



Chair of Conveying Technology

Master's Thesis



Development of an Excavation Concept for
Lunar Regolith

Dominik Höber, BSc

May 2021

Affiliation:

Chair of Mining Engineering - Conveying Technology and Design Methods
Department Product Engineering
Montanuniversität Leoben

Title:

Development of an Excavation Concept for Lunar Regolith

Author:

Dominik HÖBER, BSc

Field of study:

Mechanical Engineering - Heavy Machinery

Main Supervisor:

Univ.-Prof. Dipl.-Ing. Dr.mont. Nikolaus August SIFFERLINGER

Co-Supervisors:

Dipl.-Ing. Eric FIMBINGER

Dipl.-Ing. Dr.mont. Philipp HARTLIEB

Further Support:

Dipl.-Ing. Michael BERNER

Preface

I would like to take this opportunity to thank my family, my girlfriend, and my friends for their support during my studies at the University of Leoben. This support has brought me to where I am now. Without the motivation you gave me, I probably wouldn't have been able to finish my studies so quickly.

Furthermore, I would like to thank my supervisors Prof. Sifferlinger, Dr. Hartlieb, DI Fimbinger, and DI Berner, who made this master thesis possible for me, and supported me when there were problems.

I would also thank Andreas Taschner for the excellent cooperation during our projects.

Statutory declaration

I declare on oath that I wrote this thesis independently, did not use other than the specified sources and aids, and did not otherwise use any unauthorized aids.

I declare that I have read, understood, and complied with the guidelines of the senate of the Montanuniversität Leoben for "Good Scientific Practice".

Furthermore, I declare that the electronic and printed version of the submitted thesis are identical, both, formally and with regard to content.

Eidesstattliche Erklärung

Ich erkläre an Eides statt, dass ich diese Arbeit selbständig verfasst, andere als die angegebenen Quellen und Hilfsmittel nicht benutzt, und mich auch sonst keiner unerlaubten Hilfsmittel bedient habe.

Ich erkläre, dass ich die Richtlinien des Senats der Montanuniversität Leoben zu "Gute wissenschaftliche Praxis" gelesen, verstanden und befolgt habe.

Weiters erkläre ich, dass die elektronische und gedruckte Version der eingereichten wissenschaftlichen Abschlussarbeit formal und inhaltlich identisch sind.

18.05.2021

Date/Datum



01601916

Signature/Unterschrift

Abstract

The future goal of lunar research is a functioning ISRU chain for the production of oxygen. In-situ resource utilization (ISRU) describes the use of lunar resources for product and material generation, without transporting material from Earth. The main steps of this process are excavation, conveying, beneficiation, and processing. Each of these subsections and their interaction must function properly to enable the production of oxygen, such as for rocket fuel and to be used within lunar bases. Excavation is the first important step hereof. Due to the prevailing conditions at the celestial body, such as low gravity and thin atmosphere, and also due to the powdery and abrasive surface material, called regolith, a common mining machine as used on Earth won't work as intended. Thus a concept for a mining system that can handle these issues is developed in the course of this thesis.

There are many different functional principles possible to enable excavation. After a comparison of different implementation possibilities and their advantages and disadvantages, a bucket excavator is set to focus as a promising concept for lunar excavation. The idea is to use a horizontal bucket chain excavator that is connected with one robot on each side of the main bridge system. Because of the low gravity, scrapping of the material such as with this excavator type is preferred generally. A carrier system consisting of three beams is designed to control the excavation process by setting the mining depth, and if required, the excavation angle during operation. With this concept, a relatively large area can be processed. It is in relation to various other concepts also beneficial regarding dust and energy requirements, and it is also feasible to be used



for surface levelling, such as to prepare the ground for rocket launch/landing sites or lunar bases.

The concept development is focused on mechanical aspects, which is also supported by numerical simulation, specifically to find a suitable bucket shape. An important function is also the discharging of the excavator for further conveying purposes. Due to lunar conditions, a notching/releasing mechanism at the bucket is implemented to enhance the excavation and especially the discharging process. With this mechanism, it is possible to decrease the time of ejection.

A 3d model of the total concept is further presented, giving insight into the developed system, whereby special attention is paid to specific mechanical system components. This final system shows a promising concept that covers basic mechanical principles to allow lunar excavation as an option for further developments of excavation machines for lunar missions – but may also hold capabilities to be used in some specific application areas on Earth.

Kurzfassung

Das zukünftige Ziel der Mondforschung ist eine funktionierende Prozesskette, zur Gewinnung und direkten Verarbeitung, beziehungsweise Verwendung von Ressourcen am Mond, ISRU (in-situ resource utilization) genannt, zu ermöglichen. Die wichtigsten Schritte dazu betreffen den Abbau, die Förderung, die Aufbereitung und schlussendlich die Verarbeitung zum finalen Produkt. Jeder dieser Teilbereiche und deren Schnittstellen müssen dabei einwandfrei funktionieren, um im Speziellen die Sauerstoffproduktion, für beispielsweise Raketentreibstoff oder für die Verwendung in Mondbasen, zu ermöglichen. Der Abbau ist hierbei der erste wichtige Schritt. Aufgrund der vorherrschenden Bedingungen auf diesem erdnahen Himmelskörper, wie geringer Gravitation, dünner Atmosphäre und durch das feine und abrasive Oberflächenmaterial, genannt Regolith, eignet sich eine herkömmliche Bergbaumaschine, wie sie auf der Erde verwendet wird, nicht für diesen speziellen Einsatz. Deshalb wird im Rahmen dieser Arbeit ein Konzept für ein Abbausystem entwickelt, welches diese besonderen Bedingungen berücksichtigt.

Prinzipiell gibt es mehrere mögliche Funktionsansätze, um einen Abbauprozess zu realisieren. Nach einem Vergleich mehrerer möglicher Abbau-Ansätze und deren Vor- und Nachteile, stellt sich ein System auf Basis eines Eimerkettenbaggers, als ein vielversprechendes Konzept für den Mondbergbau heraus. Die Grundidee basiert dabei auf der Verwendung einer endlos umlaufenden Aneinanderreihung von Bechern, die einerseits zum Abbau, andererseits zum Aufnehmen des Materials, dienen. Die Führung der Eimerkette erfolgt mittels eines Brückensystems, welches zwei bereifte



Roboter miteinander verbindet. Wegen der geringen Gravitation ist das Abkratzen des Materials, wie es dieser Maschinentyp verwendet, zu bevorzugen. Das aus drei Trägern bestehende Brückensystem ist so konzipiert, dass damit die die Abbautiefe gesteuert und falls nötig auch der Abbauwinkel verändert werden kann. Mithilfe dieses Konzeptes kann eine relativ große Fläche auf einmal bearbeitet werden. Im Vergleich zu anderen Systemen, ist dieses Konzept hinsichtlich Stauberzeugung und Energiebedarf, ebenfalls vorteilhaft. Des Weiteren ermöglicht es prinzipiell auch die Vorbereitung, beziehungsweise Ebnung der Mondoberfläche, beispielsweise für die Vorbereitung des Bodens für Raketenstarts und Landungen, sowie für Mondbasen.

Die Konzeptentwicklung legt besonderen Wert auf die mechanischen Aspekte, welche unter anderem durch numerische Simulationen, wie beispielsweise für das Finden einer geeigneten Becherform, unterstützt werden. Eine wichtige Teilfunktion des entwickelten Systems betrifft das Entladen des aufgenommenen Materials, in Richtung anschließenden Förderprozess. Aufgrund der bereits erwähnten Umweltbedingungen, wird ein Klinkenmechanismus an das Bechersystem implementiert, um den Abgabeprozess zu verbessern. Damit ist es möglich, die Zeit des Materialausstoßes zu verringern.

Ein 3D-Modell des gesamten Konzeptes zeigt Einblicke in das entwickelte System, wobei besonders Systemkomponenten in mechanischer Hinsicht genauer betrachtet werden. Das finale Konzept weist vielversprechende Ansätze auf und zeigt speziell mechanische Grundansätze, um Anstöße für weitere Entwicklungen von Abbaumaschinen für Mondmissionen zu ermöglichen. Es ist auch durchaus denkbar, dass gewisse Lösungen oder Ansätze aus den Entwicklungen für spezifische Anwendungen auf der Erde eine Grundlage bieten können.

Further publications

The author of this master thesis has already done several publications in this subject area. These were worked through in a team, and are listed below:

Challenge

NASA Bucket Drum Design Challenge – April 2020 [50]

Powered by NASA Lunar Surface Innovation Initiative (LSII) and grabcad

Fourth place

Project: NASA Bucket Drum Double-Helix

Team members: Andreas Taschner, Eric Fimbinger, Stephan Weißenböck and Dominik Höber

Link: <https://grabcad.com/library/nasa-bucket-drum-double-helix-1>

Article

“Excavation and Conveying Technologies for Space Applications” [26]

Published in January 2021

BHM Berg- und Hüttenmännische Monatshefte

Authors: Dominik Höber, Andreas Taschner and Eric Fimbinger

DOI: 10.1007/s00501-020-01073-z

Presentation

SONet Talks 2021

Date: 9th of April 2021

online

Presenters: Andreas Taschner and Dominik Höber

Link: <https://youtu.be/y5z4kOHajhc>

Poster

Space Resources Week 2021 [23]

powered by LSA, ESA and LIST

19.04.2021-22.04.2021

virtual

Title: "Excavation and Conveying for Lunar Missions: System developments for the two fundamental steps of the ISRU chain"

Authors: Philipp Hartlieb, Eric Fimbinger, Dominik Höber and Andreas Taschner

DOI: 10.5281/zenodo.4707306

Cooperation Höber/Taschner

Due to the publications, two different master theses are being conducted. Dominik Höber deals with a mining unit for the Moon, and Andreas Taschner with the associated conveying unit. Since these topics have the same fundamentals, chapters 1-7 were divided and each was prepared by one person. So these chapters will be equal in both theses. This was done that each work is readable on its own.

The following chapters were written by Dominik Höber:

- Introduction (Chapter 1)
- The Moon (Chapter 2)
- Existing Robots (Chapter 4)

The following chapters and subsections were written by Andreas Taschner:

- ISRU Chain (Chapter 3)
- Transportation Systems (Chapter 5)
- Design Materials (Chapter 6)
- Boundary Conditions (Subsection 7.2)

The related part refers only to the introduction and the basic informations, the actual task is completely different in both theses. Thus, each work is independent and will be assessed individually.

Contents

1	Introduction	1
2	The Moon	3
2.1	Overview	3
2.2	The Lunar Landscape	4
2.2.1	Structure	5
2.2.2	Environmental Conditions	9
2.3	Regolith	12
2.3.1	Chemical Composition	12
2.3.2	Physical Properties	14
2.3.3	Dust	15
3	ISRU Chain	17
3.1	Excavation	18
3.2	Material Handling	19
3.3	Beneficiation	22
3.4	Processing	24
4	Existing Robots	28
4.1	Mars Rover	28
4.1.1	Spirit and Opportunity	28
4.1.2	Curiosity	30
4.1.3	Perseverance	32



4.2	NASA Rassor	34
5	Transportation Systems	36
5.1	European Large Logistics Lander (EL3)	37
5.2	NASA Lunar Lander	38
5.3	Peregrine	39
5.4	Starship	40
5.5	Blue Moon	42
6	Design Materials	44
7	Task Definition and Boundary Conditions	47
7.1	Task	47
7.2	Boundary Conditions	48
8	Excavation Concepts	49
8.1	Problems	49
8.2	Functional Principles	51
8.2.1	Back-loader / Front-loader	52
8.2.2	Scraper	53
8.2.3	Bucket-wheel	55
8.2.4	Bucket Drum	56
8.2.5	Flexible or Static Auger	58
8.2.6	Impeller	59
8.2.7	Pneumatic	61
8.2.8	Bucket Ladder	62
8.2.9	Selection of the functional Concept	64
8.3	Detailed Concepts	65
8.3.1	Basic Informations	66
8.3.2	Boom	70
8.3.3	Bridge	72



8.3.4	Selection	74
9	Simulation	75
9.1	Calibration	75
9.1.1	Density	76
9.1.2	Internal Friction	77
9.1.3	Other Parameters	78
9.2	Simulation of the Excavation Process	79
9.2.1	Field Setup	79
9.2.2	Shovel Shapes	80
9.2.3	Excavation Process	80
9.2.4	Evaluation of the Simulation	81
9.3	Discharge Process	87
9.3.1	Position of the Pivot Point	87
9.3.2	Discharge Simulation	89
9.3.3	Simulation Overview	91
10	The Design	92
10.1	Basic Structure	93
10.2	Robot at Clamping Station	97
10.3	Robot at Ejector Station	99
10.4	Bucket Mechanism	101
10.5	Design Overview	108
10.6	Further Steps	114
11	Conclusion	117
	List of Figures	121
	List of Tables	126
	Bibliography	128

1 Introduction

The universe has inspired mankind for many decades. Since the first success in reaching outer space, researchers from all over the world have been working on new technologies, for example, to position a robot precisely on Mars.

Space missions have experienced a resurgence, especially in recent years. Since private companies such as SpaceX or Blue Origin have been involved in inventing new technologies, the public interest is increasing steadily. More and more countries are launching missions into space, such as the United Arab Emirates or China. This mission mostly targets Mars because it can be a future planet for mankind, according to many researchers. [19]

The biggest problem with travelling to Mars is the long distance and the large fuel consumption. Due to the latter, another celestial body comes to the fore, the Moon. There is a chance to obtain fuel for rockets from the oxygen-containing surface material, the regolith. Thus, for example, a spaceship could fly from the Earth to the Moon, refuel and then continue its flight to Mars. This would be a great advantage because the Moon's atmosphere is much thinner than that of the Earth, and the gravitational acceleration is lower. Therefore, less energy is needed to escape from the lunar atmosphere, which would significantly increase the range of a rocket.

The abundant raw material Regolith on the Moon, due to additive manufacturing processes, can also be used as a building material for lunar bases and protection shields.



Another potential of the lunar surface material regolith is to produce oxygen for Moon bases, first for exploration missions and later for possible life on the Moon.

There are a lot of research projects ongoing to get the oxygen out of the material. They use in-situ resource utilization (ISRU), which describes a process chain from excavation to processing at the same place. However, the crucial step of this process is the excavation. Without a good mining system, the manufacturing processes cannot work. Another important step is materials handling because the medium must be brought to the manufacturing plant.

Therefore, we have made it our mission to advance this research to contribute to our knowledge of the universe.

The main part of this thesis is the development of an excavation concept from its mechanical setup, taking into account the environmental conditions. Before starting with the functional principles, several kinds of research must be done, about the lunar landscape including the special conditions and the ISRU chain. It is also important to take look at already developed robots for space applications in general, and possible transportation systems.

After that research, Chapter 7 defines the task and the boundary conditions for this thesis. The scientific part starts with Chapter 8, which is about the excavation problems and the following comparison of different functional principles with their possibilities of implementation. After that, a promising excavation concept is chosen. Chapter 9 deals with the simulation of the excavation process in consideration of surface and subsurface regolith. In the end (Chapter 10), the concept is visualized by a 3d model, and also further steps for a functioning system are mentioned.

2 The Moon

The Moon is the nearest celestial body to the Earth, with a distance between 356,000 km and 406,000 km. Because of its proximity in relation to other terrestrial bodies, mankind sees great potential in it. Due to this enthusiasm, the first missions to the Moon were already started in 1959. The first spacecraft to reach this celestial body was the Russian Lander 9 on the 3rd of February 1966, but the most famous mission was the first manned landing on the Moon on the 24th of July in 1969, during the Apollo 11 mission. The last people on this celestial body were Eugene Cernan and Harrison Schmitt of the Apollo 17 mission at the end of 1972. [58, 61]

2.1 Overview

Before starting with the main part of this thesis, it is important to take a look at the environmental and geological conditions at the Moon because these conditions lay the foundation for the development of the concept as they further set relevant boundary conditions. In Table 2.1, there is a fore comparison of some basic properties of the Moon and the Earth.

Table 2.1: Overview of properties Moon and Earth [58]

	Moon	Earth
Diameter	3,476 km	12,756 km
Mass	0.7×10^{23} kg	59.8×10^{23} kg
Gravitational acceleration	1.622 m/s ²	9.8 m/s ²
Temperature range	-258 °C (at the poles) to 127 °C (at the equator)	-89.2 °C (at the poles) to 60 °C (at the equator)
Atmospheric pressure at surface	1×10^{-12} torr = 1.333224×10^{-14} bar	760 torr = 1.01325 bar

Due to the fact that the Moon rotates around the Earth and also its axes within a month, it is always the same side that can be seen from the Earth. This gives the impression that the Moon is locked in its place. Therefore, we differentiate between “near side” and “far side”. The Moon can reflect only a fraction of the incident light, but it appears bright in the sky. The reason for this is the contrast between the Moon and the night sky, which is deep black. Actually, the brightness of the Moon is similar to the brightness of coal dust. [58]

2.2 The Lunar Landscape

Compared to the Earth on which the mountains result from an active plate tectonic process, highlands on the Moon were only created by differently sized meteorite impacts. These impacts formed not only the lunar surface over a timespan of four billion years, but also created the main subsurface material, the lunar regolith. This material will be discussed in Chapter 2.3. The core of the Moon consists of iron, with a temperature of about 1400°C, which is heated by the energy of radioactive elements. [58, 4, 13]

For the project covered in this thesis, only the surface conditions are relevant, so the inner conditions of the Moon are not mentioned further.

2.2.1 Structure

The surface structure of the Moon can be divided into two different types of landscape. On the one hand, there are dark lunar maria, and on the other hand, lighter highlands (Figure 2.1), which have a lot of craters. These hollows are characteristic for the Moon. The impacts are differentiated into craters and basins, depending on their diameters. [65]

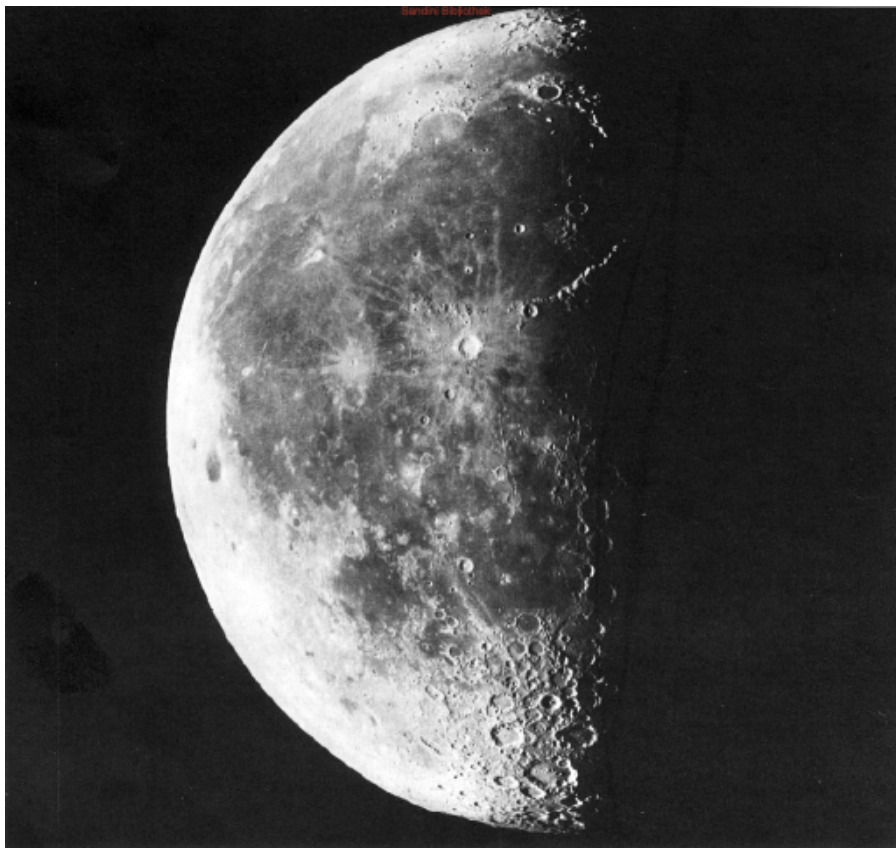


Figure 2.1: The Moon surface with maria and highlands [65]

Maria

A long time ago, people believed that the Moon has oceans and continents, as on Earth. But today, it is known that it is impossible for big oceans to ever exist because the gravity on the Moon is too low. These so-called lunar seas are just large patches of dark lava rock.

These mares, as shown in Figure 2.2, are not as old as the white highlands, so only a few craters can be found there because of fewer meteorite impacts since then. There are two classes of structure in the mare field, the mare ridges and the arcuate grabens. [65, 68]

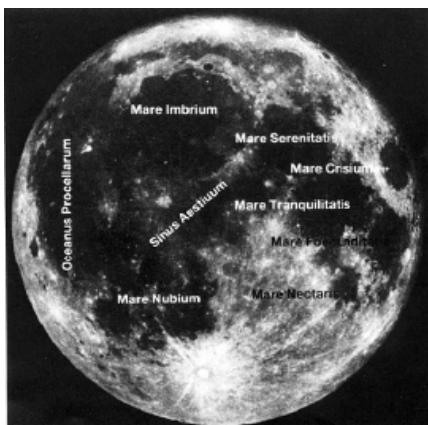


Figure 2.2: Moon mares [65]



Figure 2.3: The Apennines on the Moon [65]

Highland

Besides the craters, there are also long mountain ranges on the Moon. They were named after well-known regions on the Earth, such as the Alps and the Apennines. However, these peaks are not comparable with those on Earth, because they are only accumulations through meteorite impacts.

With their span of over 1,000 km, the Apennines (Figure 2.3) are the largest mountain range on the Moon. The peaks are up to 6,500 m high in relation to their surrounding valleys. [65, 24]

Crater

As already mentioned, the craters were created by the impact of meteorites. They have a diameter of up to 250 km. There are over 30,000 craters visible from the earth (Figure 2.4), but there are many smaller ones as well (from the Earth only those larger than 400 m in diameter are visible).

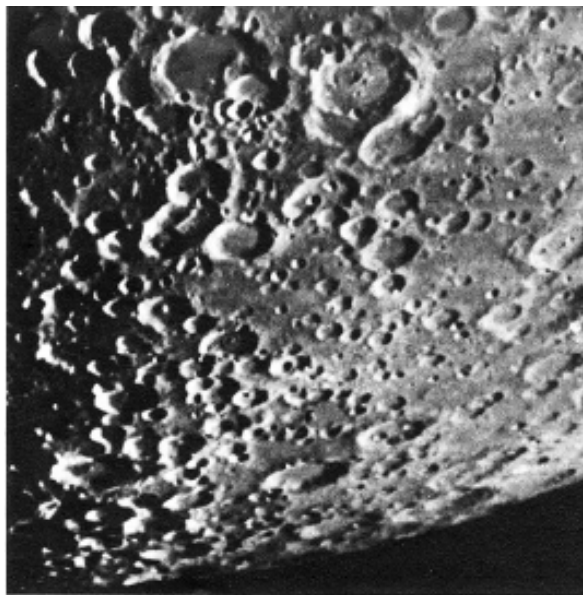


Figure 2.4: Crater landscape [65]

The crater formations can be divided into three types:

- The small craters with a diameter of 20 km
- The ring mountains (20 to 100 km)
- The wall levels (greater than 100 km)

The walls of big craters are often higher than 3,000 m, in exceptions up to 10,000 m. And because there is no water and wind, these craters remain as they are (except until the next impact of meteorites).

The biggest one is the Clavius crater with a diameter of 240 km and the highest one is the Letrone crater with a height of about 10,000 m. Other popular ones are Archimedes, Aristoteles, Copernicus, Grimaldi, Theophilus and Tycho. [65, 68]

Basins and basin rings

The large basins are an important characteristic of the Moon, which can be seen from the Earth as black circles. These bowls were created by meteorite impacts, but unlike craters, these pools have a diameter of at least 300 km. This limit is an attribute for central rings instead of central crater peaks.

The most popular ones are the Orientale Basin (Figure 2.5), the Imbrium Basin, and the South Pole-Aitken Basin. The Orientale Basin has a diameter of 930 km and four rings. Unlike the Orientale Basin, the Imbrium Basin was filled with lava. The South Pole-Aitken Basin is the largest Basin on the Moon with a diameter of 2,500 km. In addition to the large diameter, it also has a depth of 12 km. [58, 24]

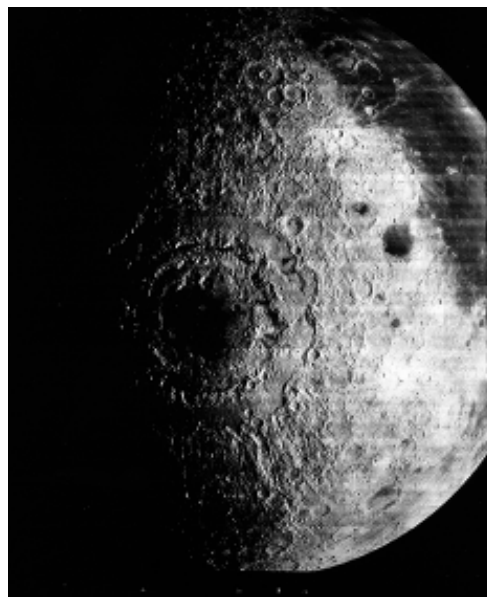


Figure 2.5: Orientale Basin [58]

Water

Evidence of hydrogen has been found on the Moon, and it is believed that there is water ice at the poles of this celestial body. Figure 2.6 shows the suspected occurrences. Water resources would be a big advantage for further missions on the Moon. [58]

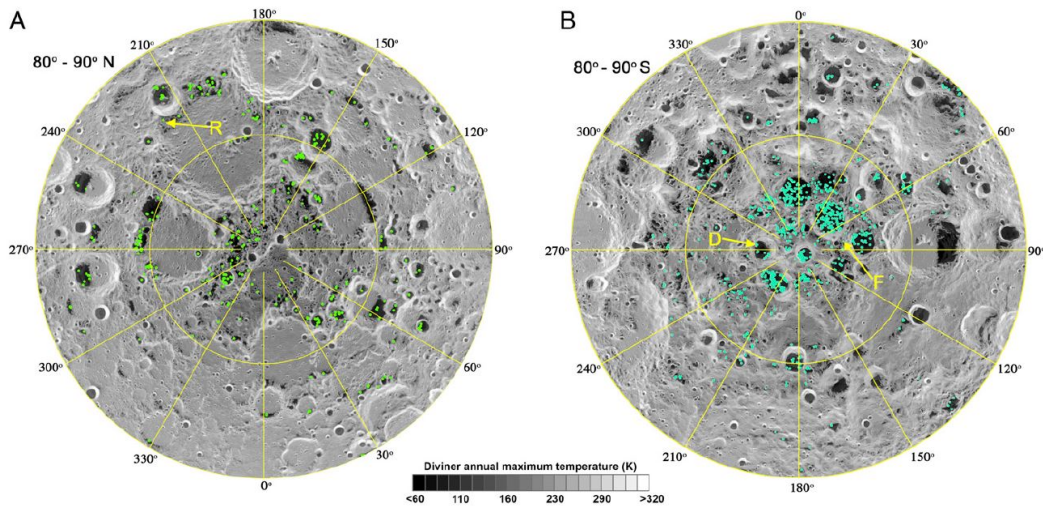


Figure 2.6: Distribution of water ice at the northern and southern polar regions [35]

2.2.2 Environmental Conditions

The environmental conditions are in many aspects different from those on Earth, notably to name the most important ones: gravity, atmosphere, temperature and cosmic radiation. Those conditions are further described on the following pages. [58]

Gravity

As already mentioned in the overview, the gravitational acceleration is only about a sixth of that on Earth. Exemplarily transferred to Earth conditions, this means that a weight of 120 kg results in a weight force on the Moon that can be compared to a weight force of only 20 kg on Earth.

$$g = \frac{G * M}{R^2} \quad (2.1)$$

The gravitational acceleration (g) depends on the gravitational constant (G), the respective radius of the Moon (R), and its total mass (M). The gravitational constant has a value of $6.673 \times 10^{-11} \text{ m}^3/\text{kgs}^2$. [64]



Atmosphere

Many people think that the Moon has no atmosphere while in fact, it has a very tenuous one. The atmosphere at the Moon has a gas concentration of about 2×10^5 molecules per cubic centimetre, which is only about one-fourteenth ($1/14$) of the Earth. In the following Table 2.2, there is the composition of the lunar atmosphere. The values are given in molecules per cubic centimetre (molecules/cm³).

Table 2.2: Gas composition of the lunar atmosphere [24]

Gas	Chemical nomenclature	Daytime	Nighttime
Neon	²⁰ Ne	$4 \times 10^3 - 10^4$	10^5
Helium	He	$8 \times 10^2 - 4.7 \times 10^3$	$4 - 7 \times 10^4$
Hydrogen	H ₂	$2.5 - 9.9 \times 10^3$	$10^4 - 1.5 \times 10^5$
Argon	⁴⁰ Ar	2×10^3	10^2
Methane	CH ₄	1.2×10^3	
Carbon dioxide	CO ₂	10^3	
Ammonia	NH ₃	4×10^2	
Hydroxide+water	OH+H ₂ O	0.5	

The composition also depends on the time of the day because there are differences between daytime and nighttime. [24]

Length of day

A day on the Moon lasts about 709 hours, which corresponds to about 29.5 Earth days, so it is nearly a month. This is a challenge and a problem for missions as there are big temperature fluctuations at night, which can also be seen in the following paragraph. [58]

Temperature

Conditions of $+127^{\circ}\text{C}$ to -173°C prevail at the equator of the Moon. These large temperature fluctuations are caused by the day and night phases on the Moon. In Figure 2.7, the temperature curve at the equator is shown. It can also be seen that an approximately constant temperature of around 240 K (-33°C) has set one meter below the surface. [58]

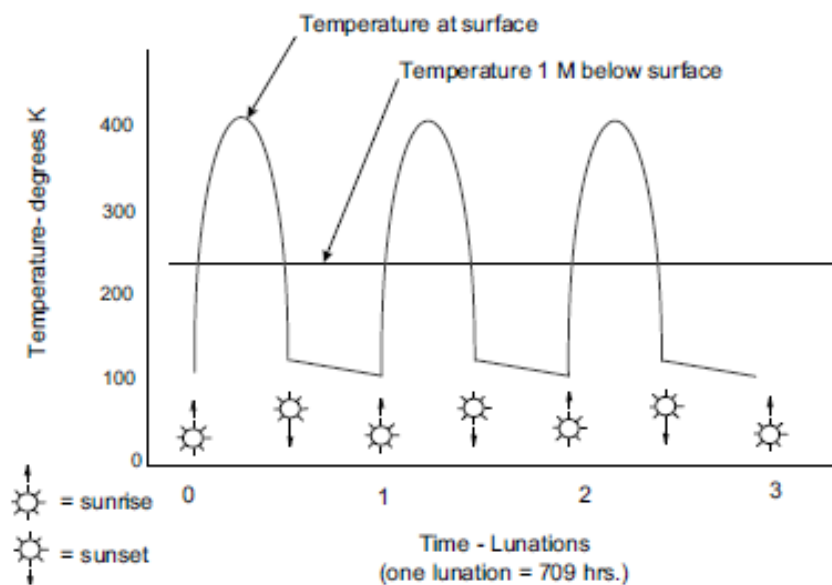


Figure 2.7: Temperature profile at the Moon's surface [58]

Ionizing radiation

There are three major types of radiation in the lunar environment, the solar wind, the solar cosmic rays, and the galactic cosmic rays. Each of them has different effects on the lunar environment. The influence of these radiations on the Moon depends on their energy and composition; for instance, the solar cosmic rays leads to ionization energy loss in the top millimetres or centimetres of the lunar surface. [24]



2.3 Regolith

There are many different minerals and rocks, which occur on the Moon, but for this application, the lunar regolith is of major importance; thus, others will not be mentioned further. Regolith results from meteorite impacts to the lunar surface. These meteorites were shattered by the impact and covered the Moons top surface layer with a fine powder: the regolith. Due to this, regolith can only be found on the surface of a celestial body, such as specifically the Moon. On the Moon, this layer covers almost the entire surface and has a thickness of four to five meters in the mare areas, and between ten and fifteen meters in the highland regions.

Regolith has two great potentials: On the one hand, it can be used as a building material because it protects against radiation, and on the other hand, it can be used to generate oxygen. The exact process of oxygen generation is described in the ISRU chapter. [58, 4]

2.3.1 Chemical Composition

The lunar regolith contains of a lot of different elements. These elements can be divided into two groups, the major elements and the trace elements. The lunar surface consists of a mixture of basaltic and anorthositic materials. It is also notable that more than a quarter of the particles on the top appears in the form of agglutinates (fused soil).

Agglutinates are composed of regolith particles and glass, which is created by the impact of the meteorites and the resulting energy conversion from the kinetic energy to heat. The unmelted fragments stick to the melted ones and thus create a new form of grain. As can be seen in Figure 2.7, these agglutinate have a very sharp shape, which is responsible for the increased wear on contacting components, such as mining equipment. [58, 12]

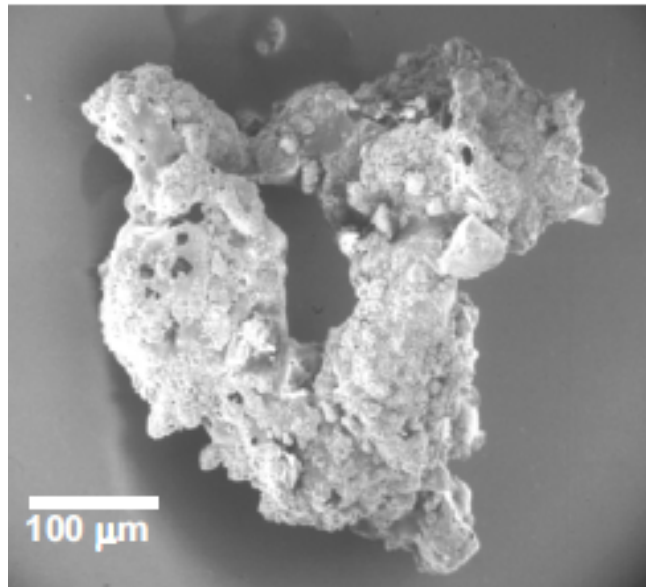


Figure 2.8: Lunar agglutinate [58]

For the listed values (Table 2.3), the average occurrence is described. The metallic components occur in the form of metal oxides. The major elements are given in the unit of percents of atoms (%) and the trace elements in grams per cubic metre (g/m^3). [58]

Table 2.3: Major and trace elements of regolith [58]

Major elements	Percent of atoms	Trace elements	Grams per cubic meter
Oxygen (O)	60.9	Sulfur (S)	1,800
Silicon (Si)	16.4	Phosphorus (P)	1,000
Aluminum (Al)	9.4	Carbon (C)	200
Calcium (Ca)	5.8	Hydrogen (H)	100
Magnesium (Mg)	4.2	Nitrogen (N)	100
Iron (Fe)	2.3	Helium (He)	20
Sodium (Na)	0.4	Neon (Ne)	20
Titanium (Ti)	0.3	Argon (Ar)	1
		Krypton (Kr)	1
		Xenon (Xe)	1

2.3.2 Physical Properties

In general, the regolith has very specific characteristics, which will be explained here, for instance, different properties due to different grain sizes.

As can be seen in Table 2.4, some properties depend on the depth. These are indicated by their average values, like the cohesion, the internal friction angle and the bulk density. High cohesion means the particles attract each other strongly and this leads to the fact that the grains can form lumps. It is also interesting that the internal friction angle, which is a parameter for the friction between the particles, changes significantly even at a depth of a few centimetres. The increase in the bulk density can be explained by the increasing compaction with depth. [24, 36]

Table 2.4: Cohesion and internal friction angle of regolith [24, 36]

Depth	Cohesion c (kPa)	Internal friction angle ($^{\circ}$)	Bulk density (g/cm^3)
0-15 cm	0.52	42	1.45-1.55
0-30 cm	0.9	46	1.53-1.63
30-60 cm	3.0	54	1.69-1.79
0-60 cm	1.6	49.5	1.61-1.71

Grain shape

There are various shapes of lunar regolith, from spherical to extremely angular. Most of the particles have an elongated shape, so the grains tend to form a denser packing. Due to this compaction, they are preferably arranged somehow parallel, along their longitudinal axes. This leads to some physical properties showing anisotropic behaviour. [58]

Grain size

The average grain size of regolith on the surface is between 60 and 80 μm . In the examined soil sample, grain sizes between 40 and 800 μm were founded. Most of the particles are glass bonded aggregates, rocks, and minerals. [24]

Another source has shown the following particle size distribution, as can be seen in Table 2.5. The values are given in percent, but the total is not 100%, because some particles were undefined and therefore not assigned.

Table 2.5: Particle size distribution in lunar soil [12]

	Size (μm)						Sample
	250-500	150-250	90-150	75-90	45-75	20-45	weighted
Weight percentage	11.91	13.13	15.99	5.48	14.45	17.37	average 78.33

Of course, there are also some bigger particles, also in the form of rocks, but these are not included in the grain size distribution because they do not appear regularly and are therefore not dealt with as part of the bulk material regolith.

It can be recognized, that there are differences between those two sources. This is because of the fact, that the distribution on the Moon is not the same everywhere. [12]

2.3.3 Dust

Particles with diameters less than 20 μm are generally called dust (in lunar context), and they can cause serious problems. Due to electrostatically loading, these small particles adhere to various surfaces. This could already be seen in the manned moon missions. They were stuck, for instance, on helmet visors, and attempts to wipe them

off, scratches the visor. Furthermore, it is getting hotter and hotter inside the overall space suit, because of the dark dust and following absorption of the solar radiation. Another issue was lower traction of the lunar rovers than initially expected. [58, 12]

Electrostatic charging

Because there is no moisture in the lunar regolith and the thin atmosphere, there is an interaction between the different radiations and the particles. Due to this influence, the regolith is electronegatively charged on the night side and positively charged on the daylight side. [58, 12]

3 ISRU Chain

In-Situ Resource Utilization, or ISRU, is defined as follows:

„In-Situ Resource Utilization is the collection, processing, storing and use of materials encountered in the course of human or robotic space exploration that replace materials that would otherwise be brought from Earth to accomplish a mission critical need at reduced overall cost and risk.“ [56]

In this section, ISRU is only considered for lunar missions, although this process chain as a whole normally includes every planet on which it is possible. ISRU includes the production with native resources as raw materials used for goods and products, which are necessary for a human being on the Moon, or space and exploration missions. For instance, ISRU contains topics like the production of life support gases, propellants, spare and wear parts, and the construction of infrastructure on the lunar surface. One essential aim, among others, is to reduce the logistics from Earth and move them to the Moon, so that rockets do not need to transport essentials to this celestial body for each consumable. Instead of delivering these from Earth to the Moon, it is better to use raw materials that exist there. Moreover, the escape velocity from the lunar atmosphere is 2 km/s, whereas the escape velocity on the Earth is about 5 times higher, 11 km/s. Thus, the reduced logistics lead to a reduction in costs. Additionally, ISRU enables long-term missions such as lunar soil excavations, where energy supply is essential. These last points describe the importance of ISRU very well and explain why so many research projects focus on it. [56, 58]

A difficult challenge is the multidisciplinary nature of this process chain. For a functional and successful ISRU, it is necessary to consider all stages – from excavation to storing the produced goods, similar to the terrestrial mine-to-product process. Therefore, many specialists from several different fields of research are required. To illustrate, for the development of an excavation robot and a chemical extraction process, different types of knowledge are needed. Furthermore, it is also crucial to link the stages properly, because without a connection between the stages, ISRU won't work.[33]

One approach is to structure ISRU into a process chain. Figure 3.1 gives a brief overview of the ISRU process chain.

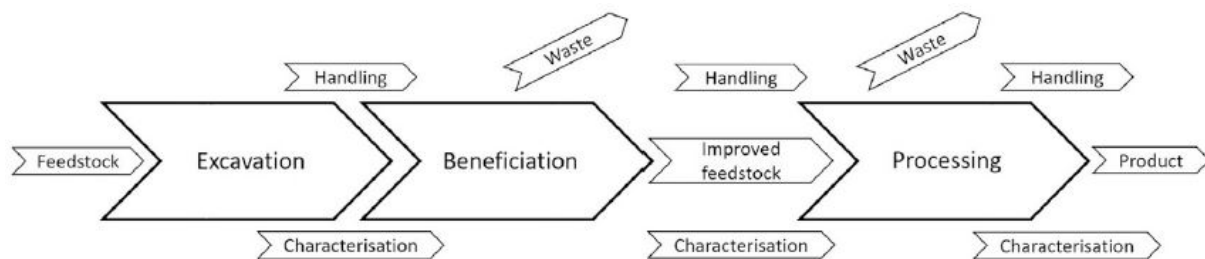


Figure 3.1: ISRU process chain [32]

It can be introduced in many different ways, but the main parts are always the same. The essential chain links are excavation, material handling, beneficiation, and processing.

3.1 Excavation

First, the lunar soil consists of regolith. Regolith is the feedstock for ISRU on the Moon. The properties and composition (e.g. ores, chemical elements) are described in Section 2.3. Regolith contains chemical elements, which can be used for mission support or to support human life on the Moon. For instance, approximately 40% of oxygen by weight is contained in the regolith. [32]



Although excavation is the initial step in the ISRU process chain, only a few research projects, compared to other steps such as chemical processing, are about the excavation on the Moon. It is currently difficult to specify the exact requirements because data about the lunar soil (e.g. composition, possible ice content) is not sufficiently available. In particular, two main issues occur when it comes to mining, conveying, and to the beneficiation of lunar regolith: First, the properties of regolith such as chemical composition and mineralogical makeup, and second, the gravitational force on the lunar surface, which is significantly different compared to the gravity force on Earth. Due to the harsh environment on the Moon, these are not the only issues that arise; for example, energy supply and tribological aspects will also be challenging. [32]

The tractive force depends on the mass of the mining unit and increases with the mass of the machine. Terrestrial excavators are designed for large vertical and lateral excavation forces without loss of traction. Therefore, almost every mining machine on Earth is a heavyweight solution. The transport of a large amount of payload from the Earth to the lunar surface leads to high financial costs and risks to deliver the payload to the Moon safely. As a result, excavators, which are operating on the surface of the Moon, have to be designed for low excavation forces and with low masses. Figures 3.2 and 3.3 are examples for this step of the ISRU chain that are under development. [32]

3.2 Material Handling

After regolith is excavated, it has to be transported to the production plant, where it goes through further steps. The material has to be delivered from the excavator, which usually operates a few hundred meters away from the base or processing plant, to the production plant as well as transported in the production plant between the individual steps. The different tasks require different conveyors. [58, 4]

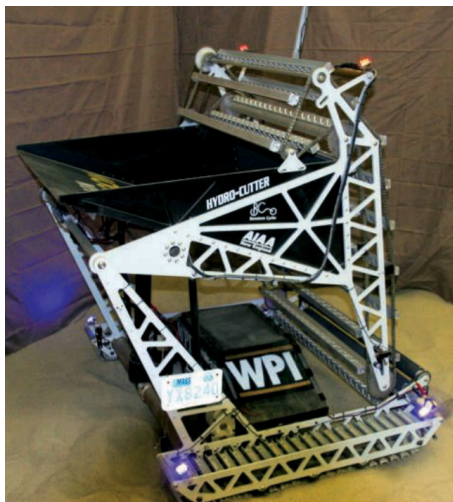


Figure 3.2: Moonraker robot [39]

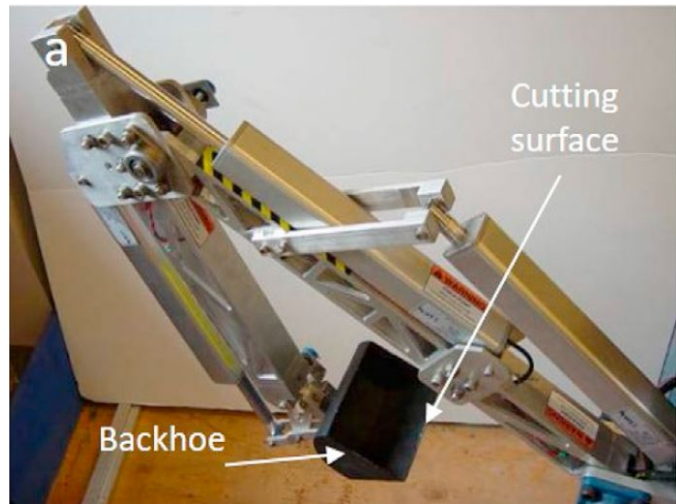


Figure 3.3: Backhoe as an excavator system [32]

There are also some major challenges in the conveying of Regolith that need to be overcome. Cohesiveness is an important property when it comes to material handling. On Earth, when the particle size decreases, the material is more cohesive. In addition, gravity also has a large influence on the powder movement and cohesiveness. Decreasing gravity level leads to an increase in cohesiveness. If, for example, a certain gravity level drops to $1/4$, there will be a huge change in powder behaviour. The result of a growing cohesiveness is that the material acquires other characteristics like clumping, difficulty in fluidizing, poor flowability, and avalanching. Furthermore, electrostatic effects have also an influence on material behaviour. On the Moon, electrostatic effects occur more often than on the Earth due to the hard vacuum and the lower gravity. The lunar surface, which is exposed to the lunar environment, receives a surface charge straight from space or even from ultra-low density plasma. Moreover, on the Moon, the particles cannot discharge themselves by the atmosphere. Besides, fine dust is part of the regolith. Dust concerns problems with mechanical machineries, such as moving parts and seals. [4]

For the transport of regolith within the production plant, there are different types of mechanical conveyors under development. Besides, pneumatic conveyors are possible on the Moon. Figure 3.4 is a graphic of the pneumatic conveying system.

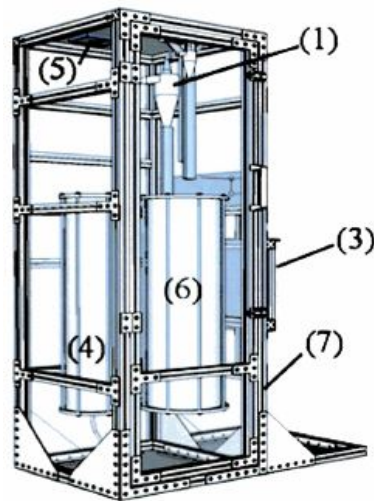


Figure 3.4: Graphic of pneumatic conveyor [40]

The delivery of regolith over longer distances is more difficult. Various types of conveying systems are being developed and studied, such as pneumatic conveying, electromagnetic conveying, railway systems, and conveyor systems. Figure 3.5 illustrates an approach for a future design of a pneumatic conveyor system. [58]

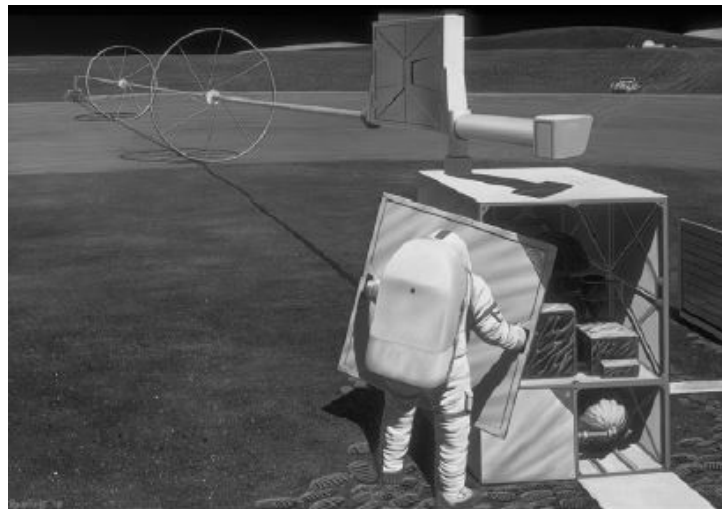


Figure 3.5: Future design of a pneumatic conveyor [58]



3.3 Beneficiation

After the transport of lunar soil to the plant and before the processing begins, the regolith has to be beneficiated or separated. Almost every processing operation requires a certain type of feedstock material. Therefore, a reliable beneficiation process, including size classification and material enrichment, is crucial for further steps. In particular, the beneficiation step ensures a consistent feedstock. Furthermore, with an appropriate raw material, no mechanical problems occur in the processing step. To illustrate, the hydrogen reduction process using ilmenite, which is patented by Gibson & Knudson, needs a feedstock containing between 80 and 90% ilmenite. [52]

Many separation and beneficiation systems on Earth use large amounts of water like density separation by spirals, jigs, froth flotation, and shaking tables. These technologies are unsuitable for beneficiation on the Moon. Every enumerated technology uses differences in physical properties to separate minerals from waste, for example, density, electromagnetic characteristics, and surface properties. As a result, beneficiation technologies without using a process fluid for separation have to be considered for lunar applications. [52]

Separation technologies based on gravity use the differences in density, particle's mass, and volume of the particles contained in the mixture. These methods, such as the shaking table, are well-known solutions for terrestrial applications. However, it would be a huge technical problem to implement such technologies for lunar separation. Instead of gravity-based separation, electrostatic and magnetic techniques are studied because they have a higher potential for beneficiation on the Moon. [52]

In electrostatic separation, changes in the Coulomb and/or dielectrophoresis forces are exploited. Both approaches have proven to be useful for generating material enrichment from several mixtures in lunar applications. Electrostatic separation, which is based on the manipulation of these two forces, has thus gained the most attention for lunar separation technologies. Due to the different surface charges of the particles,

the Coulomb force separates them. Further, in a non-uniform electrostatic field, the particles are polarized and the dielectrophoresis force is generated. Coulomb force methods require two things: charged particles and an electrostatic field. The charged particles pass through an electrostatic field. Particles, which have a positive charge, are attached to the negative side of the electrostatic field, and vice versa. Some examples of Coulomb separation techniques are Ion Bombardment, Electron Bombardment, and UV Charging. Figure 3.6 shows another technique based on Coulomb force technology called Tribocharging and Free Fall Separation. [52]

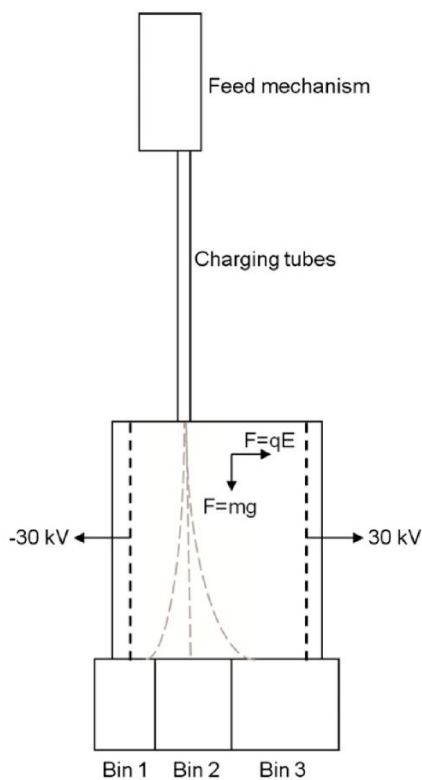


Figure 3.6: Diagram of a free fall type separator [52]

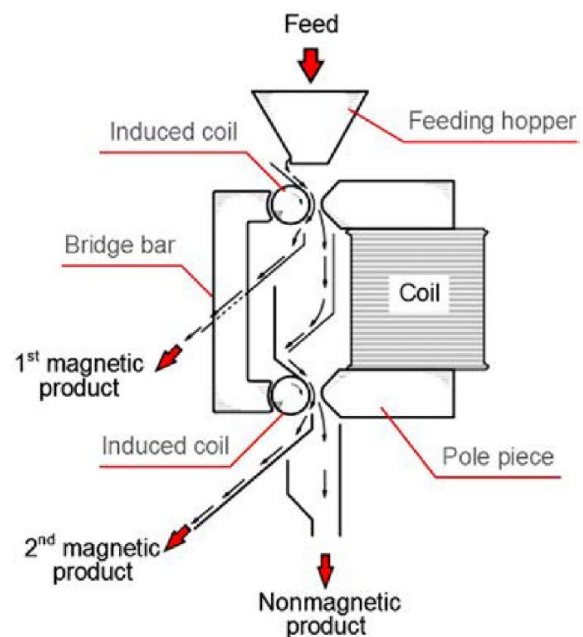


Figure 3.7: Diagrammatic representation of an IRMS [52]

Another beneficiation technique is magnetic separation. In terrestrial processing operations, magnetic separation is used. In particular to remove tramp iron from other minerals. Materials can be divided into three different magnetic behaviours: Diamagnetism, Ferromagnetism, and Paramagnetism. Diamagnetic materials, like quartz, only oppose the magnetic field if the field is very strong, whereas ferromagnetic materi-

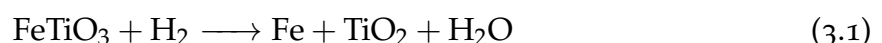


als, such as iron, can be highly magnetized. For example, ilmenite is a paramagnetic material, and without an applied magnetic field, the atoms have unaligned magnetic moments, and this results in a net-zero magnetization. But, the magnetic moments react to applied magnetic fields. Overall, the separation of paramagnetic materials from the other feedstock requires strong magnetic fields, a minimum of 2 T. In Figure 3.7, there is a high-gradient magnetic separation (IRMS) application. [52]

3.4 Processing

The production of oxygen on the Moon is a main point of ISRU. In many different types of lunar missions, oxygen is crucial, such as for ensuring human life on the lunar surface or for refuelling a rocket before launching again. As an example: 80% of the takeoff weight of Apollo 11 consisted of fuel and liquid oxygen. So, if liquid oxygen is available on the Moon, as by ISRU, the launch weight of a rocket can be significantly reduced. There are different types of experiments to produce oxygen on the lunar surface, and they can be divided into chemical reduction, pyrolysis, aqueous solvent processing, and electrochemical reduction. [4]

For feedstocks, which have a large proportion of iron ore like ilmenite, hydrogen reduction is suitable. This process works at approximately 900°C and is relatively simple.



The water is in a gaseous state after the process and is afterwards condensed. Subsequently, the water goes into an electrolysis process, and the hydrogen returns to the reduction process. The iron ore oxide content in the feedstock is decisive for the oxygen yield and depends on where the raw material was located so that a beneficiation step

prior to reduction is necessary. [4] Figure 3.8 shows two different types of reduction reactors called ROxygen, developed by NASA, and PILOT, developed by Lockheed Martin Astronautics (LMA). [57]

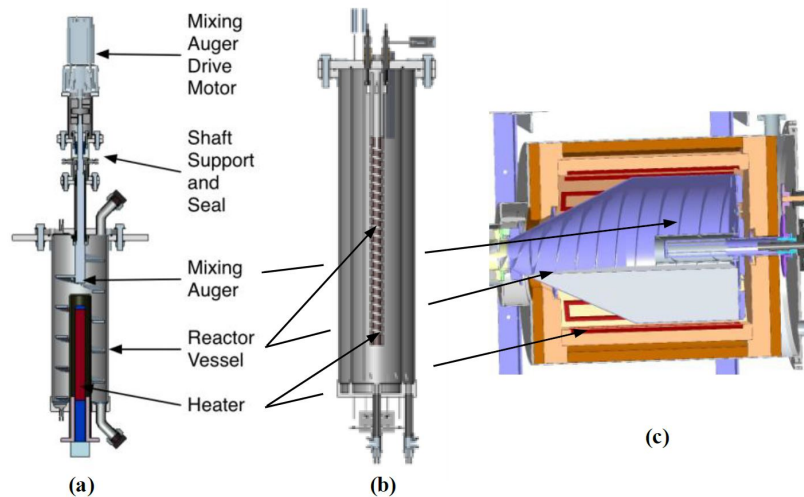


Figure 3.8: ROxygen Gen I Reactor (a), ROxygen Gen II Reactor (b), PILOT Rotating Reactor (c) [57]

Carbothermal reduction with methane is significantly different from the hydrogen reduction because it is appropriate to a bulk regolith feedstock including silicon oxide. Furthermore, this process can reach higher reduction levels. The crucial step starts at a temperature of about 1600°C:

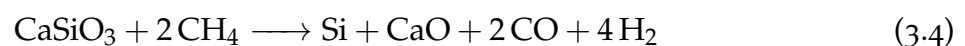
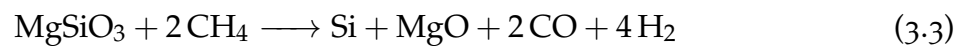


Figure 3.9 illustrates a sketch of the carbothermal reduction of lunar regolith.

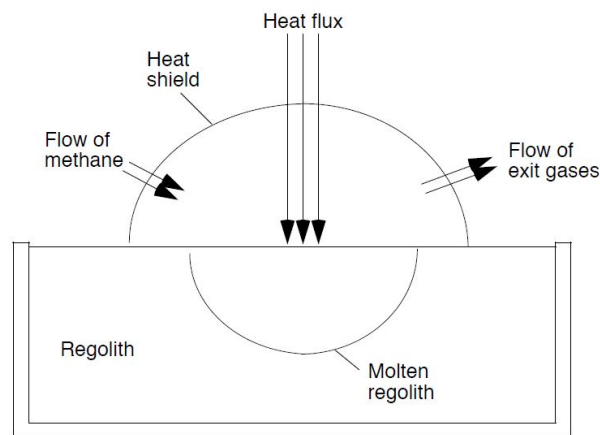


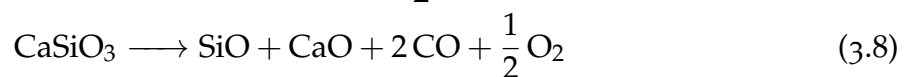
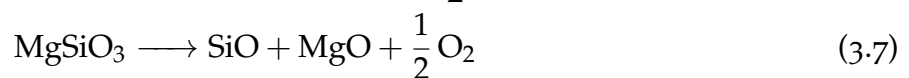
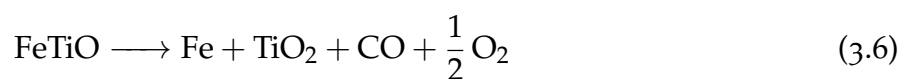
Figure 3.9: Sketch of the carbothermal reduction of lunar regolith [5]

The next step produces water over a nickel catalyst:



Then the methane is reused, and the water goes forward to electrolysis. Although ESA stated this process as their preferred way to generate oxygen, there are some disadvantages. The carbothermal reduction process requires multiple processing steps and high operating temperatures. [4]

Similarly, the vapour phase pyrolysis also works with a bulk regolith feedstock, but this process requires an operating temperature above 2000°C to decompose the strong metal-oxide bonds:





It is possible to reach oxygen yields up to 50% depending on some process factors such as temperature and duration. The rapid cooling and condensation of the oxygen obtained is an essential step in preventing the recombination of oxygen with the remaining suboxides. The major drawback is certainly the high operating temperature. [4]

There are other processes to produce oxygen, for instance, sulphuric acid reduction and the magma process, which is the simplest approach, but these processes are here not discussed in detail.

Water ice on the Moon could become a ‚gamechanger‘ due to water is the most important substance for mankind. NASA’s mission called LCROSS detected water ice in the polar regions in acceptable quantities in October 2009. According to the LCROSS mission, the lunar soil in the polar regions, especially in the permanently shaded craters, contains about 5.6% water ice, but this is a model-based estimation, so it must be confirmed first. If the prediction is correct, the astronauts will be able to extract up to 100 litres of water from one cubic meter of lunar soil. The presence of water ice on the Moon represents a great opportunity for lunar missions; nevertheless, many challenging problems are still ahead. For instance, ice-mining operations will be technically problematic because of the low temperatures to -230°C and below. Moreover, the extraction of water ice will be energy-consuming, expensive, and the transportation of the extracted water ice will also be problematic due to the mountainous terrain and the rough environment. [4]

4 Existing Robots

The following pages will describe some existing robots which were already used in space or are planned to start soon. The structure of the robots is the most important aspect of this research; hence, a selection of modern robots used in space exploration (therefore also including Mars) is being examined in more detail in the following.

4.1 Mars Rover

The Mars rovers from the National Aerospace and Space Agency (NASA), are the most popular space robots, and even if they aren't/weren't mining robots, there is a lot of knowledge for further use. For example, the drive or the energy supply. The Mars Rover project consists of several missions: the missions Spirit and Opportunity are already considered completed. [47]

4.1.1 Spirit and Opportunity

These robots (Figure 4.1) were structurally identical, and they investigated the geological circumstances on Mars. The landing sites Gusev Crater and Meridani Planum were specifically selected because water was suspected there most. [49, 47]

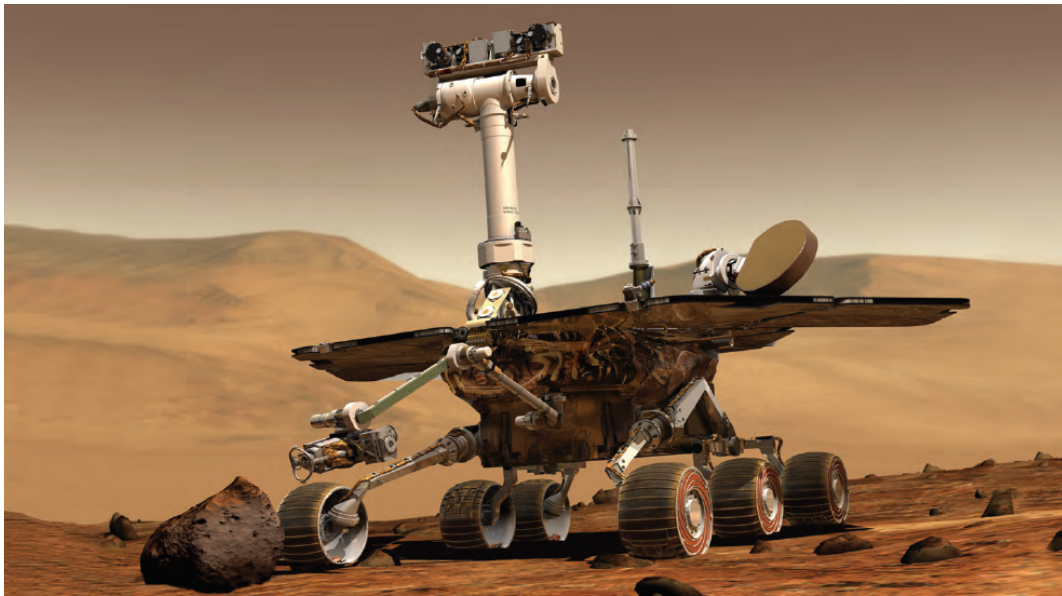


Figure 4.1: Spirit and Opportunity [49]

Table 4.1: Facts about the missions Spirit and Opportunity [49]

	Spirit	Opportunity
Launch	10th of June 2003	7th of July 2003
Arrival	4th of January 2004	25th of January 2004
Landing place:	Gusev Crater, Mars	Meridiani Planum, Mars

While NASA lost the connection to Spirit on the 22nd of March 2010, the mission of Opportunity lasted until the 10th of June 2018. On the 12th of February, the mission was finally declared finished (Table 4.1). [49, 47]

Structure

The rover was 1.6 m long with a width of 2.3 m. The total height of the robot was 1.5 m, and it had a total weight of 175 kg. It also had a robot arm with three instruments to remove rocks and brush surfaces. [44]

The core structure was made of composite material in a honeycomb setup, and the energy supply was realized by solar panels, with a total area of 1.3 m². The panels could

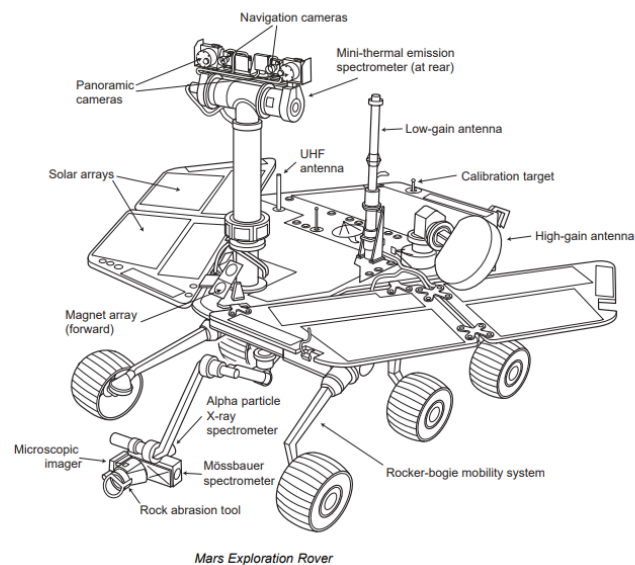


Figure 4.2: Structure of Spirit and Opportunity [44]

produce up to 900 Wh of energy by martian day. The rover also had six wheels (figure 4.2) and a special system for driving over relatively big rocks. Sensitive components such as the battery were stowed in a warmed box so that they survived the cold Martian nights. The rover was also equipped with a few cameras for navigation and collecting data. [43]

4.1.2 Curiosity

Curiosity (Figure 4.3) is the follow-up development of the rovers Spirit and Opportunity. The main mission is to deal with the question if there were ever viable conditions on Mars. Curiosity is especially looking for moist climatic conditions as well as rocks and minerals. The mission (Table 4.2) still continues today.

Unlike its predecessors, it does not use solar panels for power supply. Curiosity uses a Multi-Mission Radioisotope Thermoelectric Generator that provides about 2,700 Wh per sol (Martian day). [46, 45]

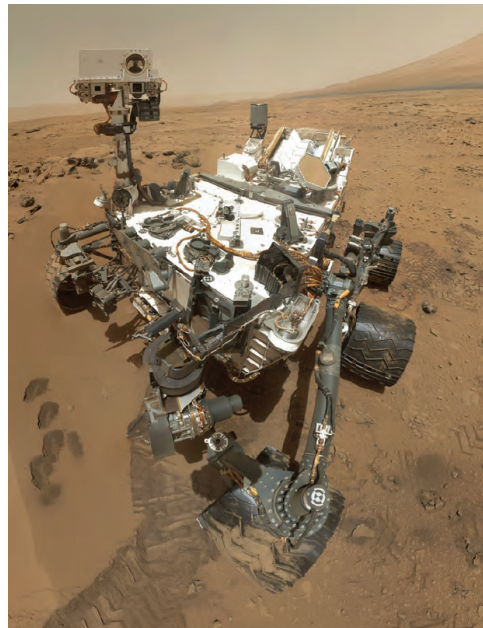


Figure 4.3: Curiosity [46]

Table 4.2: The Curiosity mission [46, 45]

Mission		Structure	
Launch	26th of October 2011	Length	3 m
Arrival	8th of August 2012	Width	2.8 m
Landing place	Gale Crater, Mars	High	2.1 m
		Mass	899 kg

The robotic arm is probably the most important tool for Curiosity. It is 2.1 m long and is constructed like a human arm to ensure maximum flexibility. The hand at the end is called turret (Figures 4.4 and 4.5) and has many functions. These include a drill, for collecting powdery rock samples, a brush, and a shovel (DRT) for collecting surface samples. Furthermore, an Alpha Particle X-ray Spectrometer (APXS) is used for the identification of chemical elements, and a subsystem named Collection and Handling for In-Situ Martian Rock Analysis (CHIMRA) that is used for sample processing, is located there. Another equipment is a camera called Mars Hand Lens Imager (MAHLI). With this, Curiosity can research the geological conditions on Mars. [46, 45]

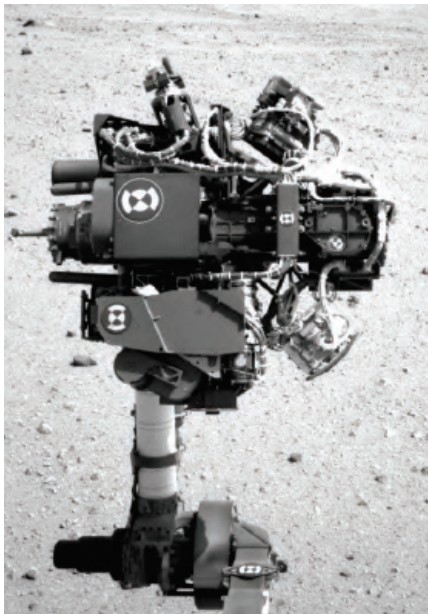


Figure 4.4: Curiosity's turret [46]

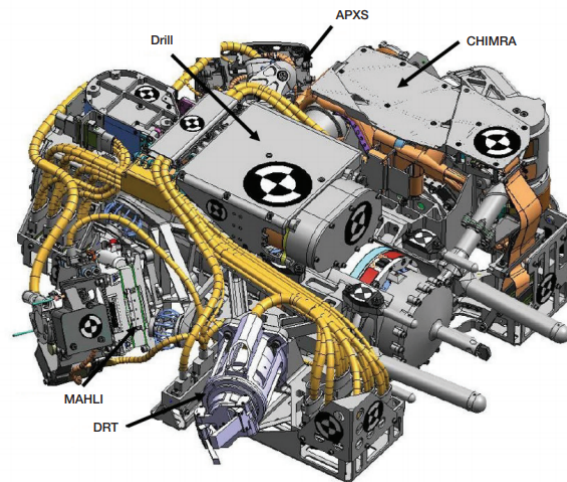


Figure 4.5: Structure of Curiosity's turret [45]

4.1.3 Perseverance

Perseverance (figure 4.6) is the latest Mars rover landed on Mars. This mission can be divided into four goals, which are defined as follows.

- Determine whether life ever existed
- Characterize the climate
- Characterize the geology
- Prepare for human exploration

With its launch on the 31st of July 2020, Perseverance landed on the 18th of February 2021 in the Jezero Crater. With a length of 3 m, a width of 2.7 m, and a height of 2.2 m, it is quite similar in size to its predecessor Curiosity. Although in terms of weight, this rover is about 126 kilograms heavier (total 1025 kg). For its power supply, a Multi-Mission Radioisotope Thermoelectric Generator, like the last generation of Mars rovers, is used. [42, 37]

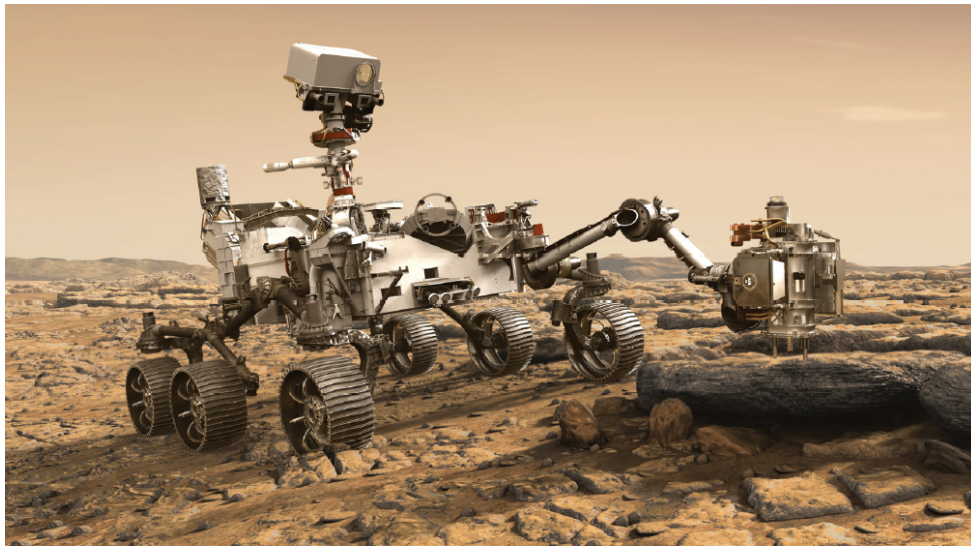


Figure 4.6: Perseverance [42]

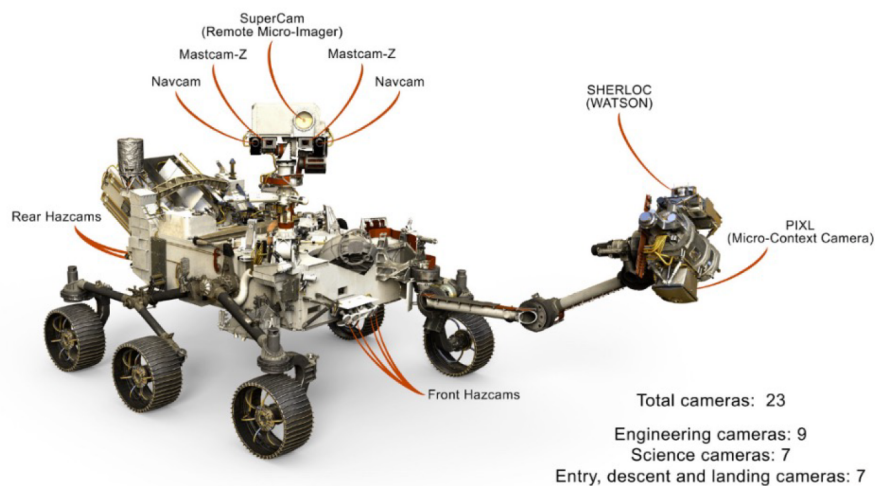


Figure 4.7: Perseverance and its cameras [42]

As can be seen in Figure 4.7, Perseverance has a total of 23 cameras for taking pictures and for orientation on Mars surface. Nineteen of them are located directly on the rover, three on the back shell, and one on the descent stage. There is also a lot of other scientific equipment for various purposes. In addition to its robot arm, it is also equipped with numerous sensors and detectors to examine every movement in the best possible way. [42, 37]

Ingenuity

The remarkable thing about this mission is that the Mars rover is hosted by a helicopter for the first time. This helicopter is called Ingenuity (Figure 4.8). Aside from its exploration mission, it is mainly used to plan the best route for the Mars rovers.

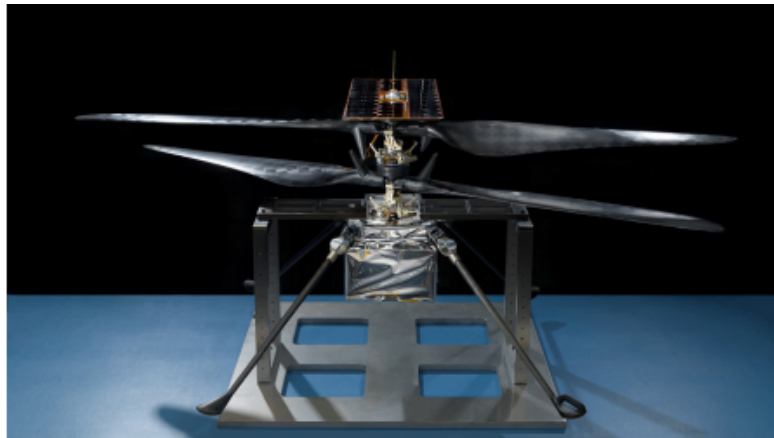


Figure 4.8: Ingenuity [42]

Ingenuity weighs 1.8 kg, is 0.49 m high and the span of its two pairs of rotors is 1.2 m. It is equipped with two different cameras, and it gets its energy from a solar panel that charges lithium-ion batteries. With this power supply, it can fly 90 s per Martian day. [42]

4.2 NASA Rassar

The Regolith Advanced Surface Systems Operations Robot (RASSOR) Excavator is a robot, which should be used on the Moon to mine and transport regolith. It consists of four drums (Figure 4.9), which take up and store the regolith until it is dropped out at the unloading point. The mining takes place by rotating the drum in one direction and the discharge by changing the direction of the rotation. Therefore four drums are used so that the forces cancel each other out as good as possible. [41, 48, 59]



Figure 4.9: NASA Rassar [48]

The RASSOR should meet the following requirements:

- Mining of 700 kg regolith in 24 h
- Equipped with a camera
- Recharging its batteries at the lander
- Lifespan of minimum 5 years
- Ability to improve itself

[41]

The expected weight of the RASSOR will be about 100 lb which ensures 45 kg. But this low weight is also problematic because if the robot is lighter, the excavation process is more difficult. This is because the drums can not be pressed into the regolith with relatively high forces; the robot would lift itself while digging.

The robot is currently still in the planning phase; a start date is not known yet. [59]

5 Transportation Systems

In this chapter, lunar landers are described, which would be able to transport the mining and conveying unit to the Moon. Before the transportation from the Earth to the Moon starts, the mining and conveying unit is housed in the lunar lander until its arrival on the lunar surface. The whole lunar lander is a part of the launch vehicle. For illustration, the lunar lander of the mission Apollo 11 “Eagle” was placed in the tip of the rocket Saturn V. Launch vehicles consist of several stages; the majority of launch vehicles have three stages. After a certain amount of time after launch, the first stage gets disconnected from the rest of the vehicle. The other stages also disconnect from the vehicle until the lunar lander is close to the Moon. The remaining distance is covered by the lunar lander itself – until arrival at the lunar surface.

Commercial rocket launch companies are developing rapidly. Nowadays, there are already about 100 companies working on solutions for rocket launches, such as SpaceX or United Launch Alliance (ULA), a joint venture of Boeing Defense, Space and Security (BDS), and Lockheed Martin Space Systems. As an example, Figure 5.1 shows the rocket Vulcan Centaur, which is developed from ULA. The first launch of Vulcan Centaur is planned for June 2021. Soon, rocket launches are going to be different from them today: There will be launch providers with reusable first stage engine compartments, reusable first stages, and completely reusable two-stage launch vehicles. [14]

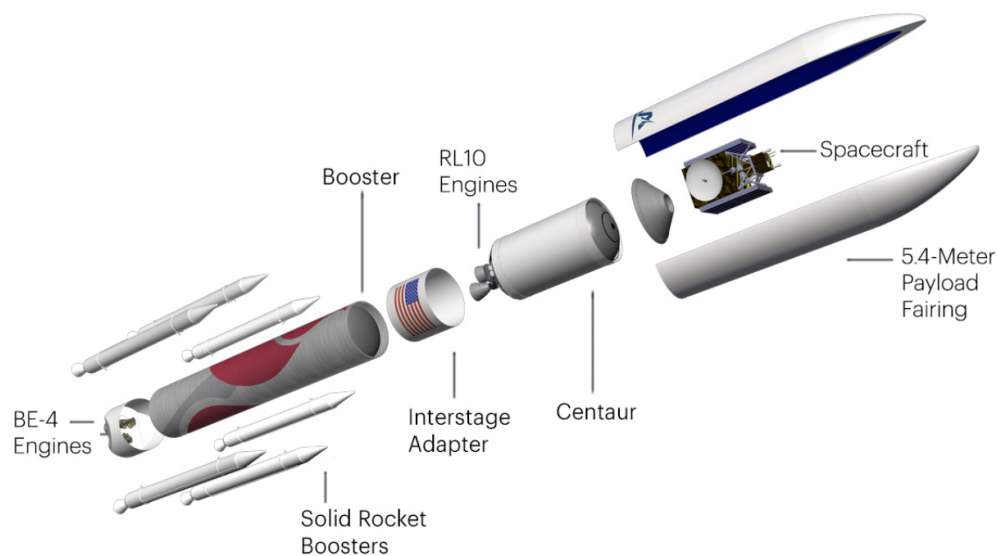


Figure 5.1: Vulcan Centaur [66]

5.1 European Large Logistics Lander (EL3)

The European Large Logistics Lander, which is shown in Figure 5.2, is a project of the European Space Agency (ESA). At this time, the EL3 is in an intensive study and development phase. If the project proves, it becomes a complete space project [18]

Although EL3 is not yet a full-fledged project, it is important for Europe to take part as an essential organization in various research topics related to the Moon. In particular, the goal of the Artemis program, which is a collaboration of ESA, the US government and NASA, is to bring people to the Moon in 2024, including the first woman ever.

As the name suggests, it is a lunar lander that is mainly developed to transport cargo. First, two payload options were approved: delivering logistics to support human expeditions on the lunar surface; and second, autonomous science missions without humans on board to return samples from the lunar soil. For the future, certain missions should be combined, like technology demonstration and cargo delivery. One main goal is to have a wide variety of mission, which can be done by EL3. Furthermore, EL3 is designed to survive the lunar night. [18]

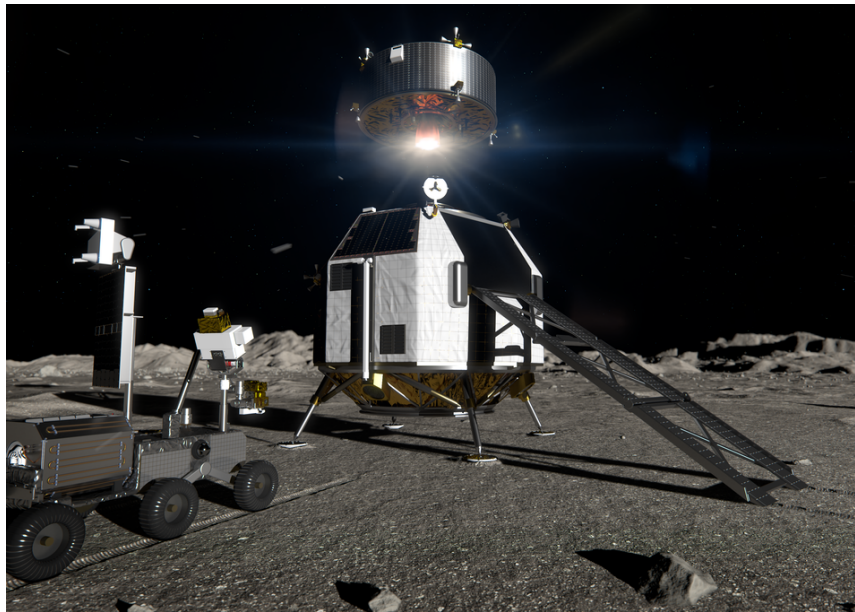


Figure 5.2: European Large Logistics Lander [18]

In the following, the essential properties of EL3 are listed [18]:

- Size: 4.5m in diameter, up to 6m tall
- Mass on Earth: 8500kg
- Mass of delivered cargo: 1500kg
- Mission types: cargo, science rover, in-situ resources, and more
- Launcher: Ariane 64
- Launch Site: Kourou, French Guiana

5.2 NASA Lunar Lander

The NASA Lunar Lander (Figure 5.3) is a pallet concept to transport mainly robotic mobility systems, like rovers, to the lunar surface. The design is not complete and several subassemblies are at different levels of development.[34]

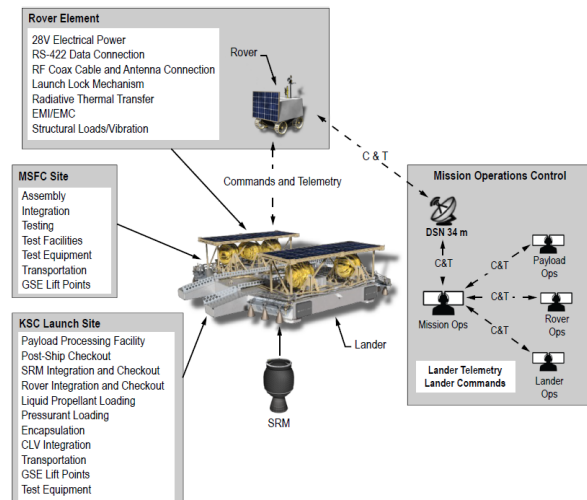


Figure 5.3: NASA Lunar Lander [34]

This lander will deliver medium-sized payloads, up to 300 kg, to the polar regions of the Moon. Shortly after the landing, power will be provided to the payload by the lunar lander. Additionally, this lunar lander is not able to survive the lunar night. One essential target in the development amongst others was to design a lander that is simple and affordable. So the requirements were set to a minimum. In other words, the main parameters risk, mass, and performance were weighed lower than cost. [34]

5.3 Peregrine

Peregrine is a lunar lander from the company Astrobotic. In general, Astrobotic is a company, which works in the field of lunar logistics and provides delivery services from the Earth to the Moon. Figure 5.4 shows the lunar lander. [3]

The maximum payload delivery capacity is 100 kg. Peregrine is designed for a surface mission duration of 192 h. Almost every kind of payload is able to get to the lunar surface with Peregrine. 1 W power and 10 kbps bandwidth per kilogram is provided



Figure 5.4: Peregrine [3]

for the payload by this lunar lander. From the lunar poles to the lunar equator – Peregrine can bring payloads to several locations on the Moon. Like the NASA lunar lander, Peregrine flies the missions autonomously, in other words, without humans on board. [3]

Astrorobotic already offers commercial cargo flights to the lunar orbit and lunar surface for various institutions, for instance, governments, companies, individuals, and universities. Transportation of the payload to the lunar orbit costs \$300,000 per kilogram, delivery to the lunar surface \$1,200,000 per kilogram. In addition, for mobility on the lunar surface, every customer can book a delivery rover, which transports a certain payload to the target location. [3]

5.4 Starship

Starship is a spacecraft system of the company SpaceX, which was founded by Elon Musk. It is a two-stage vehicle, composed of the "Super Heavy" rocket as the launch vehicle and the spacecraft called Starship. The whole system is a completely reusable delivery system for missions to the Moon and Mars as well as for Earth orbit delivery

missions. As shown in Figure 5.5, both types of missions, crewed and uncrewed, are possible with the different configuration types of the Starship. [62]

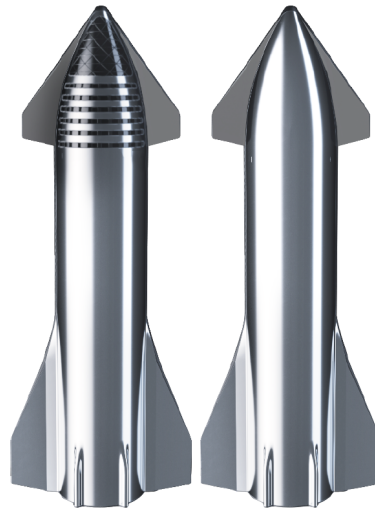


Figure 5.5: Crew configuration (left) and uncrewed configuration (right) [62]

Starship can do a wide variety of transportation missions without humans in the spacecraft. It has the ability to deliver satellites, cargo, large observatories, refueling tanks, and many more. This spacecraft has the capability to transport more than 100 t of cargo to the Moon and Mars fully autonomously. Additionally, this system is available to transport cargo from one location on Earth to another location on Earth very quickly. Figure 5.6 illustrates the dimensions of the Starship payload volume. [62]

Moreover, another target of the Starship design, among others, is to make life multi-planetary. So, the crew configuration of the Starship can transport up to 100 people from Earth to the Moon and Mars. [62]

According to SpaceX vice president of commercial sales, Jonathan Hofeller, launching satellites by 2021 is the firm's goal. There are two launch sites: Kennedy Space Center, and Boca Chica launch pad. [62, 38]

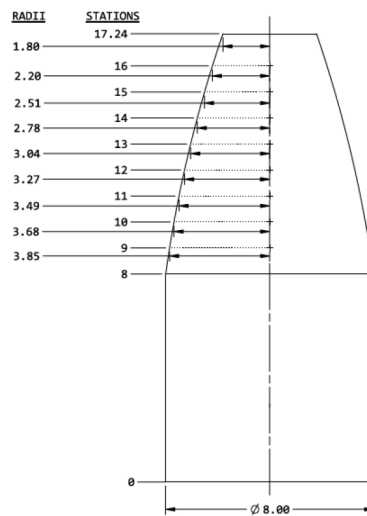


Figure 5.6: Starship payload volume [62]

5.5 Blue Moon

Blue Moon (Figure 5.7) is a lander from the company Blue Origin. The founder of Blue Origin is Jeff Bezos, who also founded Amazon. This lunar lander also has two configurations: as a fully autonomous cargo lander and as a human landing system. Blue Moon can be launched with multiple launch vehicles, for instance, Blue Origin's New Glenn, or the Vulcan Centaur from the company ULA. [8]

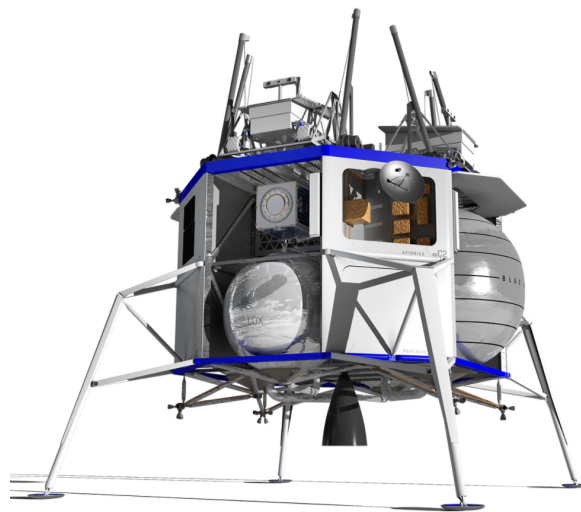


Figure 5.7: Blue Moon [8]



This lander has a 23 ft (about 7 m) payload bay, which provides much space for the cargo. The bay stays about 4 m above the ground on the four landing legs. Blue Moon weighs about 16.5 t in total, with the maximum amount of fuel and cargo. It is possible to load about 4.5 t of payload into the lander. [22]

Furthermore, Blue Moon is capable of conducting different types of missions, such as science, in-situ resource utilization, and infrastructure development missions. The unloading system of the lunar lander uses a crane to drop off certain payloads. This davit system is able to drop up to four lunar rovers onto the lunar surface simultaneously. Also, cargo missions with the Blue Moon lander will be available for different institutions, like universities, government, and commercial customers. [8, 22]

6 Design Materials

In this chapter, the requirements for the design materials, and which materials are suitable for the excavation and conveying system, are discussed.

The harsh lunar environment leads to a variety of requirements for the design materials. The following essential factors lead to large differences in material requirements between terrestrial and lunar applications:

- Temperature
- Radiation
- Atmosphere and Pressure
- Meteorites
- Gravity
- The length of the lunar day
- Dust
- Electromagnetism

Especially the points Pressure, Temperature, and Electromagnetism are essential in terms of mechanical equipment/materials. [29]

The low pressure on the Moon leads to outgassing effects in the design materials. Outgassing is the release of molecules into a vacuum, which were closed on or in a material. Outgassing can occur in different types of mechanisms: desorption, evaporation, and diffusion. This (in this particular case) negative process often appears



with polymeric materials. As a result, outgassing cause structure distortion, change in properties, loss of dimension stability, loss of mass, and surface contamination. On the Apollo 8 mission, for example, the silicone rubber seals of the observation window were outgassed during the first lunar orbital flight. Subsequently, the large window was contaminated, and the astronauts couldn't take pictures and videos from this window and had to use another one. [2, 17, 31]

Another important difference among others is the temperature. One lunar day lasts for about 28 Earth days, including about 14 Earth days of lunar night and 14 Earth days of the lunar day. Due to the thin atmosphere and the long days/nights, the temperature has a large variation of approximately 140 K in the equatorial zone of the Moon. Therefore, the design materials for lunar missions must have high thermal resistance. Also, the thermal expansion of the design materials must be taken into account, as the thermal expansion can lead to problems, e.g. with bearings or seals. [29]

If lunar mission objects rove on the lunar surface, charge differences relative to the lunar surface occur. The reason for this is an additional charge source: triboelectric charging. Triboelectric charging appears at the regolith-wheel junction. Atmospheric static discharge is not possible due to the lack of atmosphere. Moreover, dust with an electrostatic charge has a high tendency to adhere to exposed surfaces. For instance, the adhesion of lunar dust could be the reason for a not feasible lunar mission. Dust adhesion to solar panels on the moon can decrease the efficiency of the solar panels. [10, 30]

In table 6.1, some materials, which are possible for lunar applications, are compared. [67]

Aluminium is one of the most commercial structure material in aerospace application. It has a low density relative to steel and low costs in fabrication. Furthermore, there is a large variety of aluminium alloys, so this material has a broad range of essential properties. [67]

Table 6.1: Design materials for lunar applications [67]

Material	Density [kg/dm ³]	Melting Point [°C]	Thermal Expansion [10 ⁻⁶ /K]	Youngs' Modulus [GPa]
Aluminium	2.7	660	23.8	71
Beryllium	1.7	1287	11	293
Titanium	4.5	1668	8.2	108
Steel	7.85	900-1500	11-13	210
CFRP	1.6	-	0.2	140

Although pure beryllium does not fit the requirements of space applications, beryllium-aluminium alloys are some of the rare light metals with a high melting point, relatively high strength, and high ductility. It is used particularly in space and aircraft applications. [60]

Titanium is a high-strength structural material, characterised by good stiffness, lightweight, and high-temperature capabilities. Similar to aluminium, there is a variety of alloys with titanium, so the properties are also different depending on the alloy. Drawbacks are the high costs and difficulties to manufacture, especially welding. [67]

Steel is the material with the broadest range of applications in all areas of technology. Specific alloys, such as stainless steel, which are appropriate for lunar missions, are also possible for lunar systems.

Carbon fibre reinforced plastic (CFRP) is also appropriate for lunar missions. It has high strength and high stiffness with the graphite fibres. In addition, it is a lightweight material. The properties, especially stiffness and strength, are depending on the direction of the fibres. The main disadvantages are outgassing and complicated manufacturing. [69]

7 Task Definition and Boundary Conditions

In this chapter, the task and the boundary conditions are defined. Some of the boundary conditions are considered rather as a recommendation or as an additional (nice-to-have) aspect, since especially the maximum weight can only be achieved by ultralight construction.

7.1 Task

The task of this thesis is to concept and design an excavation concept for the application on the Moon, from its mechanical side. Regolith is set as the material to be mined/excavated. In addition to the already conducted research, work should include the areas of conceptual development and design, specifically regarding mechanical system setup, which can also be supported by numerical simulation for the material handling aspect.

It is set to elaborate a wide variety of concepts and then compare functions with advantages and disadvantages. After the concept selection, a simulation of the functional principle should be carried out if necessary. Finally, the selected concept must be graphically prepared. Concerning the design, it should be noted that only components that are important for major operational tasks need to be detailed. The maximum



dimensions and the maximum total weight are defined in the boundary conditions. The excavator should also be able to interact with the conveyor system, of the mentioned second thesis, in the future. Due to that, some kind of transmission system should be integrated.

7.2 Boundary Conditions

Initially, the maximum dimensions and weight of the system are specified. In chapter 5, several lunar landers, which can deliver both units to the lunar surface, are described. These transportation systems are either built by commercial companies (i.e. Blue Moon, SpaceX) or space agencies, such as NASA or ESA. Although there are only a few lunar landers offering a delivery service to the moon compared to terrestrial delivery services, there is a wide variety of maximum weights and maximum dimensions of the payload compartment of the transporters. To illustrate, SpaceX's Starship will deliver a maximum weight of about 100 t, whereas the maximum payload delivery capacity of Astrobotic's Peregrine is 100 kg. After studying various lunar landers in Chapter 5, ESA's European Large Logistics Lander (EL3) is defined as the delivery unit for the two systems. EL3 has a maximum payload capacity of 1.5 t. The maximum weight of the excavation- and conveying system is respectively about 750 kg, or 1.5 t in total, so both systems can be transported to the moon simultaneously. The maximum dimensions of each system are 6 m in length, 4 m in width, and 2 m in height.

Furthermore, the volume flow rate is also defined. The first step is the search for the annually required oxygen mass. About 10,000 kg of oxygen is needed for initial human lunar missions. Additionally, the same amount of oxygen is required for two launches from the lunar surface. Assuming the least efficient oxygen extraction method, a volume of 660 m³ is required, which corresponds to an area with the size of 8,250 m² (about one soccer field) excavated 8 cm deep. As a result, the mining target is set to 2 m³ per Earth day (equals 0.083 m³/h). [56, 57]

8 Excavation Concepts

The excavation of regolith is the first important step in the ISRU chain. This is because the envisaged processes require a large amount of lunar surface material to be gathered. There are several different ways to carry out the excavation, and these are discussed in this chapter. The selection is made by comparing the advantages and disadvantages of individual concepts.

8.1 Problems

However, due to the environmental conditions on the Moon, the excavation process poses some problems. These mainly concern low gravity, soft surface, high cohesion, sharp grain shape, and temperature variations by day and night.

The low gravitation leads to the fact that mining processes, which mainly use their high own weight, are not as easy to realize on the Moon as on Earth. Because of the lower gravitation (about $1/6$), the pressing of a blade into the surface is not easily possible or at least not very effective. If looking on a backhoe-loader, for example, it would rather lift itself off the ground than dig into the ground. And it is not a suitable solution to just make the machine six times heavier, due to the high transport costs and also the high mass to move consequently. A compromise with the final weight of the excavator is needed.



Also, driving on the surfaces is not as easy as expected. As mentioned in Section 2.3, the regolith covers most of the lunar surface. This powdery material results in a soft Moon ground and, as a consequence, in the sinking of wheels or chains. This sinking in is a few centimetres deep, which, in turn, increases the required drive power and furthermore the wear.

High cohesion can lead to clumping of the material. Depending on the application, this can be seen as a proximal and a distal part, but for excavation, this usually is not beneficial. It should therefore be noted that constrictions due to the risk of clogging are avoided. If this is not possible, systems or actuators have to be planned to remove the blockage.

As already mentioned, there are agglutinates in the regolith. These agglutinates have sharp grain shapes, and this significantly increases wear and tear. For this reason, machine parts that are regularly in engagement must be designed to be as wear-resistant as possible. Remedial measures are the use of materials, which are harder than the agglutinates and a higher wall thickness to prevent breakage.

With the high-temperature fluctuations, the demands on the used material also increase. They must be able to withstand the maxima of around 200°C as well as function smoothly at the minimas down to -150°C. These temperatures also have a great influence on the control units. If it is not possible to use them in the deep minus range, it is planned to operate only during the day and heat the sensitive components at night.

The maintenance is also a big problem for machines on the Moon, because it is not that easy to carry out repairs or replace wearing parts as on Earth. The structures should therefore be kept as simple as possible because more moving/interacting parts means more sources of error and thus probably require maintenance.

So it can be recognized that some influences have to be considered, which are not known on Earth. Thus the majority of the mining units on Earth, do not apply to the Moon as they are. [58, 26]

8.2 Functional Principles

Before discussing the different concepts, first, a closer look at various functional principles should be taken. There is a wide range of possible functions (Figure 8.1), which one would perhaps not consider for use on the Moon.

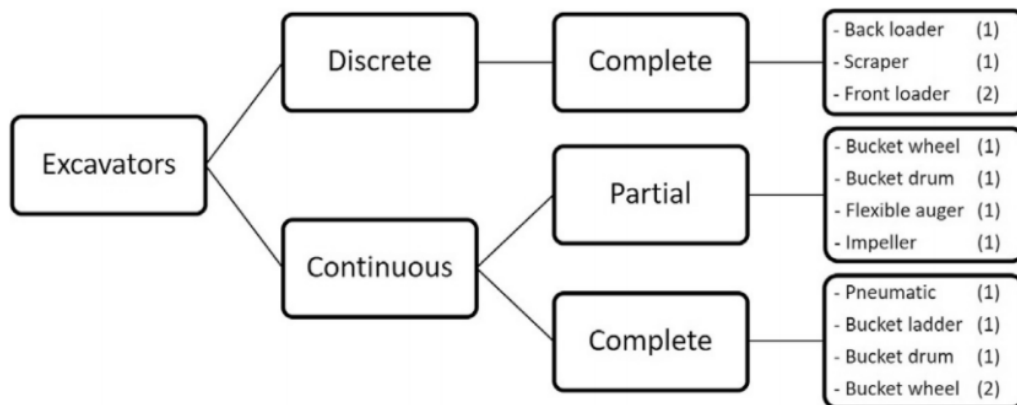


Figure 8.1: Functional principles [32]

There can be a differentiation made between discrete and continuous concepts. The discrete functionals may have a lower mass flow rate, but may show less wear and tear. This is because continuous functionals have more frequent contact with the material. It is important to mention, that some of these principles are normally used for conveying on Earth, but with some modifications, it is possible to use them for excavation. Conveyors are only used for the transport of the material, while mining

On the following pages, these functional principles are described. There are also some possible pros and cons of using this principles for the lunar excavation process. Also, the possibility of the implementation on the Moon is explicitly considered. These advantages, disadvantages, and possibilities of implementation are established and evaluated referring to the research. [32]

8.2.1 Back-loader / Front-loader

Function

A backhoe loader is usually the combination of three different machines, a tractor, a loader, and a backhoe (Figure 8.2). The tractor part is not of interest for this thesis, so will not mention in more detail. The loader part is located at the front and the backhoe in the back. They use their shovels to dig out material. The contact pressure is generated by the high dead weight. The backhoe consists of three segments, which are named boom, stick, and bucket. There are three joints for the connection of these parts. With these joints, the backhoe is flexible similar to a human arm. These movements are mostly carried out by a hydraulic system. [27]



Figure 8.2: Backhoe loader [9]

Advantages

- few moving components
- robust



Disadvantages

- high weight required
- discontinuous mining
- low mass flow rate
- hydraulic critical because of tightness

Possibility of implementation

As already mentioned, to use this variant efficiently, the machine must have a high dead weight. A higher transport weight is not possible, so it could be considered to design the loader with a kind of empty tank. This tank can then be filled with regolith by itself, and this will significantly increase its weight. However, a compromise would have to be made with the sinking depth and resulting effects such as on the wheels.

8.2.2 Scraper

Function

The most important components of the scraper are the deflection roller, the drive roller, the drive chain, and the scraper plates (Figure 8.3). With its sharp blades, the scraper can easily graze material from the surface and then pushes it in front of itself until its endpoint is reached. There, the material is dammed up and is ready for further use. Because it uses several plates, the wear is better distributed and the longevity of the installation is increased. [51]

Advantages

- lower weight needed
- robust
- resistant to temperature fluctuations

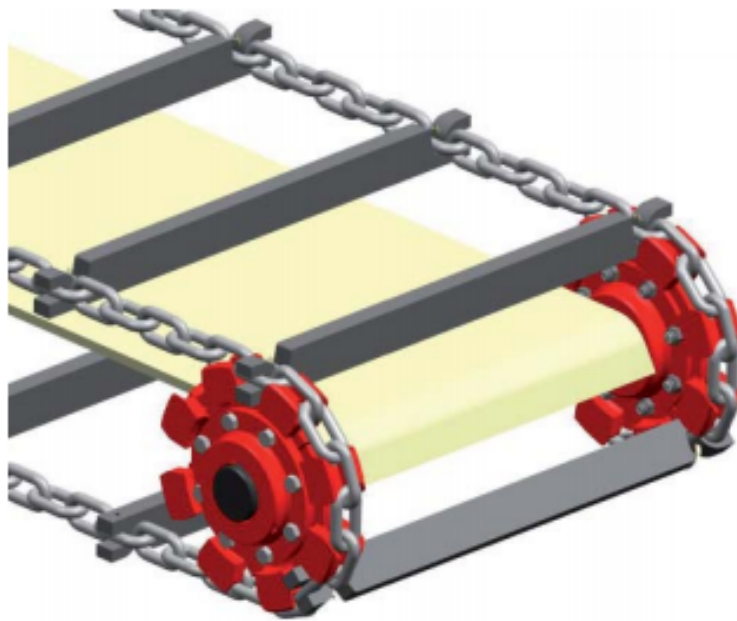


Figure 8.3: Scraper [53]

Disadvantages

- high energy requirement
- separate collecting system necessary
- only surface mining

Possibility of implementation

Using two or four scraper booms, which transport the material into the center of the robot. There is a conveyor unit that picks the regolith up and carries the material to further use. These booms are rotatably mounted to achieve the largest possible excavation area.

8.2.3 Bucket-wheel

Function

This operating principle is used on Earth mainly for coal mining. The bucket wheel excavator is a giant plant, which scrapes the material from the surface by the front bucket wheel (Figure 8.4). The material is emptied by gravity into the inside of the wheel when it reaches its highest point. This causes the material to fall onto a belt conveyor and get transported away. [7]



Figure 8.4: Bucket-wheel excavator for coal mining [55]

Advantages

- continuous mining
- high mass flow rate possible

Disadvantages

- critical at low gravity
- high wear
- selective mining



Figure 8.5: Lunar excavator by the Colorado School of Mines [15]



Figure 8.6: Bucket-wheel excavator with a bucket wheel in the middle [32]

Possibility of implementation

Some have already tried to implement this principle for use on the Moon; two different approaches were considered. On the one hand, the function of a bucket-wheel excavator which is mentioned above (Figure 8.5), and on the other hand, the use of a wheel in the middle of the robot (Figure 8.6). With both alternatives, the material must be delivered through the bucket wheel into the centre and due to the poor flow properties of the regolith, problems could arise. [15]

8.2.4 Bucket Drum

Function

The bucket drum should be used to excavate material and store it inside. When the drum has been filled to its maximum filling level, the entire machine must return to the discharge point to unload the material. When the drum is empty, it returns to the mining point. So machines that are equipped with a bucket drum are both: a mining and a conveying machine. [41, 48, 59]

Advantages

- continuous mining

Disadvantages

- low mass flow rate
- possible blockage of the drum
- long driving distances, because of mining and conveying

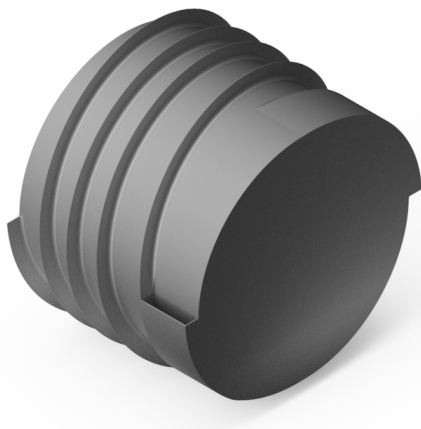


Figure 8.7: Bucket drum concept [50]

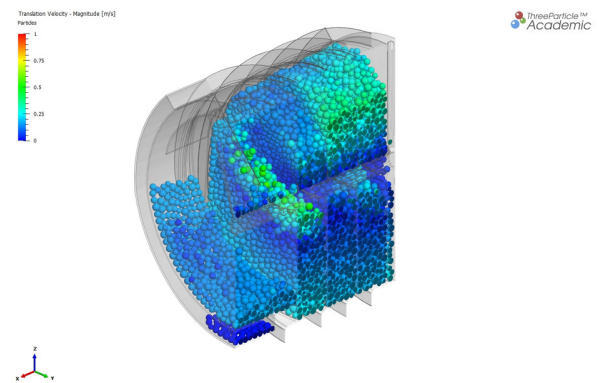


Figure 8.8: Bucket drum DEM simulation [50]

Possibility of implementation

NASA is currently researching such a concept, so it will not be discussed here in detail. An overview of the planned NASA Ressor mission can already be found in Chapter 4.2. In the Figures 8.7 and 8.8 a bucket drum of the mentioned “NASA Bucket Drum Design Challenge” can be seen, including a representation of the DEM simulation.

8.2.5 Flexible or Static Auger

Function

Screws are normally used on Earth to transport material from one point to another. But it is also possible to use them for mining, if they are used to scrap material off the surface. The main component is the screw shaft, with its helically arranged sheet metals. By rotating the shaft, the materials get pushed to one side until it reaches the outlet. This conveyor can be used for both, horizontal and vertical transport. The screw can be designed with or without an axle (Figure 8.9), which can sometimes be an advantage. And of course, there are different possibilities to arrange the screws, as single or multiple applications and flexible or static. [11]



Figure 8.9: Shaftless screw conveyor [11]

Advantages

- simple structure
- continuous mining via surface scrapping

Disadvantages

- high energy requirements
- risk of clogging
- wear
- digging not possible

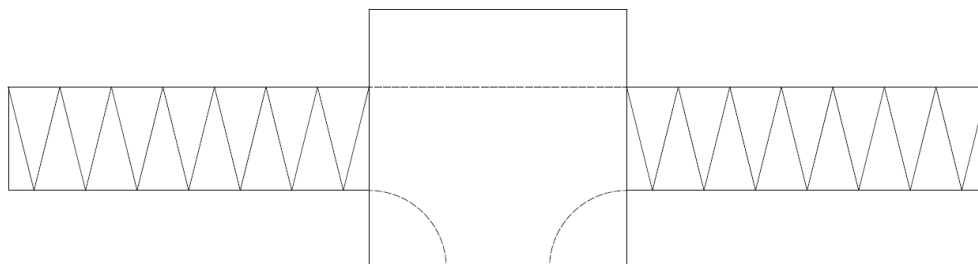


Figure 8.10: Concept bilateral screw conveyor

Possibility of implementation

It would be possible to use two bilateral screws, which are fixed on a rover (Figure 8.10). These screws are adjustable in their height and their angle of rotation. The material gets transported into the centre and is then discharged at the back, but there is the problem, that the screw always is in contact with the regolith; thus wear increases with every rotation.

8.2.6 Impeller

Function

This principles function due to utilization of centrifugal force through high rotational speeds. A blast wheel is driven, and thus, the material is quickly accelerated to high speed. Due to low gravity and the soft surface, there are high litter widths possible,

and the material could easily be steered to the further conveying system. But this implementation is problematic regarding wear for the wheel blades, because of the high rotational speed, and also for the diverting shore.

Advantages

- simple structure
- continuous mining

Disadvantages

- high rotational speed
 - wear
 - problems with harder spots
- only for the surface
- higher dust generation

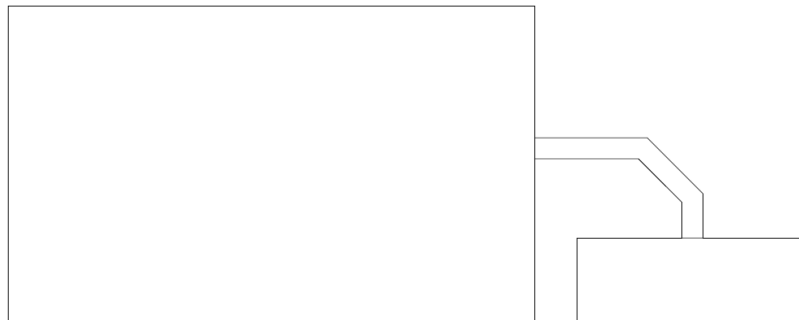


Figure 8.11: Sweeper concept for dismantling regolith

Possibility of implementation

It would be possible to use the concept of a sweeper (Figure 8.11) by using two brush heads or paddle wheels. The two wheels rotate in opposite directions and the material is thrown through the middle of the two wheels towards the robot. There the material is picked up for further use.

8.2.7 Pneumatic

Function

Pneumatic excavators normally use air to transport material. This method can typically be applied to transport materials with low density. An important parameter for the function is the flow velocity of the air; in general, it must be higher than the velocity of the material that is moved. The material is transported through a mostly tubular container. There are three different variants for the implementation of a pneumatic conveyor, the vacuum conveyor, the pressure conveyor, and a combination of both (Figure 8.12). [21]

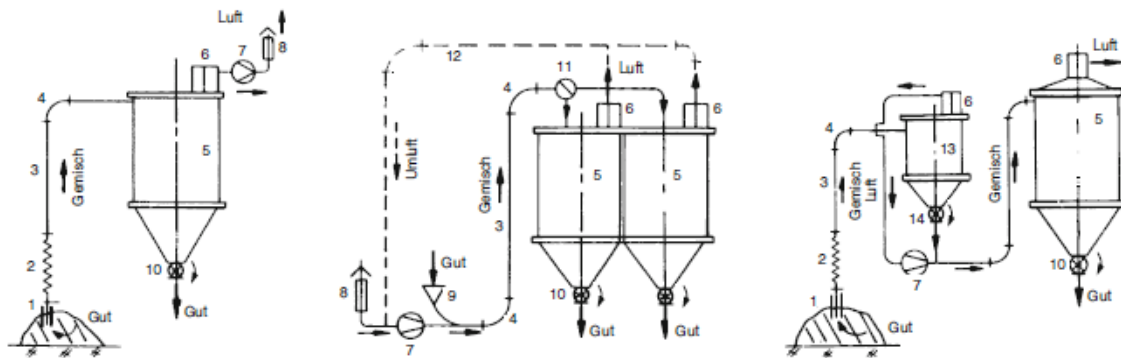


Figure 8.12: Types of pneumatic systems: vacuum conveyor (left), pressure conveyor (right) and the combination (right) [21]

Advantages

- no moving parts (except air flow generators, etc.)
- continuous process
- lower energy needed

Disadvantages

- difficult to implement
- transportation gas or fluid needed
 - tightness
- no actual mining, only collecting

Possibility of implementation

There is a big potential by using pneumatic conveyors for dismantling processes on the Moon. The structure reminds of a vacuum cleaner. But the biggest difference results from the thin atmosphere. Due to that, no air can be used as transport gas; the drag forces are low. Therefore, an alternative in the form of another gas or liquid must be found. That is a big problem for this concept, because the carrier medium would have to be filled into the machine on Earth, and if the medium escapes due to a leak, the excavator would not work anymore. Also, there is the need for a gate to get the material in and out of this flow/stream medium.

8.2.8 Bucket Ladder

Function

A bucket elevator consists of an endless loop of cups arranged one behind the other (Figure 8.13). They are typically used for conveying above an angle of inclination of about 70° . The pendulum bucket ladder is a special design form, allowing lower and even horizontal bucket conveying. [21]



Figure 8.13: Bucket elevator [20]

Advantages

- continuous mining
- high mass flow rate
- large area removal
- lower dust generation
- robust

Disadvantages

- higher weight
- shock loads
- risk of clogging

Possibility of implementation

The implementation can be similar to the scraper, where a boom is used to move regolith towards the centre of the robot. However, the big difference is that the bucket ladder does not require a separate collection system because of the buckets. An example

of this construction is a bucket chain excavator, which can be seen in Figure 8.14. It is also possible to use a concept with a bridge connection between two mobile robot carriages. In any case, the bucket ladder is used as a scrapping system in horizontal form for both variants.



Figure 8.14: Bucket chain excavator [54]

8.2.9 Selection of the functional Concept

British scientists have already conducted experiments for these functional principles. Table 8.1 shows an extract of their results. For the selection of a suitable system, mass flow and penetration depth from these previous researches are considered, as well as the mentioned advantages and disadvantages of this chapter.

Although the different systems may not have been tested under the same conditions, there are clear differences. Of course, it has to be kept in mind that certain variants are probably already better optimised/developed than others.

Because of the importance of a high mass flow rate for mining regolith, only three functional principles make it onto the shortlist. These are the scraper, the bucket wheel, and the bucket ladder principle. With the bucket wheel, it is only possible to remove a very narrow area. A larger excavation area and, therefore, a smaller mining depth would



Table 8.1: Mass flow & depth of different functional concepts [32]

Process	Mass flow [kg/h]	Maximum depth of excavation [cm]
Backhoe	100	100
Scraper	900	-
Bucket-wheel	180-1050	5
Bucket drum	90 kg per trip	-
Flexible auger	50	Not applicable
Impeller	6-30	-
Pneumatic	6	Not applicable
Bucket ladder	800-2400	10-15

be better because it is easier to mine the superficial regolith. The bucket chain excavator could be implemented with a function that is quite similar to that of the scraper, but with the advantage that there is no separate receiving system required. Therefore, a bucket chain excavator is selected here as more promising than the others.

8.3 Detailed Concepts

The possible implementations of this functional principle were already mentioned in Section 8.2.8, the bridge version, and the boom version. In this chapter, these concepts are now considered more closely and decisions are made. There is also some basic information about bucket elevators that are used on Earth for clarification.

8.3.1 Basic Informations

Before the concepts are considered in detail, the general function and special features of the bucket elevator are described. This information refers to a bucket ladder that is in operation on Earth.

As already mentioned, bucket ladders are normally used for vertical conveying. There is an image of such an implementation in Figure 8.15.

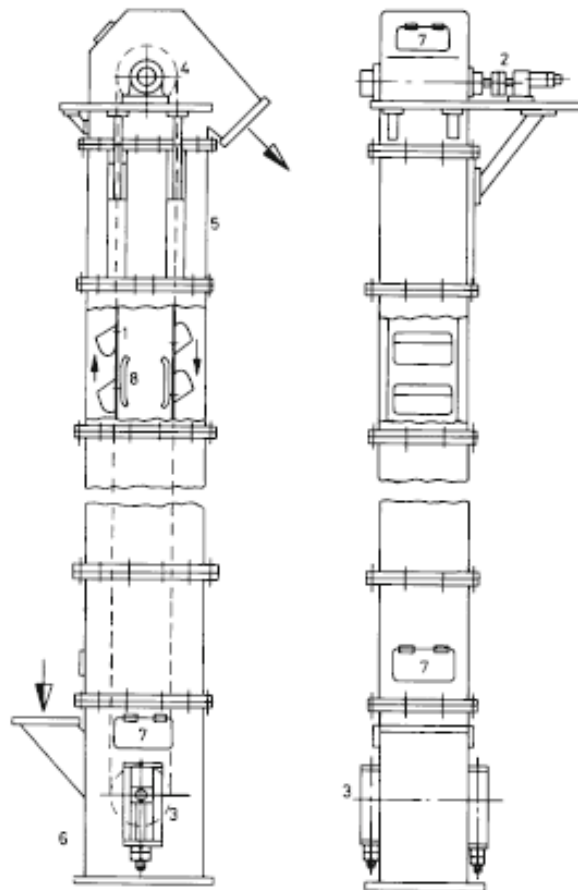


Figure 8.15: Vertical bucket ladder [21]

As indicated by the arrow, the bulk material is fed into the system through the chute (6). The buckets (1) are attached to an appropriate pulling device, which is held in position by guides (8). The bucket elevator is driven by a motor (2), which here drives the upper

deflection drum. The upper arrow describes the dropping direction, the discharge (4) will be described later in more detail. The entire plant is covered by an enclosure (5), which is equipped with maintenance flaps (7). A very important component is the clamping station (3), their tensioning allows operation. [21]

Technical data

Bucket elevators on Earth can convey bulk material with a mass flow up to 400 t/h, to a height of about 60 m, with a velocity from 0.3-3 m/s. Typical buckets have a volume up to 140 dm³ and a maximum width of 1250 mm. There are also many specific solutions possible. It should also be noted that the buckets are typically partially filled with bulk material. The degree of filling depends on the grain size and the conveying velocity and is normally between 0.4 and 0.88. The form and the material of the buckets depend on their application. [21]

Discharge

There are normally two different methods of discharging a bucket of a bucket elevator: the centrifugal discharge and the gravity discharge (Figure 8.16). [21]

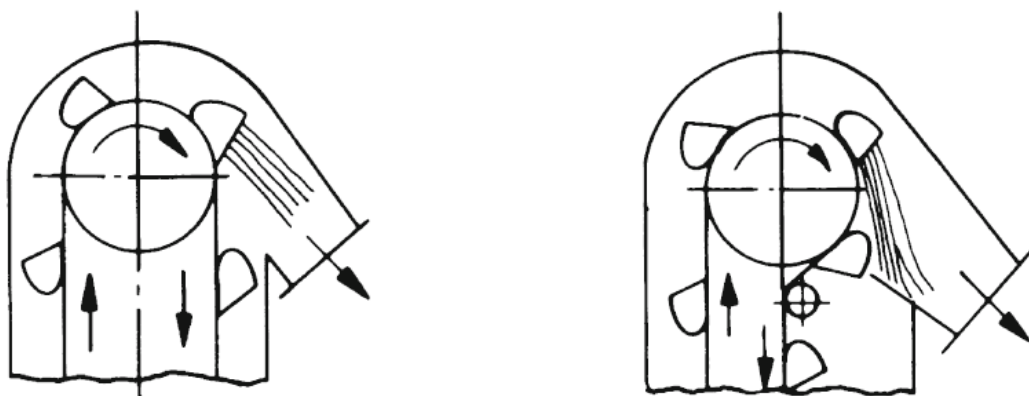


Figure 8.16: Methods of discharging a bucket, centrifugal discharge (left), gravity discharge (right) [21]

Both methods can use the same components, the only difference is the bucket speed. A high velocity in combination with direction change ensures that the material is ejected from the cup. With gravity discharge, a slower speed is used, thus the material moves from the bucket in the discharge chute by gravitational forces. [21]

This transition can be determined by further formulas. The basis for this calculation is the occurring forces, which can be seen in Figure 8.17.

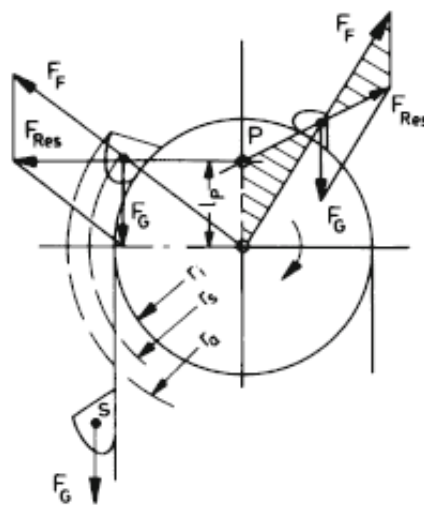


Figure 8.17: Forces of a bucket ladder at the discharge [21]

As can be seen, the weight force (F_g) and the centrifugal force (F_f) are decisive factors. The weight force is described by mass (m) multiplied with gravitational acceleration (g). [21]

$$F_g = m * g \quad (8.1)$$

For the centrifugal force, the angular velocity (ω), mass (m), and the deflection radius (r_s) are important. [21]

$$F_f = m * \omega^2 * r_s \quad (8.2)$$

While comparing these two forces, it is evident, that the mass does not influence the method of emptying. [21]

$$\frac{F_g}{F_f} = \frac{m * g}{m * \omega^2 * r_s} = \frac{g}{\omega^2 * r_s} \quad (8.3)$$

Now a further parameter is introduced into the calculation, namely the pole distance. These results form the formula above and serve as a comparative measure for the type of discharge. The pole distance describes the distance of the pole point from the centre axis. [21]

$$l_p = \frac{g}{\omega^2} \quad (8.4)$$

The following conditions apply for the type of unloading:

- $l_p < r_i$: centrifugal discharge
- $l_p > r_a$: gravitational discharge

For the area between r_i and r_a there is a mixture of these two types. [21]

Pulling device and bucket fixing

There are different types of traction devices, which are used in bucket elevators. There are belt conveyors, round steel chains, and rubber chains. The selection of the appropriate tensile member may differ depending on the application. Criteria for this are mechanical and thermal stress, type of bulk material, and planned lifetime. [51]



Figure 8.18: Different principles of bucket attachment [28]

Generally, three different principles are used for the cup attachment. The chain bow, the plug driver, and the screw connection (Figure 8.18). Especially for the latter, there are several possibilities, such as fastening with a segmental screw or rubber-bonded metal. A distinction is made depending on the application; the selection mainly concerns the attachment on the side of the bucket or the back. [21, 51]

8.3.2 Boom

Function

The concept with the boom (Figure 8.19) has two to four cantilever bucket chains. These bucket ladders pick up the material and transport it to the centre of the machine. After the discharge, there is a separate conveying system, which takes the regolith to further processes. The outriggers are adjustable in height as well as in their direction of rotation. While the excavation process with four booms, the machine stands still.

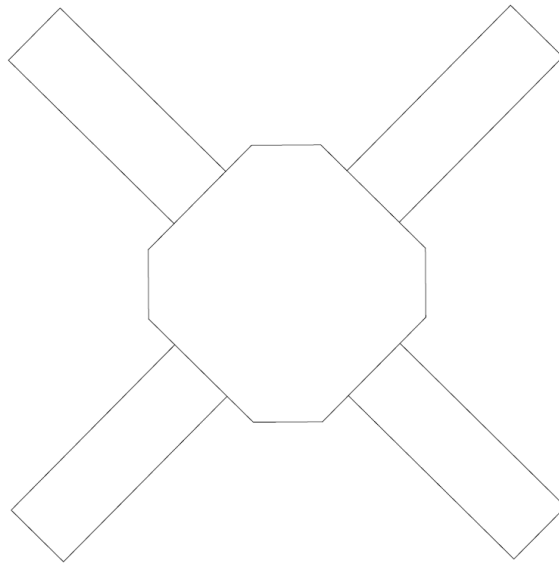


Figure 8.19: Concept bucket ladder with boom

Excavation area

The mining area varies depending on the number of booms. With four booms the area will be almost circular, as on the left side of Figure 8.20. With two booms it will look like a slotted hole (in the middle). A full rectangular mining area with ideal space utilisation cannot be achieved with this concept, because there will always be a not excavated field between the two booms (right side), where the robot drives.

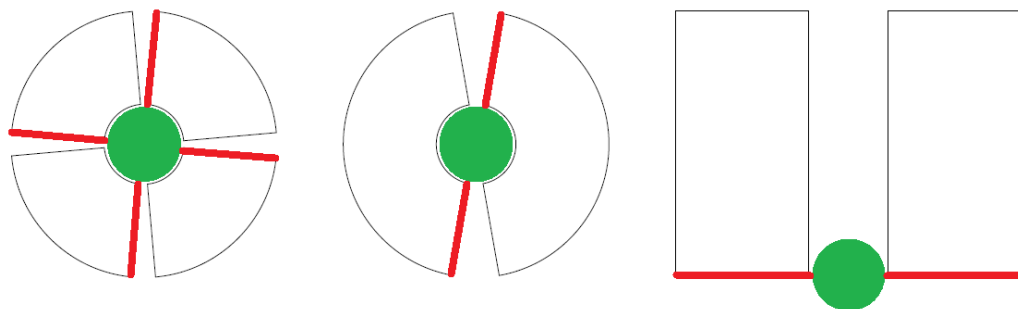


Figure 8.20: Excavation area boom concept: circular (with four booms), slotted hole and two rectangular areas (both with two booms)

Advantages

- adjustable height
- adjustable rotation position
- high mass flow rate

Disadvantages

- higher dead weight because of two/four independent systems
- small excavation area
- difficult combination with conveyor system

8.3.3 Bridge

Function

A bridge is used to connect two chassis (Figure 8.21). The bucket chain, which is responsible for the material removal, runs on this bridge. The bridge consists of three segments hinged together. The material is discharged at one end of the bridge. How the material would be dropped will have to be clarified later.

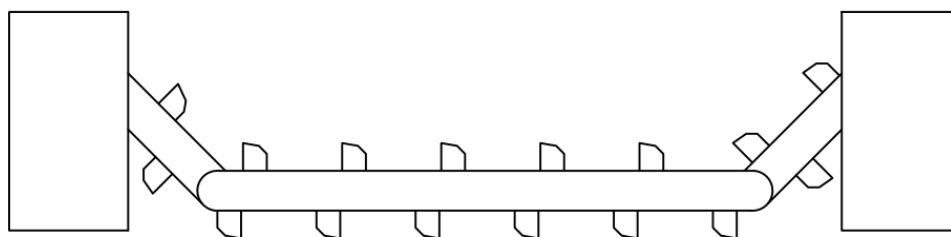


Figure 8.21: Concept bucket ladder with bridge [26]

The two outer segments can be individually adjusted in height (Figure 8.22). This allows the middle segment, where the mining takes place, to be set at different angles, and

the mining depth can be also regulated. Thus, the mining of uneven surfaces can be realized.

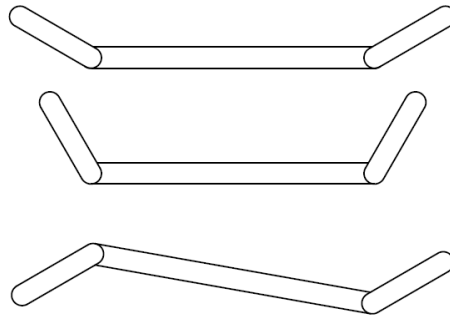


Figure 8.22: Variation of the middle segment

Excavation area

There are two different ways to mine material with this concept (Figure 8.23). In one case, one robot stands still and the other moves 180 degrees around the stationary one. This results in a semi-circular extraction area (left side of the graphic), with the advantage that the material is always discharged at the same point. This would be a great advantage for many conveyor systems. The second possibility is that both robots move together in the same direction while the bucket chain excavator removes material. In this way, a rectangular mining area (right side) could be achieved and the resources could be ideally utilised.

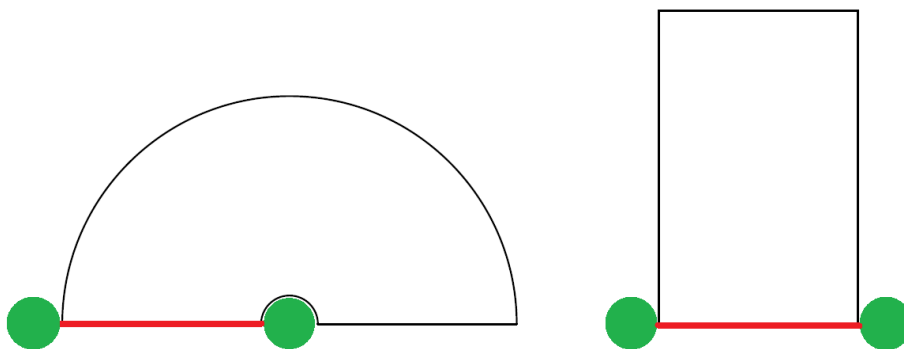


Figure 8.23: Excavation areas bridge [26]

Advantages

- lower dead weight
- better relation mined/unmined surface areas
- adjustable height
- easier combination possibilities with separately attached conveyor system
- lower (and relatively constant) energy needed

Disadvantages

- lower mass flow, because of only one bucket chain

8.3.4 Selection

Both concepts offer great potential and could principally work on the Moon. The decision is made for the bridge variant since the advantages outweigh. Due to the lower dead weight, the bridge can be extended, and the mining area can be increased. Furthermore, the possibility of making better use of the lunar surface was also a decisive reason. The energy supply is always an important aspect of space missions, and the bridge concept also holds benefits in comparison to the boom concept in terms of energy requirements.

9 Simulation

The simulation of the bucket design is used to support the design process. With an improved bucket design, higher mass flow rates are possible, and the characteristics at the discharging can be improved as well. The simulation will be split into three parts. These are:

- Excavation on the surface
- Excavation 60 cm under the surface
- Discharge process

The two different mining processes are necessary due to the different properties of the regolith on the surface and a few centimetres below. But prior to the start of the simulation, there are parameters to calibrate.

This simulation is only for first general comparison of different designs. For a detailed simulation, many more parameters like the grain form must be considered.

9.1 Calibration

Regolith contains low grain size particles. These small particles would require high computing power. Due to this, the small particles are combined into larger ones, which represent the properties of the fine-grained regolith. This process is called coarse graining. A typical simplification that is assumed is the grain shape. While the regolith

has complex forms, a spherical one is used for the simulation. For both material properties, spheres with a diameter of 15 mm are used. Except for these assumptions the solid density and the friction coefficient for internal friction must be calibrated.

9.1.1 Density

First, a cylindrical body is created, which is placed on a flat surface and then filled with particles (Figures 9.1 and 9.2). The used program, ThreeParticle/CAE by BECKER3D [6], enables to export the positions of every particle, in every axis, into a CSV-file. This file can be loaded into the DEM Calibration Tool [25] (Figure 9.3). This tool calculates the volume and fill-level of the specified space. After uploading, the desired bulk density can be entered and the required solid density, that will be used in the simulation, is calculated.



Figure 9.1: Density calibration: cylinder filling

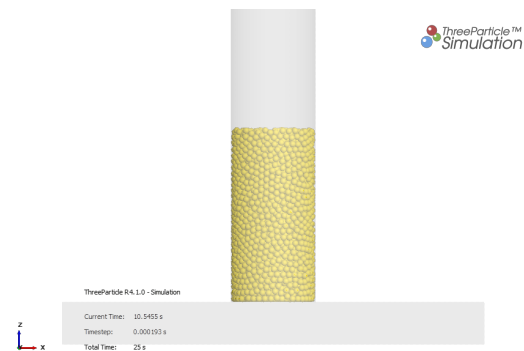


Figure 9.2: Density calibration: full cylinder

In Table 9.1 there are the results of the calibration. As can be seen, there are differences of 340 kg/m^3 at the used bulk density and 524 kg/m^3 at the solid density.

The difference between the solid density and the bulk density is that the bulk density describes the density of the entire material (particles including space between them), and the solid density describes only the respective particle density.

Target Bulk Density 1790

Please check if fields from csv matched correctly:

Field	X-Coordinate	Y-Coordinate	Z-Coordinate	Volume
↓	↓	↓	↓	↓
Field from csv	'Position_x'	'Position_y'	'Position_z'	'Volume'

Information for test volume:

	X	Y	Z
Minimum coords	-0,0922	-0,0922	0,0079
Maximum coords	0,0922	0,0922	0,4072
Size	0,1844	0,1843	0,3993
Center	0,0000	-0,0000	0,2076
Particle diameter min	0,0150		
Particle diameter max	0,0150		
Particle count	4.471		

Advanced Settings ^

Figure 9.3: DEM Calibration Tool

Table 9.1: Density calibration: results

	Solid density [kg/m ³]	Bulk density [kg/m ³]
Surface	2234	1450
60cm under the surface	2758	1790

9.1.2 Internal Friction

To calibrate the internal friction, the angle of repose from the literature is compared with a simulated result (figure 9.4). These required angles are mentioned in Table 2.4 in Chapter 2.3.2. The friction coefficient is changed, and the simulation iteratively restarted, until the two angles match. For an accurate result, the angles are measured on both sides in two planes (x and y), and the average value is then used from these four angles.

The determined values for the internal friction can be seen in Table 9.2 with their associated angle of repose.

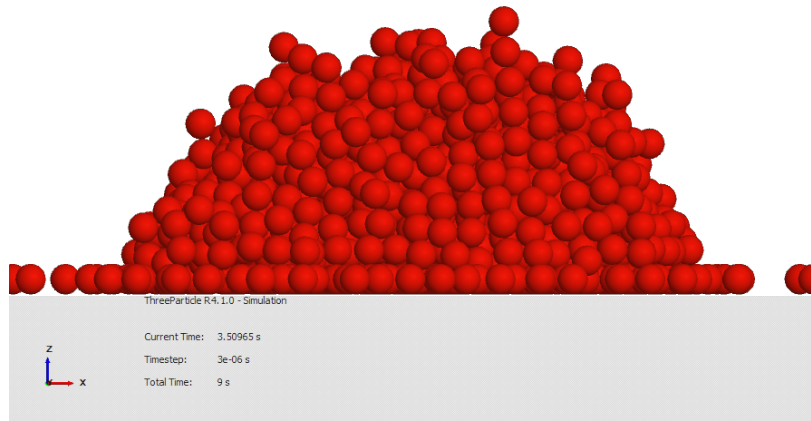


Figure 9.4: Angle of repose for the subsurface Regolith

Table 9.2: Internal friction calibration: results

	Internal friction coefficient	Internal friction angle
Surface	0.338	42°
60cm under the surface	0.497	54°

9.1.3 Other Parameters

Other parameters are important for the simulation, like the external friction coefficients, such as between, the bucket and the regolith. There are also attempts to determine this parameter, but due to the lack of comparative values, these cannot be carried out completely, as physical data is not available as required. The friction coefficient for the external friction is set for comparative values with that one for internal friction (as a conservative approach).

The cohesion should also be taken into account, but as this has hardly any influence on the simulated function, it is not considered further.

Other set properties, like the coefficient of restitution, the Poissons ratio, and the Shear Modulus can be seen in table 9.3.

Table 9.3: Used DEM parameters

Coefficient of restitution	0.1
Shear Modulus	3 MPa
Poisson 's ratio	0.5

To simplify and further to enhance the calculation, and as spherical particles are used, the rotation of the particles is locked.

9.2 Simulation of the Excavation Process

The simulation of the excavation process is used to optimise the shovel shape. For this purpose, various design models are compared with each other to select the most promising one from these as designed. For a comparison between the influence of the different blade shapes, only the inner surface (cross-section) is of relevance for the simulation. To prevent the material from falling out at either end, virtual planes with an ideally smooth material (no friction) are used.

9.2.1 Field Setup

The first step of the simulation is to recreate a lunar surface. For this, an empty box is designed first. Then a particle mix with a specific particle size distribution is put on that in a thin layer, so that in the end, the surface results in a waviness and is not perfectly flat. These particles are fixed so that they cannot move in the further simulation. In addition, the actual regolith particles are added on top of this layer. It is important to ensure that enough particles cover the sublayer so that the blade does not collide with it. In Figure 9.5 there is the box with the sublayer and in Figure 9.6 the completed surface setup. These steps must be performed for both, surface regolith and subsurface regolith.

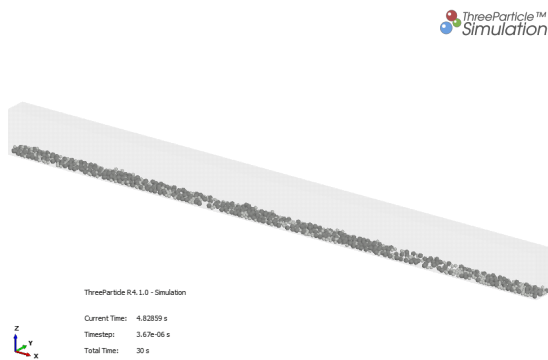


Figure 9.5: Sublayer

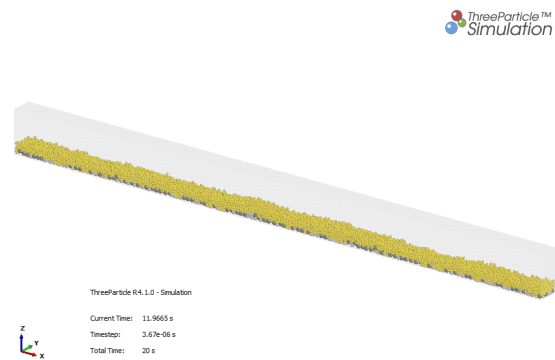


Figure 9.6: Field setup for surface Regolith

9.2.2 Shovel Shapes

As already mentioned, there are many possibilities to implement the shovel design. In Figure 9.7, there are five forms, which will be compared with each other. Every form has specific aspects, therefore differences are occurring in various effects. In order to make them comparable, all forms have the same outer dimensions, while some are designed more angular, some more rounded, as can be seen.

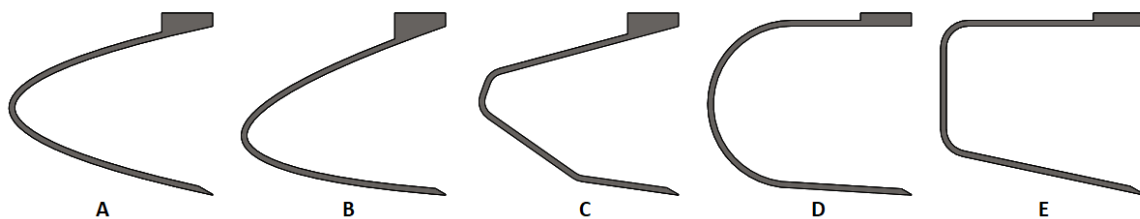


Figure 9.7: 5 different shovel shapes from A to E

9.2.3 Excavation Process

The mining process consists of bucket plunging into the material (Figure 9.8), horizontal mining movement, and the bucket turning out (Figure 9.9). The excavation speed was set at 0.3 m/s and the pivot point 190 mm above the upper edge of the shovel. The excavation depth for an ideal comparison must be determined empirically and is

subsequently the same for all blade shapes. But there are differences between the surface and the subsurface simulation because of a different field setup.

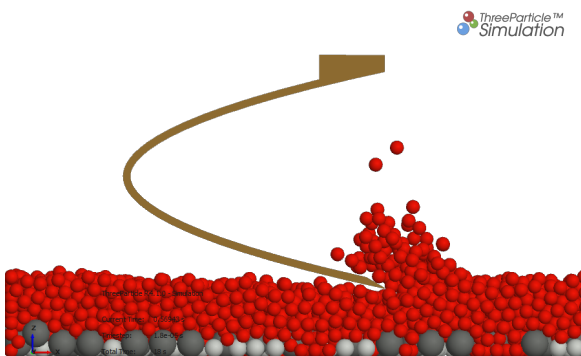


Figure 9.8: Bucket plunging Form A

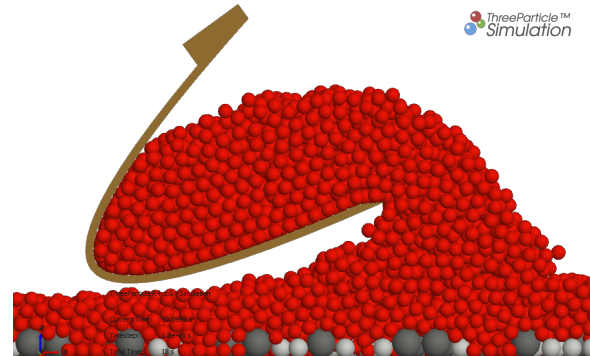


Figure 9.9: Bucket turning out Form A

9.2.4 Evaluation of the Simulation

The blade shapes are now compared with each other concerning the following aspects:

- Force progression
- Number of scooped particles

Force Progression

The measured values of the respective blade forces are exported into CSV-files. These files are processed further using MATLAB2017b [63] to plot respective curves. As can be seen in Figures 9.10 and 9.11, it is hard to determine differences from the pure results. Therefore, the measured values must be converted into a final curve. To get a representative curve showing the trend, the averages of twenty-five measurements are calculated and assigned a point in the diagram. These smoothed curves can be seen in the Figures 9.12 and 9.13.

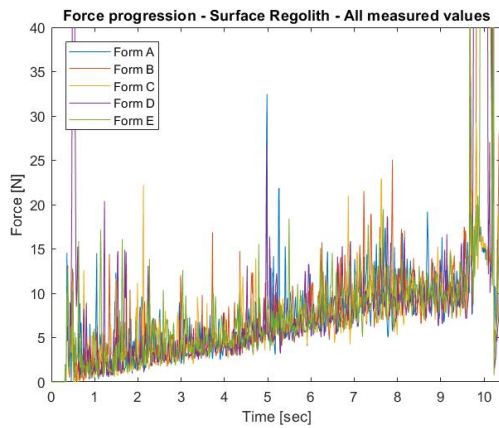


Figure 9.10: Force progression - Surface - All values

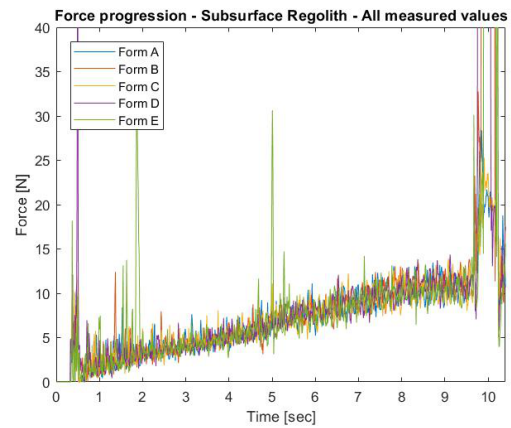


Figure 9.11: Force progression - Subsurface - All values

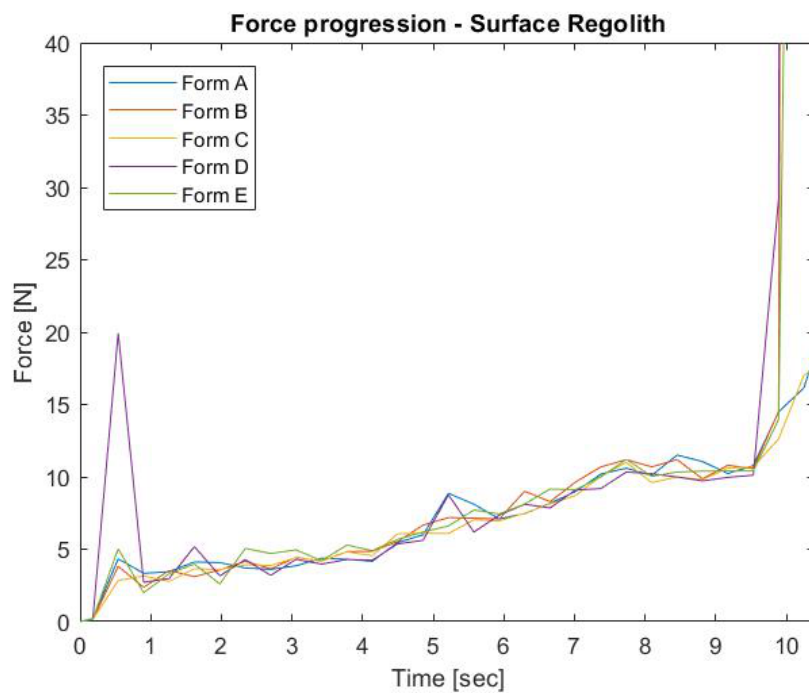


Figure 9.12: Force progression - Surface - Smoothed curve

In these curves, there is a little difference in force during the constant linear excavation, except in form E. However, serious deviations do occur while bucket plunging (left end of the graphic) and bucket turning out (right end). So these subdivisions need to be studied more closely.

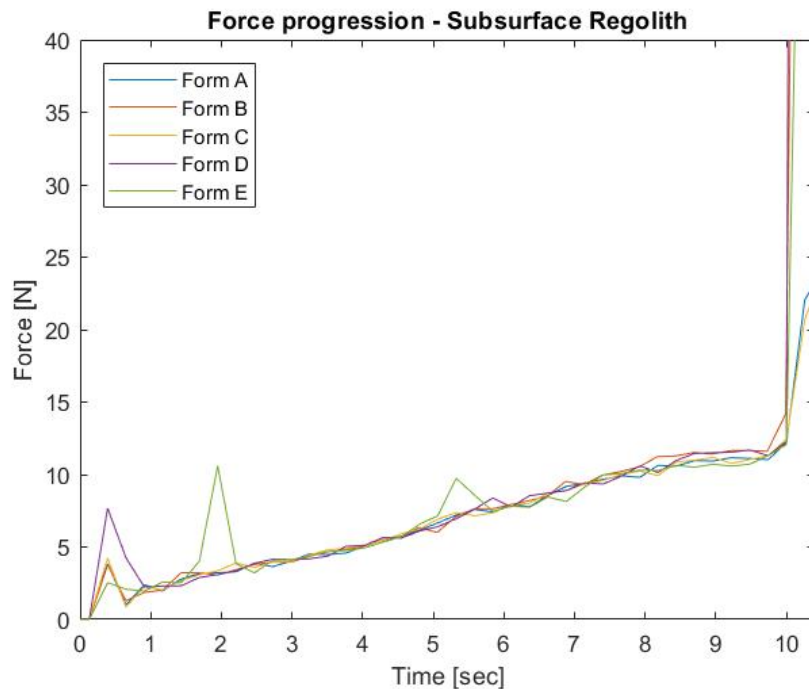


Figure 9.13: Force progression - Subsurface - Smoothed curve

It can be seen that in both regions, surface and subsurface (Figure 9.14 and 9.15), shape D has the largest deflections. The others are very similar, so there are three forms left. These are the forms A, B, and C. Furthermore, the detail at the bucket turning out must be considered (Figure 9.16 and 9.17).

Owing to the fact, that only form D and C have not a sharply increasing curve, these two forms are left. These rises, of the three eliminated buckets, comes from the contact of the back of the bucket with the base during the tipping up of the cup. With adjustment to this aspect, the eliminated designs could also work, but this thesis deals only with the basic designs.

It is interesting that particle parameters also have an impact on blade shape performance. While form E still appears to be the second-worst solution when entering the surface regolith, it is the best below the surface.

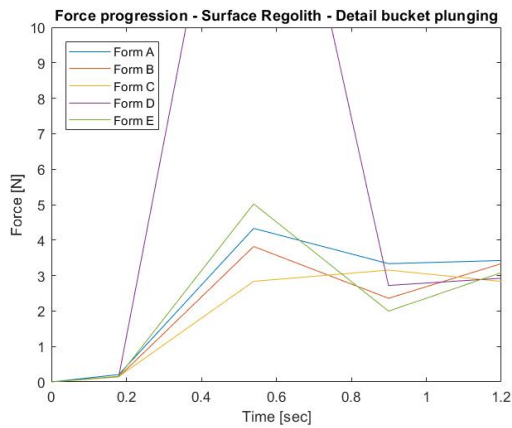


Figure 9.14: Force progression - Surface - Detail bucket plunging

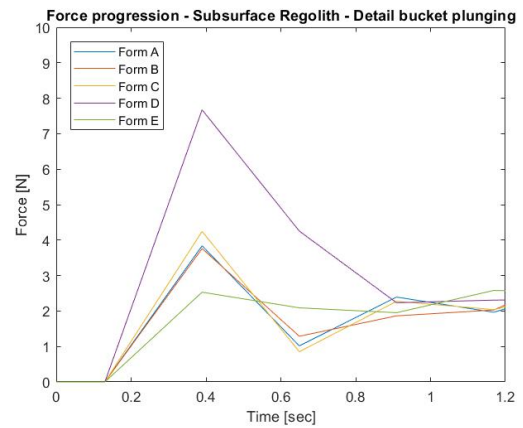


Figure 9.15: Force progression - Subsurface - Detail bucket plunging

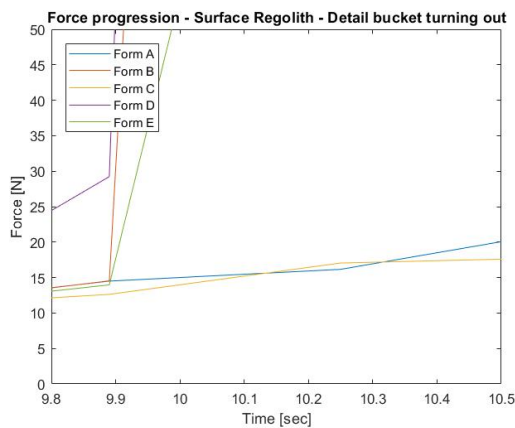


Figure 9.16: Force progression - Surface - Detail bucket turning out

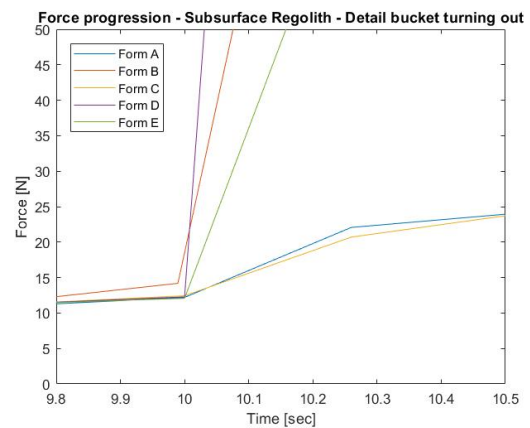


Figure 9.17: Force progression - Subsurface - Detail bucket turning out

It is also important to note that the calculated forces may differ from the actual one, because of the simplifications, so these loads are only for comparison.

Number of scooped particles

Another important parameter for the selection of the shovel shape is the number of scooped particles, because a low force form is not beneficial when there are only fewer particles scooped. The number of particles can be used as a measure for the later volume. In Figures 9.18 and 9.19, a clear division in the values of the respective blade

shapes can be seen. This has to do with the different bulk material on one the hand and the different field setup on the other hand. Because of this different setup, the excavation depths are not identical.

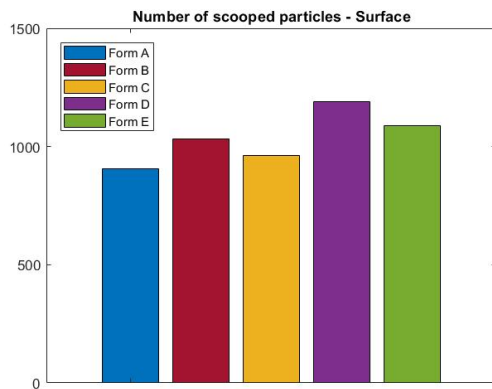


Figure 9.18: Number of scooped particles - Surface

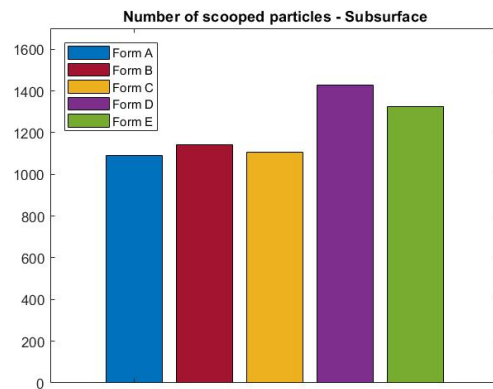


Figure 9.19: Number of scooped particles - Subsurface

It was to be expected that form A and E would be able to accommodate more material since the empty volume inside the bucket is significantly higher. But form B showed higher filling compared to form A, as they are very similar. In comparison of the number of scooped particles Form D is the best one, followed by E, and B. The forms D and A are close up to form B concerning the excavated volume.

Shovel Selection

Due to the force comparisons, only two of the five forms are left; form A and C. The three other ones were already eliminated. Form C performs better regarding filling than form A in both areas, thus form C will be the selected design. Another advantage is the large slope on the back of the bucket, which probably favours the ejection of material.

Due to the required conveying volume of two cubic decimetres per shovel, the width must be set accordingly. The widening is performed according to the following formulas:

$$V_p = \frac{4 * r^3 * \pi}{3} = \frac{4 * 7.5^3 * \pi}{3} = 1767.09 \text{mm}^3 \quad (9.1)$$

$$V_r = \frac{w_{new}}{w_{old}} * V_p * n_{part} * k \quad (9.2)$$

First, the volume of a single particle (V_p) must be calculated. Formula (9.2) is for the required shovel conveying volume (V_r) and consists of the width of the simulated shovel (w_{old}), the width of the widened shovel (w_{new}), particle volume (V_k), number of particles at the simulation (n_{part}) and a correction factor k . This factor takes into account the influence of the blade side surfaces. By transforming this equation, the new width can be calculated as follows.

$$w_{new} = \frac{V_r * w_{old}}{V_p * n_{part} * k} = \frac{2 * 10^6 * 120}{1767.09 * 963 * 0.7} = 201.48 \text{mm} \cong 205 \text{mm} \quad (9.3)$$

Figure 9.20 shows the completed bucket design.

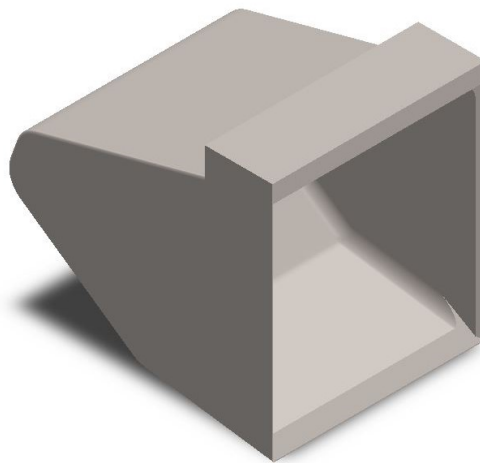


Figure 9.20: Chosen bucket design

9.3 Discharge Process

The bucket course can be seen in figure 8.21 and is already described there. For a fast discharge of the bucket, it must swing out while moving vertically upwards. To make this possible, a mounting block is inserted between the chain and the bucket, which has a swivel joint at the end (figure 9.21).

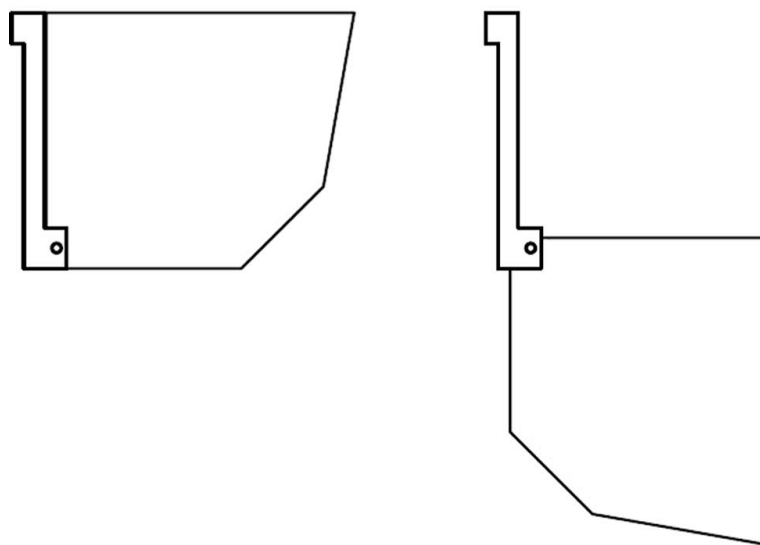


Figure 9.21: Function of the notching mechanism [26]

9.3.1 Position of the Pivot Point

The position of this swivel is important for further function. There are significant differences in both, x-axis and y-axis. Each of these positions has advantages and disadvantages. Some of them need the use of springs for the initial acceleration.

x-axis (horizontal)

The pivot point can be located between the top edge as upper point and the bottom edge as the lower one. Springs are additionally used so that the bucket already gets an initial speed, clamping is thus prevented, and also the discharge time is reduced.

Without springs, only the shovel top variant would be possible because of the restoring torque. By changing this distance in the x-axis, the initial speed of the bucket varies, as well as the ejection position along the axis. Setting the pivot point at the bottom edge of the bucket is not useful, since this part is engaged when the bucket is removing material. Figure 9.22 shows three possibilities graphically, left is always the normal position, and right the end position after swing-out.

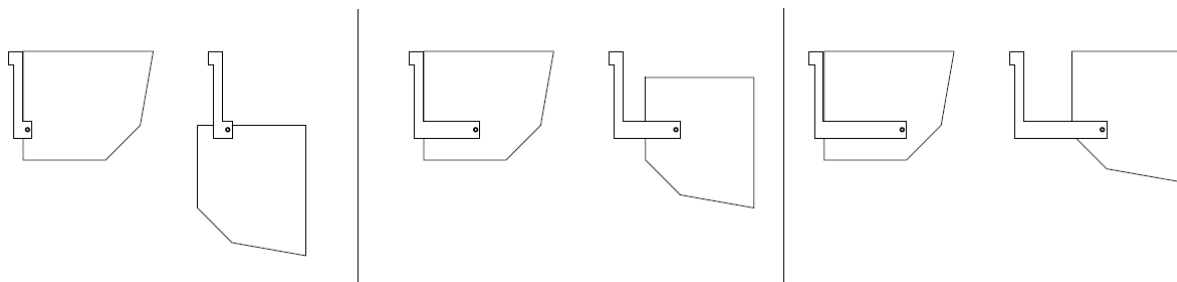


Figure 9.22: Pivot-Point: x-axis positions

y-axis (vertical)

There are also several solutions for the y-axis. These are:

- Pivot point above the end of the bucket
- Pivot point at the level of the cup rim
- Pivot point above the rim of the bucket

The positions are shown using the variant x-axis equals blade top edge. They are only for representation, the pivot point can be set at every position along this axis.

It can be seen in Figure 9.23 that the longer the hinge, the further to the side (in this case to the right) the bucket ejects the material and the higher the rotational energy. A discharge variant in which the lower edge of the blade in the swung-out state protrudes over the lower edge in the normal state would be a great advantage for the unloading process to the following chute. This could prevent the material from the bucket from being emptied into the following bucket during unloading.

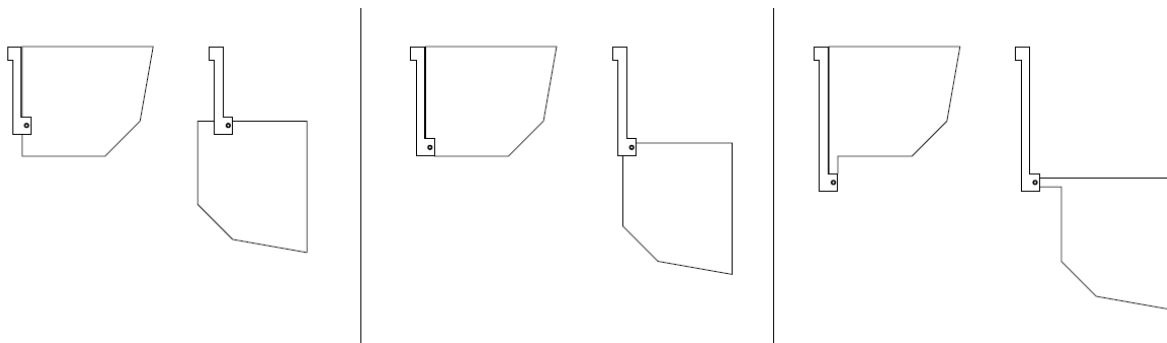


Figure 9.23: Pivot-Point: y-axis positions

9.3.2 Discharge Simulation

To determine the position of the pivot point, the discharge process is simulated. The aim is to discharge as quickly as possible with a slight overhang of the lower edge of the blade, as mentioned before. A multi-body system is used for this purpose. The blade is freed in all six degrees of freedom, and the mass moments of inertia are defined. The vertical forward movement is performed by inserting a part that induces the dragging of the bucket. Markers are set to define the linking of the parts (the bucket and the drag part) accordingly. Therefore, these two markers are linked with constraints. At this point, a revolute joint is inserted. To simulate the spring force, a force impulse is applied when releasing the bucket from the hinge.

Figure 9.24 shows a possible pivot point (in the middle of the blade) in the simulation, and Figure 9.25 the blade spinning out.

For fastening the discharge process, a punch block is used. The blade hits this block while swinging out. This leads to an impact, and the particles get a higher velocity. This effect can be seen in Figures 9.26 and 9.27. The punch block can be the green one in Figure 9.26.

The simulation of several pivot points has shown that the solution requires a compromise, due to the possibility of changing the position and spring force. Therefore, the point from Figure 9.24 was set as the pivot point. So it can have a clear overhang and an

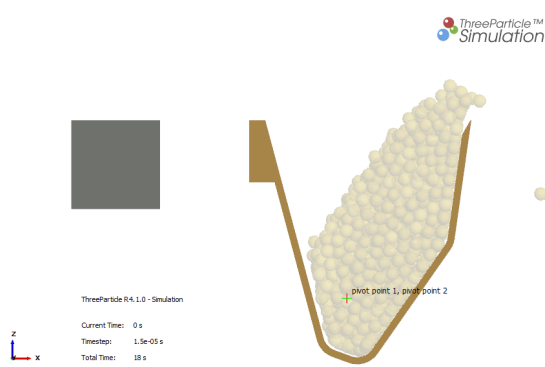


Figure 9.24: Possible pivot-point

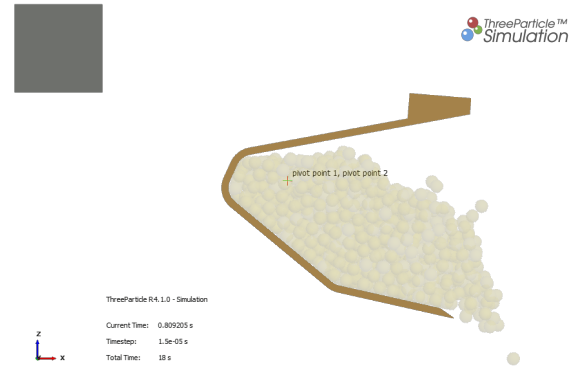


Figure 9.25: Bucket spin out

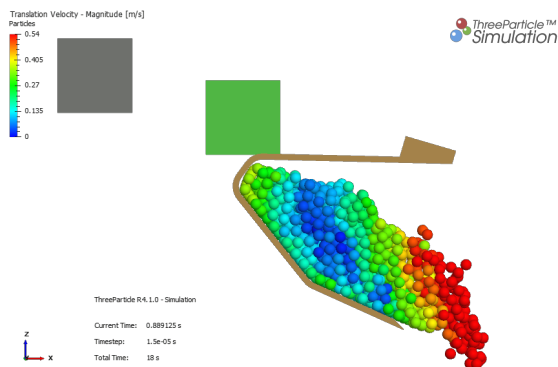


Figure 9.26: Bucket before hitting the block

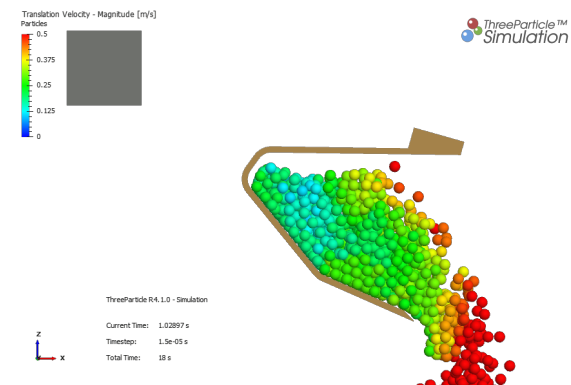


Figure 9.27: Bucket after hitting the block

acceptable emptying time with less spring force. The discharge time could be reduced if the pivot point was outside the bucket, but this would be a more cumbersome option. The rotational energy would also be significantly higher at the impact, which would result in a sharp increase in the enclosure.

In this position of the pivot point, the simulation showed, that the blade must be fixed in the position after impact with the punch block, because this prevents the bucket of a swing back, and the blade is emptied more quickly. Another important fact of this bounce block is the determination of the maximum swing. This ensures that all the material can be unloaded as centrally as possible.



9.3.3 Simulation Overview

With these simulations it was possible, to chose a promising shovel design out of the five options. It could also be seen, that the different excavation depths, with the following different parameters, influence the forces and number of scooped particles.

The definition of the pivot point was another important step, and the simulation has shown, that a punch block can decrease the discharge time, and also that a use of springs for the initial speed are necessary. A low discharge time is important for the further conveyor system. Because it can be an advantage when the whole material, that was excavated with one bucket, can be transferred in a compact package instead of constant trickling.

The conclusions of this chapter are important for the further thesis, especially for the designing of the mechanical system.

10 The Design

In this chapter, the selected operating principle is presented graphically and discussed in more detail. For this description, the construction is divided into several subgroups (Figure 10.1), which are the basic (beam) structure, the robot at the clamping station, the robot at the ejector station and the bucket mechanism.

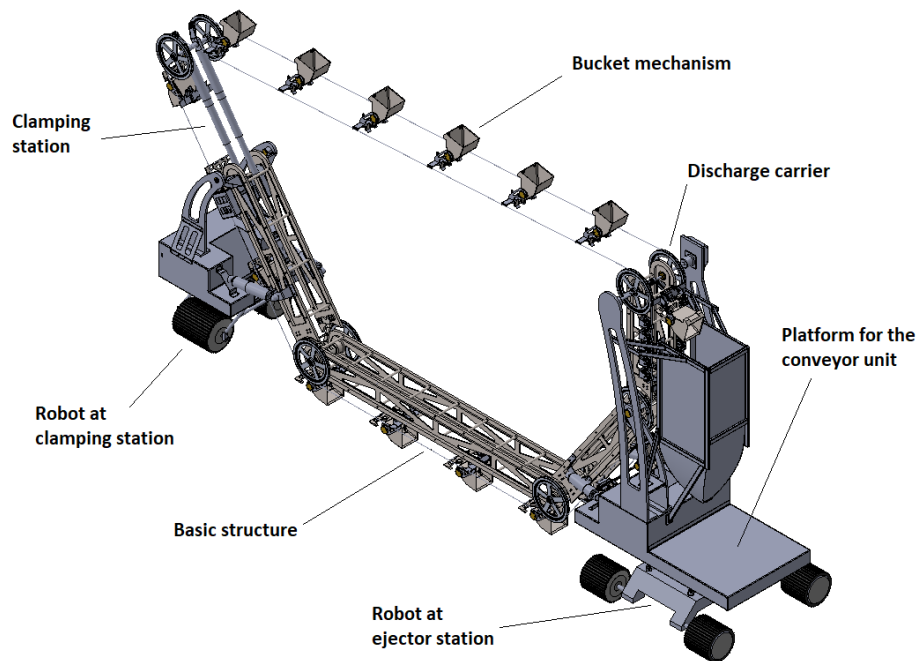


Figure 10.1: Design explanation

This design is only a mechanical concept. Some components are not shown in detail, and there may be various other solutions for individual designs in the future. For the design process SolidWorks2019 [16] is used.

10.1 Basic Structure

The basic framework consists of four beams. Three of them were mentioned in Subsection 8.3.3 and are responsible for the basic structure; the fourth one is the discharge beam. These carriers are hinged together to allow adjustment of the mining depth and to respond to surface irregularities. Each beam contains two basic elements, which are bolted together through rods. Figures 10.2, 10.3, 10.4, and 10.5 show the graphic of every single carrier and Figure 10.6 the whole structure.

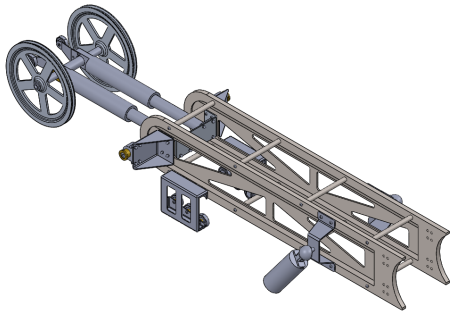


Figure 10.2: Carrier clamping station

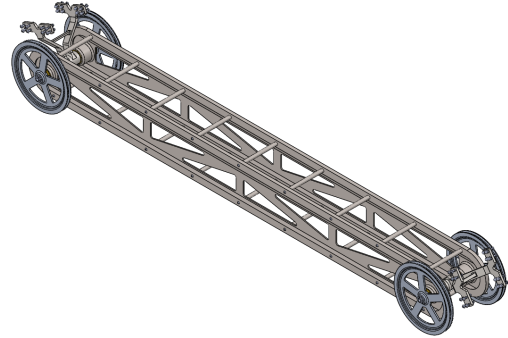


Figure 10.3: Main beam

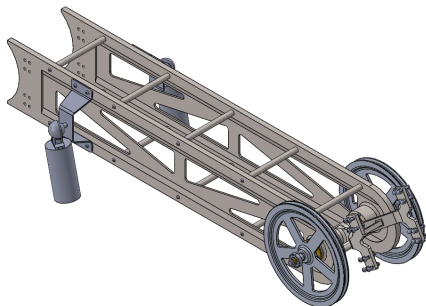


Figure 10.4: Connector

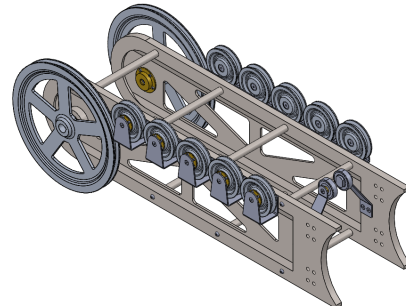


Figure 10.5: Discharge carrier

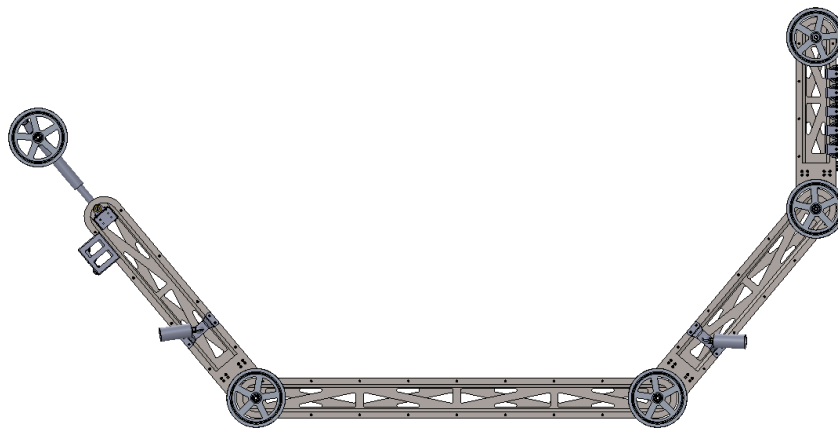


Figure 10.6: Basic structure

Traction device

At the connection points, there are diverter rollers to guide the steel cable. Three different options are available for the traction means, a steel cable, a chain, and a belt. The belt is not a sensible solution, since the required elastic rubber materials are susceptible to radiation, as according to Chapter 6. Chains would result in a lot of points where each two chain elements interact with each other, so friction/wear is relatively high, specifically with dust considered. The decision consequently fell on steel cables, as those provide relatively simple solutions with less susceptibility to error.

Bearing

The rotation of these carriers relative to each other is realized by a plain bearing. A roller bearing could also have been used, but the low twist and rotational speed make this heavier solution impractical; also the relative movements of even more mechanical parts are thus avoided.

The deflection rollers are supported by ball bearings, as they are subjected to constant rotary motion. Figure 10.7 shows both types, the rolling bearing on the outside and the plain bearing on the inside. The plain one is designed as a hollow shaft, which makes

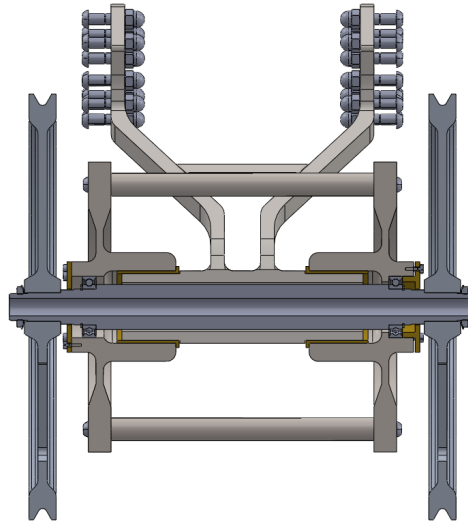


Figure 10.7: Bearing combination

it possible to position the shaft for the deflection rollers inside the gliding cylinder. A continuous shaft is used for the pulley so that they run synchronized. Also, feather keys were used for the rollers.

Clamping station

To allow the function with the most diverse beam arrangements, the steel cable must in every position be specifically tensioned. In order to implement this, two synchronized electric telescopic-cylinders, which are positioned at the outer point opposite to the discharge station, are used. They can control the pretension of the tractions means by extending and retracting. It would principally also be possible to position a tensioning pulley somewhere along the steel cable course, but this would have introduced additional locking parts into the system, as the buckets are attached to the cable in a specific form allowing limited guidance only.

This shown solution using two cylinders is one of a few possibilities. For example, it would also have been feasible to use a central cylinder with a rail-guidance system. However, the simple and low-wear design are aspects to this two-cylinder system. As

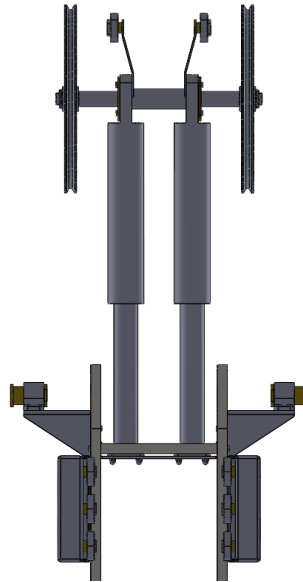


Figure 10.8: Clamping station

can be seen in Figure 10.8, the cylinders were placed inside the beam structure to save space. As a result, there is a risk that the cylinders are not equally loaded such as resulting from one-sided blade charging. Position-controlled cylinders can be useful to avoid such problems; another option would be to place the two cylinders each on one side (outside) of the beam structure.

Discharge station

As mentioned before, there is a fourth carrier. This beam is positioned vertically upwards and is responsible for the discharge of the bulk material. A peculiarity is, that this beam is not changeable in position. The main function of this carrier is to guide the cable while using the bucket plunging mechanism. This dropping mechanism is explained in Section 10.4 in more detail. At this section, the cable is guided during various forces act on the cable.

Drive

The drive is located on the discharge carrier. For this concept, the motor is positioned inside the robot and the torque was redirected to the top of the support structure utilizing a shaft and bevel gears. It would also be possible to place the motor directly at the top, but the high motor weight would significantly increase the risk of tilting of the whole system. Chain drives or belt drives are options, but the disadvantages have already been mentioned (such as dust-related wear; maintenance).

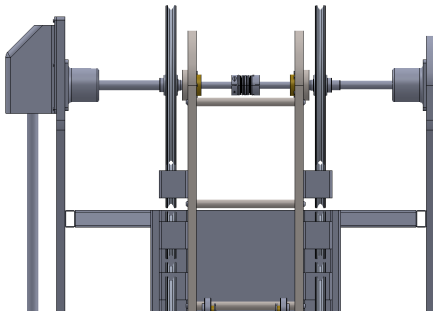


Figure 10.9: Two shafts connected via shaft coupling

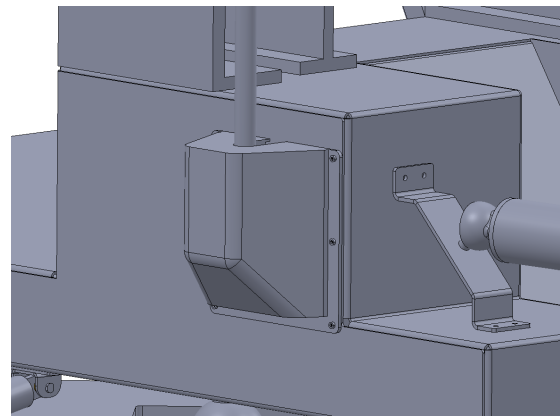


Figure 10.10: Second deflection of the drive shaft

Figure 10.9 shows the two drive shafts. On the left side is the 90-degree deflection through a pair of bevel gears. Figure 10.10 shows the second deflection on the basic structure of the robot of the discharge station, with the placed motor inside (not visible).

10.2 Robot at Clamping Station

The excavation machine is composed of two robots. The robot at the clamping station (Figure 10.11) is the smaller one. It consists of two assemblies: the chassis, and the superstructure. The chassis includes two wheels, as well as control units, and a

radioisotopic generator, as used on the latest generation of Mars rovers (Chapter 4). The wheels are driven by hub drives.

The two wheels are larger than those on the other robot (discharging side; see next Section), because of the dismantling tactic. While the main robot on the drop-side always drives in the already excavated (thus paved) field, its opposite (this robot with the two wheels) is intended to drive offroad. The two wheels including dampers, and a revolute joint (Figure 10.12), enable the robot to drive over stones and other obstacles.

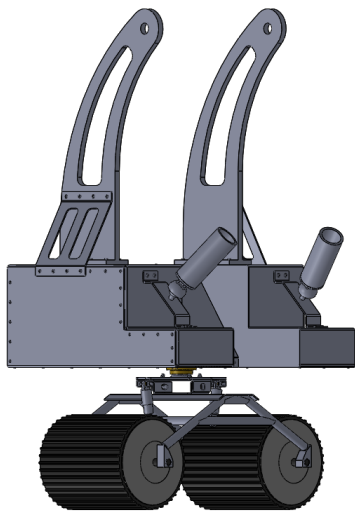


Figure 10.11: Robot at clamping station

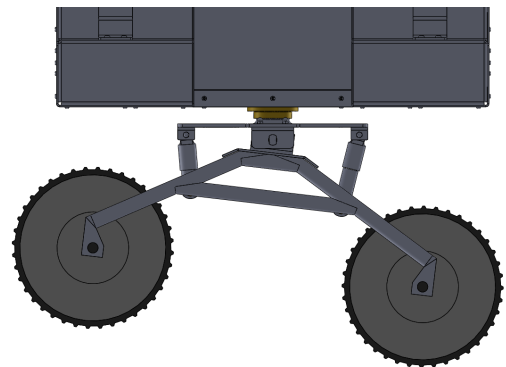


Figure 10.12: Revolute joint for offroad driving

On the superstructure is the attachment of the support structure, as well as two electric cylinders. These cylinders can be used to vary the position of the attached girders. The connection is made via ball joints. This adjustment would also have been possible with a pulley system, but the simplicity and reduced wear parts tipped the scales. Inside the housing are control units, generators, and sensors. Cameras and sensors can be mounted on the outside for orientation.

10.3 Robot at Ejector Station

Compared to the robot at the tensioning station, the robot at the discharge has more components (Figure 10.13). The chassis system is bigger to increase stability. In the base, there is an additional generator nearby the mentioned motor for the bucket chain system.

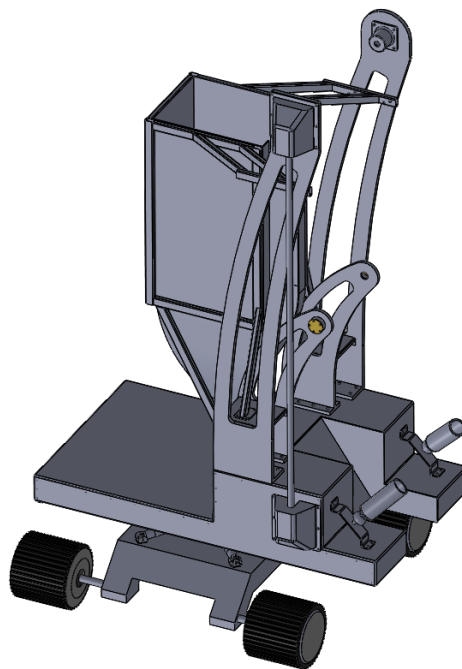


Figure 10.13: Robot at ejector station

In the structure, the beams are mounted twice, as compared to the opposite side, the vertical drop beam is added. Furthermore, a relatively large platform is also prepared for the attachment of the conveyor unit (covered in the mentioned thesis by Taschner, see Instruction to Cooperation Höber/Taschner).

This robot has four wheels, and the drive is the same as the one on the other robot. The connection between the chassis and the superstructure is made by a ball joint with

attached dampers (Figure 10.14) to compensate for unevenness so that, for example, the robot can drive diagonally upwards while the other drives diagonally downwards.

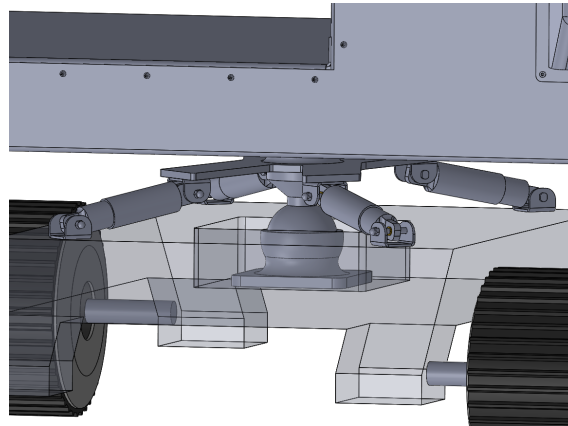


Figure 10.14: Ball joint against unevenness

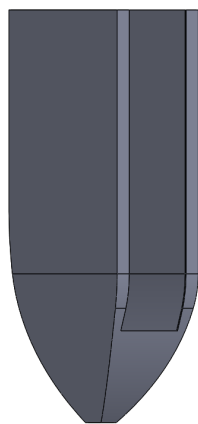


Figure 10.15: Chute

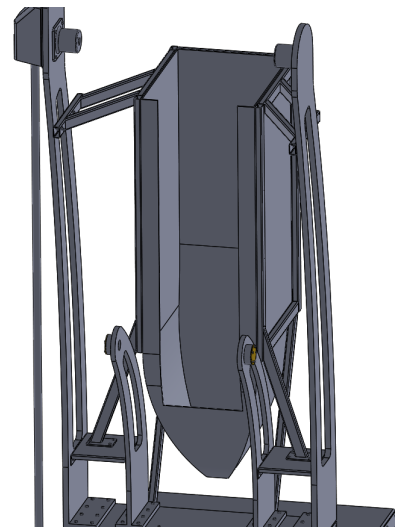


Figure 10.16: Chute in the assembly

A chute is used to transfer the bulk material to the conveyor system (Figures 10.15 and 10.16). In this concept, a chute with a tapered cross-section is used, which has tangential transitions. This allows the material to be transferred in a smooth way. For the exact shape optimization, a DEM simulation would have to be carried out. The chute is closed until the top, with the intention to reduce dust generation near the conveyor unit.



10.4 Bucket Mechanism

The swing-out mechanism of the bucket is one of the most important functions. The basic principle has already been explained, which is implemented in the concept as described. There are a variety of options for implementation with three basic concepts, magnetic, electric, and mechanic. The magnetic concept is the simplest, but since regolith can be attracted by magnets, is probably not suitable. Another possibility consists of electric cylinders that empty the bucket, but there are some problems. On the one hand, additional energy is required and, on the other hand, the rotational energy cannot be used for emptying. Thus, a mechanical concept is the most promising.

A large number of components is required to implement this mechanism. Therefore, the individual functions are explained separately in each case. Figure 10.17 shows a overview of the whole bucket system, with all its special components, and Figure 10.18 the bucket at its swing-out end position.

Another important components are the parts, that activate this different types of functions. For this applications, rollers are used for triggering the unlocking and the resetting. These rollers are described in the each subsection in detail. Figure 10.19 shows the position of this important components

Attachment to the steel cable

The fastening from the bucket to the cable is done by a clamp, which is compressed through screws. This results in a force-fit connection between the bucket attachment and the steel cable. Figure 10.20 shows this attachment component.

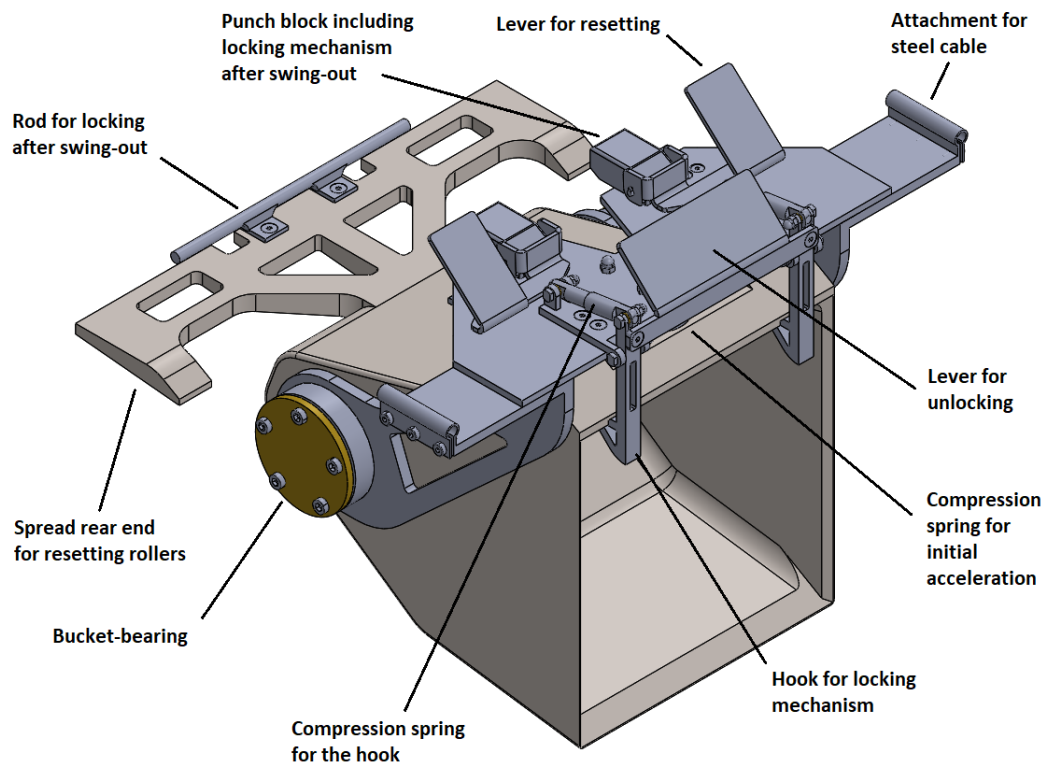


Figure 10.17: Overview of the bucket mechanism

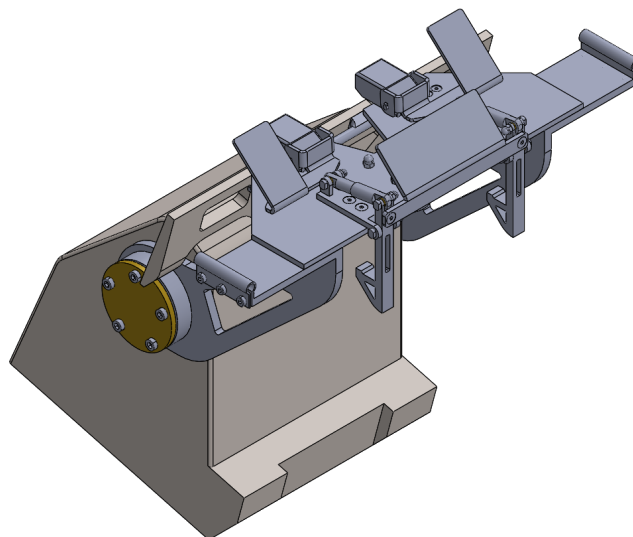


Figure 10.18: Bucket at swing-out end position

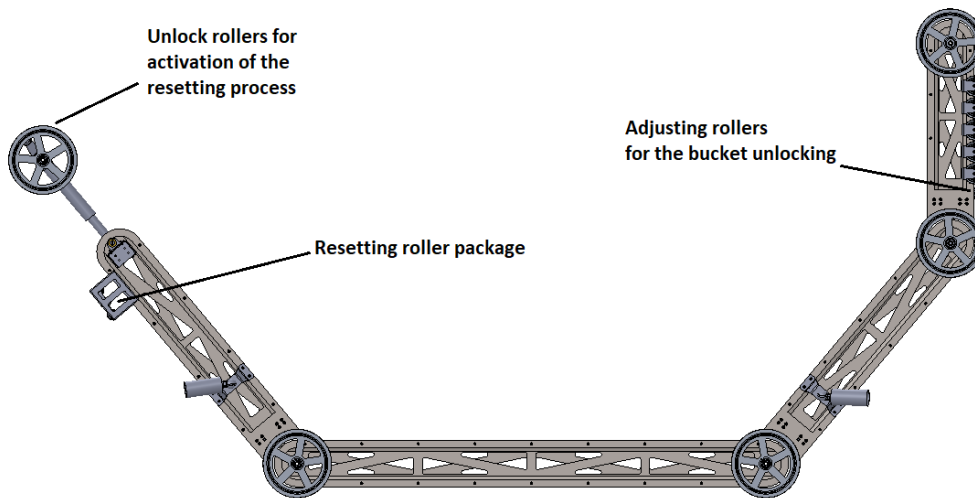


Figure 10.19: Positions of the activation rollers

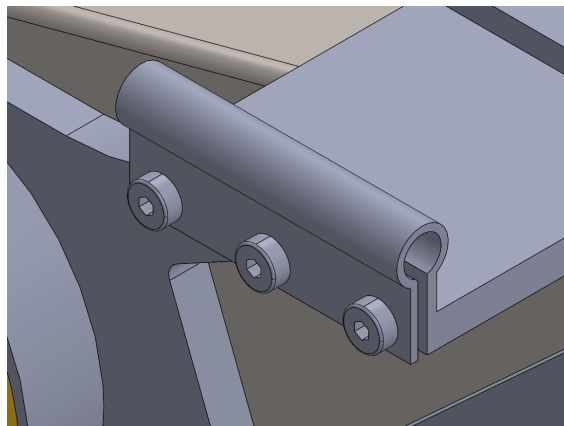


Figure 10.20: Steel cable attachment

Bucket-Bearing

A ball bearing is used to make the rotation of the bucket possible. This enables low-friction swivelling and less energy loss. Figure 10.21 represents the bearing assembly without cover, and Figure 10.22 with cover. The bearing is attached with the inner ring to the stub shaft of the blade. The cover protects the bearing from dust ingress.

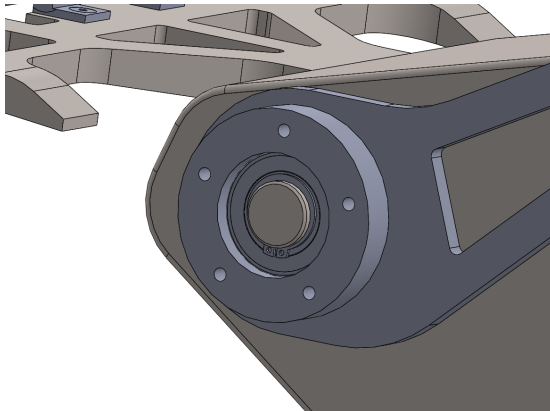


Figure 10.21: Bearing of the bucket

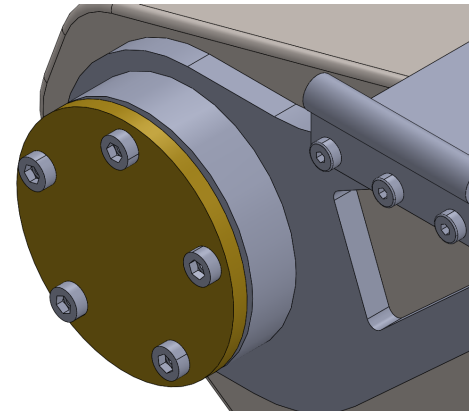


Figure 10.22: Cover of the bearing

Locking of the bucket

The locking mechanism is responsible for the blade to swing out at the desired position and to fix it at the remaining positions. A hook (Figure 10.23) is used, which engages the bucket. The hook is rotatably mounted on the upper plate and is loaded by a compression spring. As a result, the blade is locked in place. A total of two hooks are used, which are connected by plate with lever. This plate makes it possible to unlock the bucket (Figure 10.24). After passing over a roller, the lever is pressed down and the bucket swings out. This roller is located at the lower end of the drop beam and is shown in Figure 10.25. Between the two hooks, there is the spring for the initial impulse.

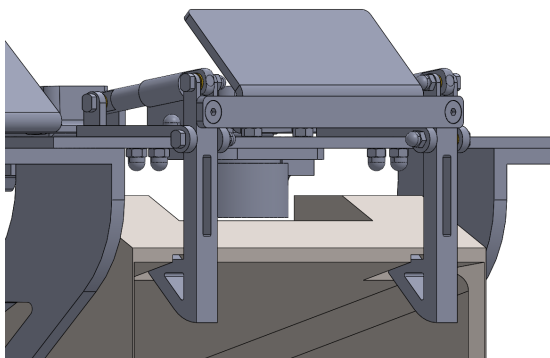


Figure 10.23: Locked hooks

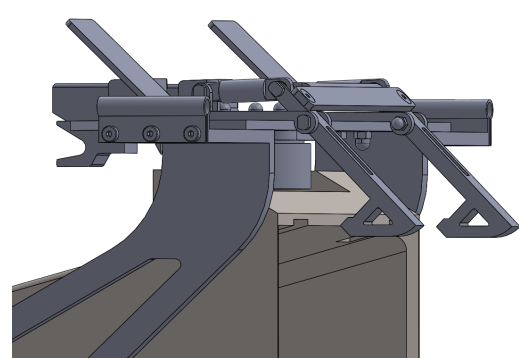


Figure 10.24: Unlocked hooks

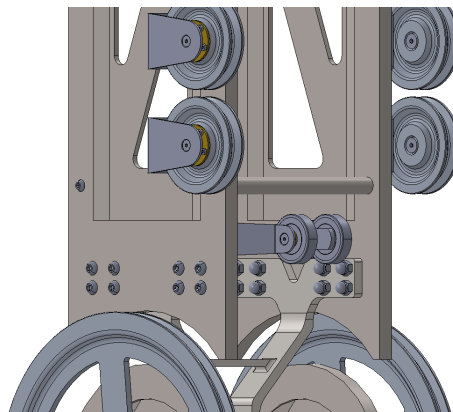


Figure 10.25: Adjusting roller

Punching block

It is necessary to lock the bucket after reaching the punching block. For this, a latch lock is used in combination with this block. At the rear end of the bucket, there is an arm on which a cylindrical rod is fixed. This rod pushes the wedge of the latch bolt upwards when reaching the punching block while swinging out. A spring is used in the inner-side of this block to take the wedge back down after the rod has passed through. The rod bounces against the block and this lock makes spring back impossible. The function can be seen in Figures 10.26 and 10.27.

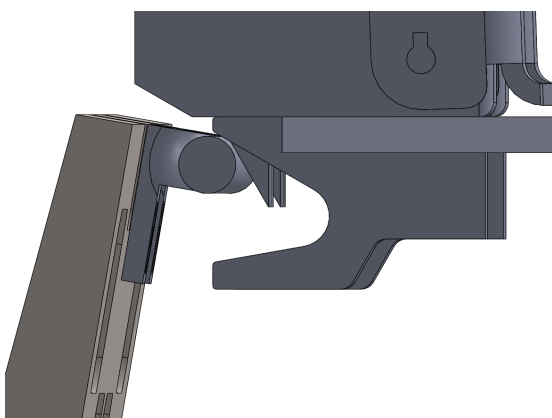


Figure 10.26: Punching block before locking

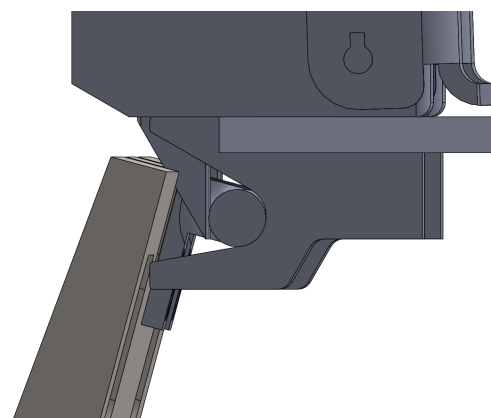


Figure 10.27: Locked punching block

As with the locking mechanism, a lever with actuating rollers is used to release this fixation. Figure 10.28 shows that this roller is attached to the tensioning station. This means that the bucket is fixed during the movement from the upper guide roller of the discharge carrier to the tensioning station.

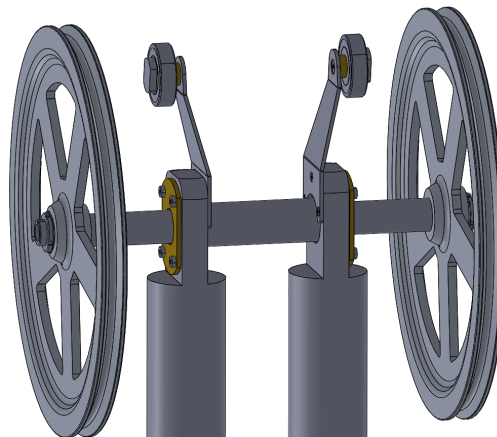


Figure 10.28: Unlock rollers tensioning station

Resetting of the bucket

Resetting takes place after the clamping station has been overhauled by actuating the lever. The rotational energy should cause the blade to swing back and push the bevelled hooks way from their original position (Figure 10.29). Furthermore, this pre-loads the spring for the initial energy. The pressure spring returns the handles to the locked position.

In case that this rotational energy is not sufficient to reset the bucket successfully, a separate system is implemented. An assembly with differently arranged rollers is installed. Due to that, the arm at the rear end of the bucket is spread, so these roller system can roll over. These rollers ensure that the bucket is reset after passing over this roller track. In Figure 10.30, the rollers were arranged linearly. In the optimized case, this arrangement would not be linear to avoid shock loads and smooth the entry. Further simulations would have to be carried out to determine the exact shape.

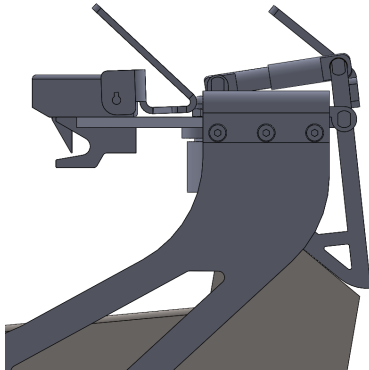


Figure 10.29: Bucket reset

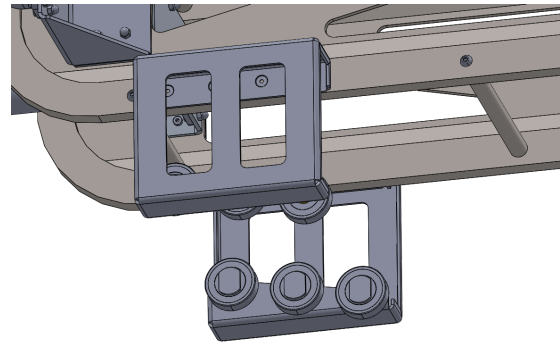


Figure 10.30: Resetting rollers

Final bucket design

Figure 10.31 shows the final design of the bucket including all mentioned mechanisms, Figure 10.32 the unlocking of the bucket, and Figure 10.33 the resetting process.

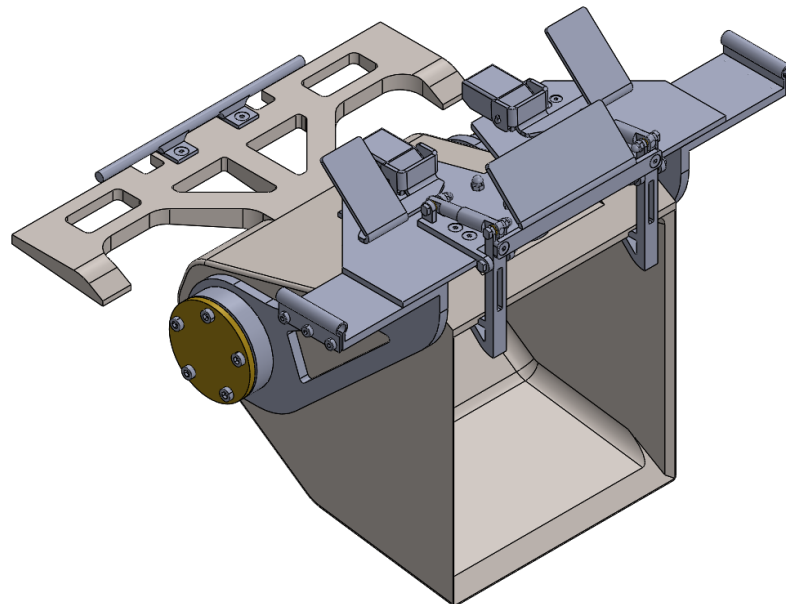


Figure 10.31: Final bucket design

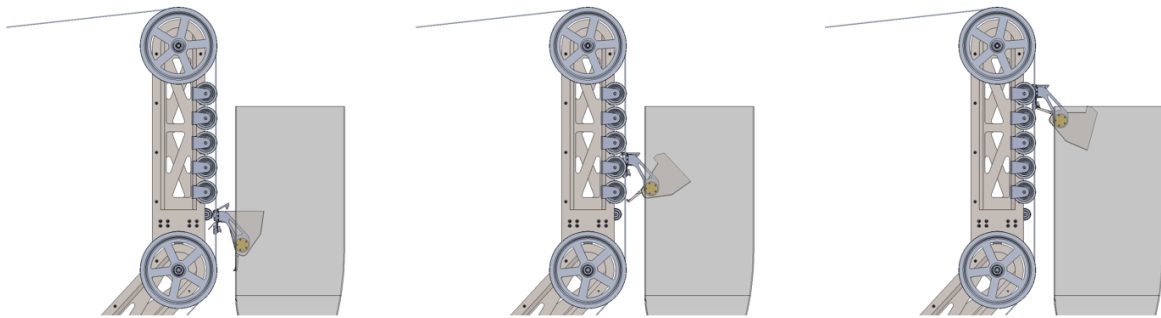


Figure 10.32: Bucket unlocking timeline

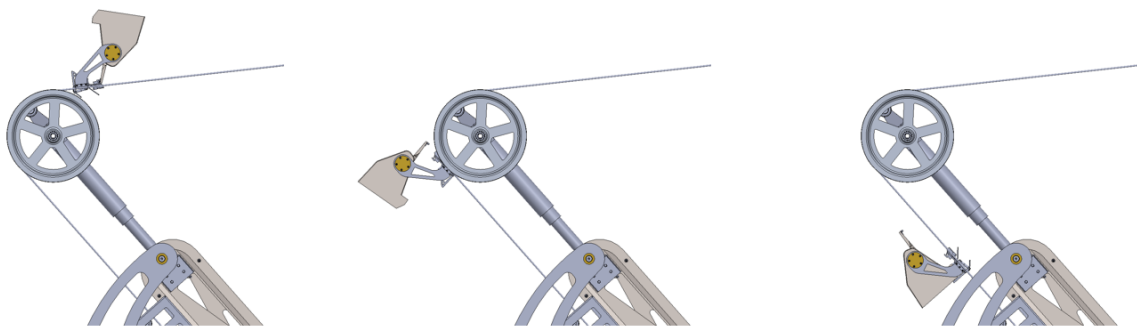


Figure 10.33: Bucket resetting timeline

10.5 Design Overview

While designing, it was found that varying the angle of the support structure is useful only to a certain extent. Therefore, the angles to each other were limited between 125 and 150 degrees. The upper and lower end position are shown in Figures 10.34 and 10.35. The lower end position is also the maximum excavation depth, and the upper-end position was chosen as safety position. For instance, if the bucket cannot be reset successfully, a sensor recognize this issue. This leads to the activation of the safety program. In this program the beam structure is adjusted to the upper-end position, so that the buckets are lifted of the ground. Due to this, the incorrect reset bucket makes a total movement around its course, until it is reset at the resetting station successful. This upper-end position will also be set while driving to the excavation area.

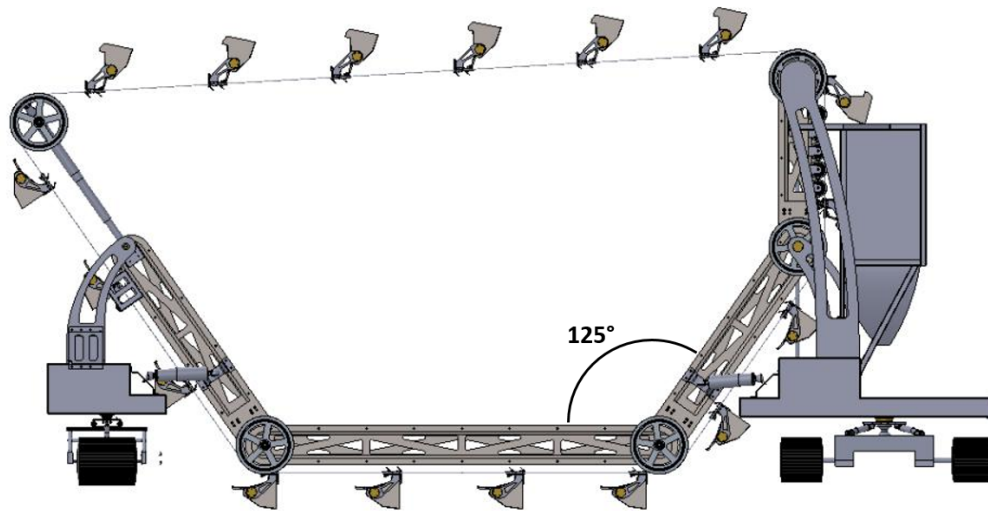


Figure 10.34: Lower end position - maximum excavation depth

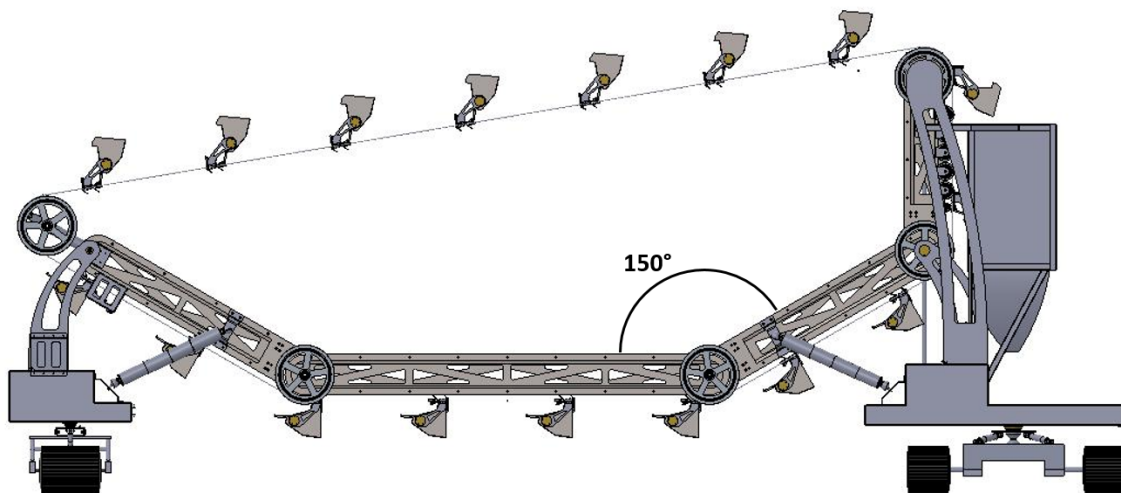


Figure 10.35: Upper end position

Due to the low excavation depth, bigger rocks might be no crucial problem for the system. Because this excavator will be equipped with many different sensors and cameras to scan the surface. So it is possible to trace the problematic rocks before hitting them with the bucket. If there are rocks, which are too big for the bucket, the robot can lift its buckets, and passing these obstacles. For further development stages,

it is also possible to use shields for pushing away them away or develop own robots, for preparing the excavation area and removing the big rocks.

The dimensions of the whole excavator are also important parameters. While the the length depends of the adjustment of the side legs (set angle), the height, and the width are independent from this. It is important to note, that these values are only approximate and could change minimally due to modifications. This excavator is 1150 mm wide, and 3600 mm high, the length has a range of 7750 to 8850 mm (Figures 10.36 and 10.37) including the platform for the conveyor system. For transport by rocket, the unit can be folded to less than 6 m in length. This will fit with the boundary conditions.

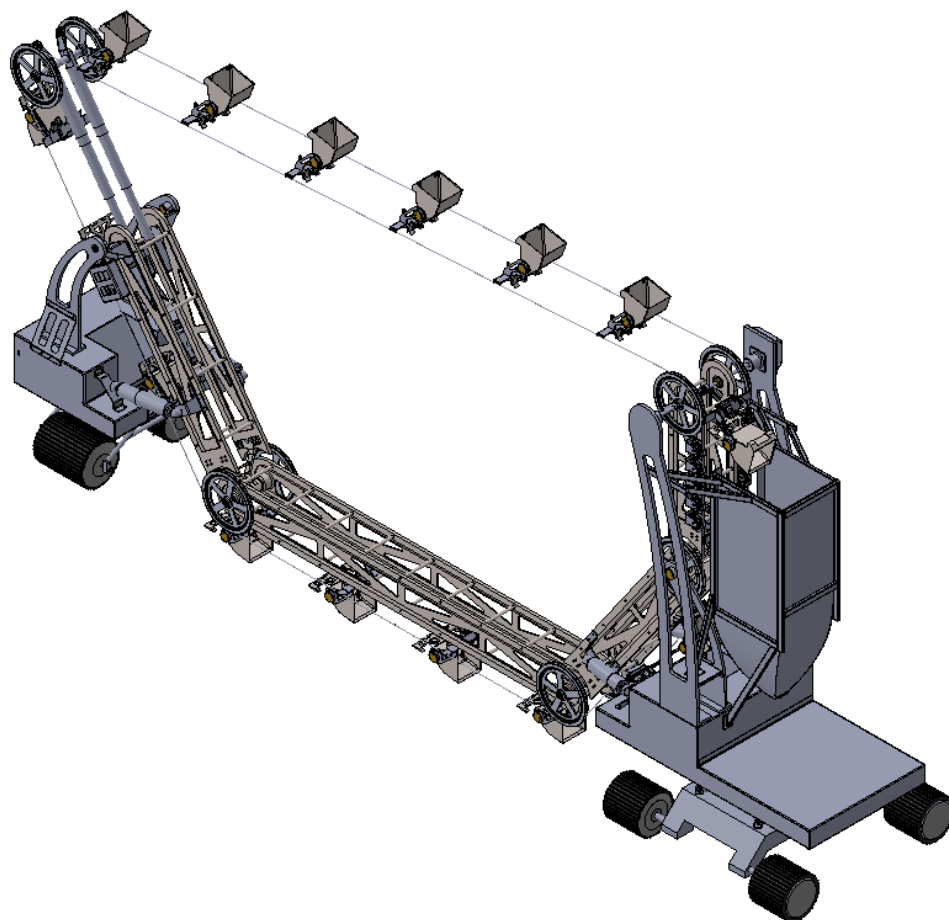


Figure 10.36: Lower end position - isometric view (shortest length)

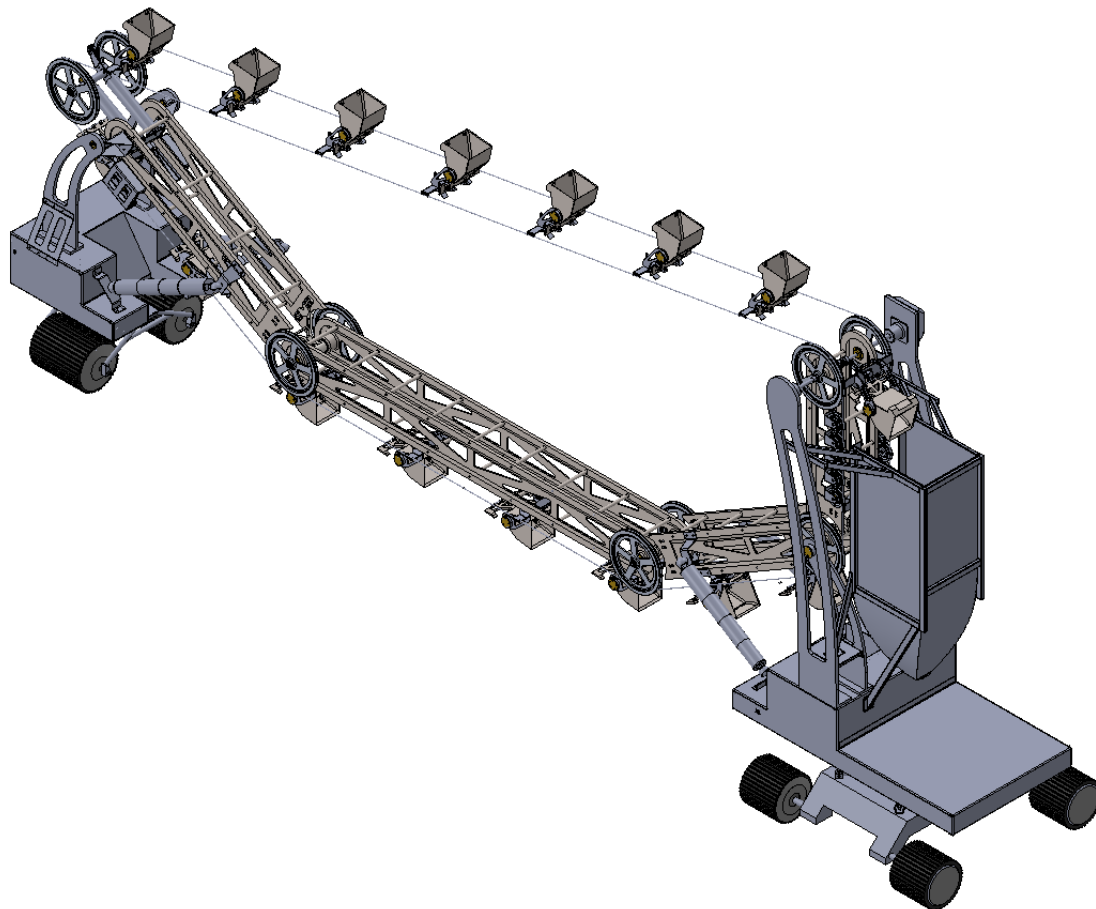


Figure 10.37: Upper end position - isometric view (longest length)

Seventeen buckets are used in the excavator, with a distance of 1000 mm to each other. This relatively large distance, in combination with the number of buckets is an advantage, because more cups decrease the wear of every single one. The bucket speed is set at 0.2 m/s, which results that a bucket is discharged every five seconds. The excavation volume of about 2 dm³ per shovel leads to an average volume flow of 0.4 dm³/s. As mentioned in Chapter 7, 330 m³ regolith are necessary to produce enough oxygen for one rocket launch. As the excavation takes place only at lunar days, this excavator, this would last 460 hours. Referring to Section 2.2.2, a lunar day lasts 29.5 Earth days or 708 hours. So it would be possible to gather enough material to launch three rockets every two lunar days.

In the following graphics there are two other views of the excavation system, set at the upper end position. Figure 10.38 shows the concept from the top, and Figure 10.39 from the clamping station side.

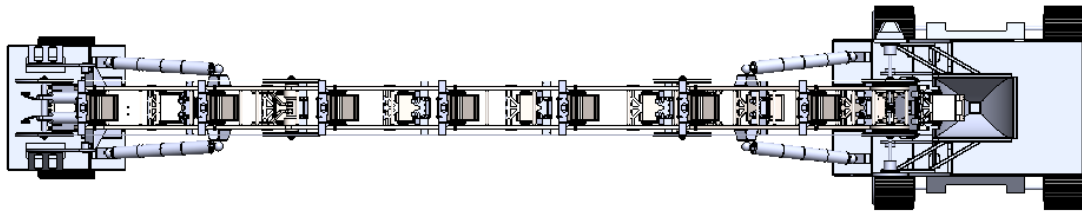


Figure 10.38: Excavation System from the top

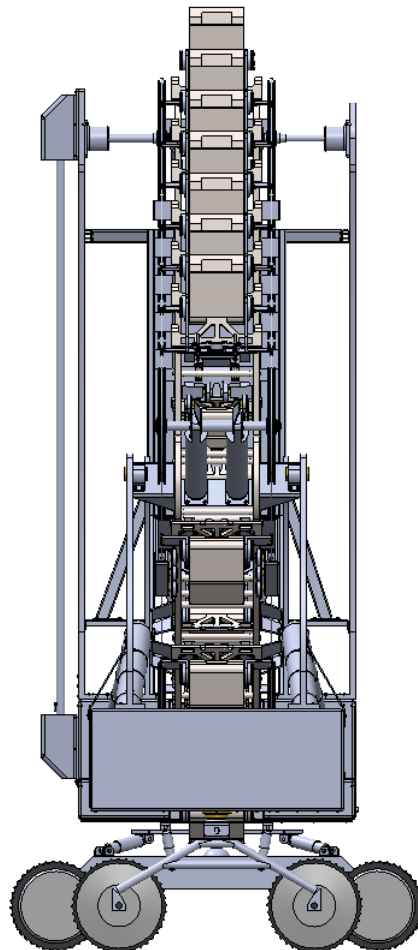


Figure 10.39: Excavation System from clamping station side

Figure 10.40 represents the final design in action. The smaller robot drives off-road, and the discharge robot at the already dismantled area. In this picture, a rectangular excavation area is created.

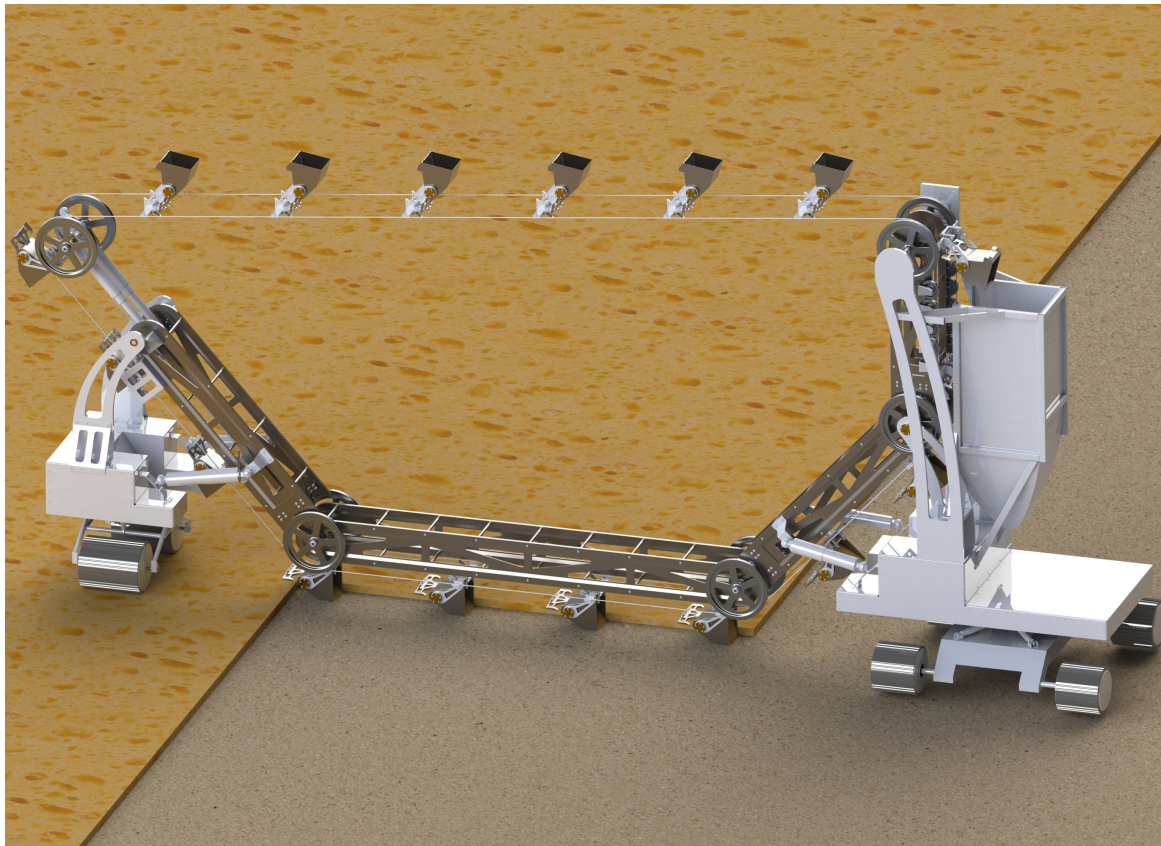


Figure 10.40: Lunar excavation in operation [23]

The final design (10.41) shows an excavator in terms of its mechanical setup. Some considerations about the implementation were made. Especially the carrier parts and the bucket mechanism are prepared in more detail. For these realisations, there were many different possibilities feasible in principle; one promising was chosen and prepared as shown. For further development further studies/design/optimisation etc. must be performed in more detail - also resulting in various changes.

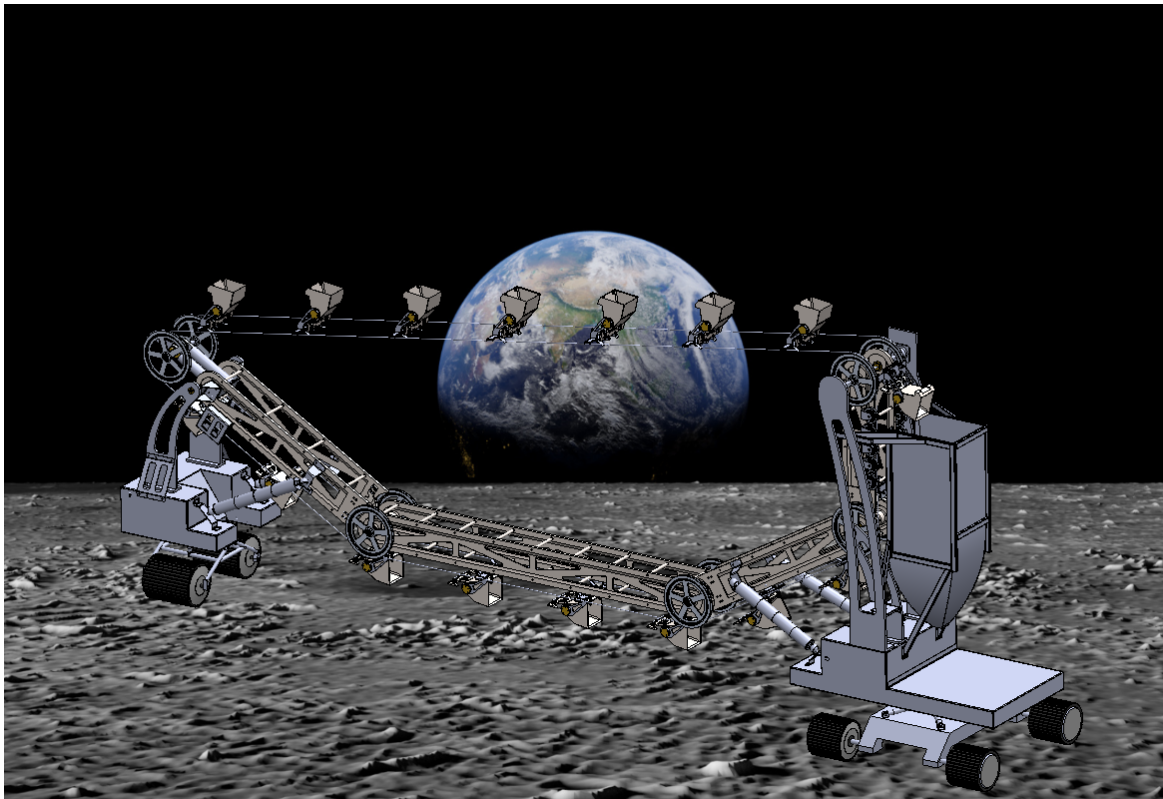


Figure 10.41: Lunar excavation concept on the Moon (Background: [1])

10.6 Further Steps

The main part of this thesis was to develop a principle concept, for an excavator for lunar missions - with the focus on the mechanical functionality and mechanical components. There are still many further steps to be taken to realize excavation as principally proposed, ranging from basic subsystem discussions/redesigning to highly detailed developments such as specific material determination or topology optimisation. Some of these further necessary steps are mentioned below.

Dust protection

As mentioned in Subsection 2.3.3, lunar dust is the main problem on space missions. Therefore, the protection of moving parts against these small particles is important, and various covers/anti-dust-mechanisms would need to be installed. These were

not included specifically in this concept explicitly. Maybe it is possible to use dust collectors like dust extractors or dust separation.

Another crucial step beneath the dust protection is lower dust generation. First of all, the excavation of material would cause dust in some way. Some steps for reducing dust were already considered, like the low excavation depth and the relatively low bucket speed; but some more precautionary measures would have to be researched in that regard. However, it can be said that the mining regions will beneficially be located also some distance away from the bases. Therefore, the lowered local dust, which is still generated although minimised as effective as possible, affects probably more the machine (excavator/conveyor) itself than other equipment, such as at the base.

Lightweight optimization

The overall concept was created with lightweight solutions in mind but at a minor level. However, for further developed implementation, every single component and every single connection need to be optimized closer because every kilogram requires more financial resources for transportation and should be avoided. For these improvements, various types of simulations, like FEM or topology analysis, can be used. Because such further specifications would be required at a further stage of development, no information regarding a specific weight value can be given so far, as this depends on a lot of factors, such as actual defined material to be used, or also further attached systems (such as sensors/cameras etc.).

Energy calculation

Another important issue for lunar robots is the availability of energy. For this system, isotropic generators are proposed. At this stage, it is not possible to define specifications about this regard, as closer energy-considerations would be required considering the total final development at an further developed stage (and not at this conceptual stage). Initial calculation attempts were made, but, as for instance, standard components (e.g.

mechanical parts, such as cylinders, drives etc.) are most likely not used, specific energy consumptions are relatively unclear. Research about the Mars rovers has shown that components that are used in such environments, need significantly less energy because of their grade of optimization/manufacturing etc.

Automation/Controlling

The excavator has been analysed from its mechanical side; for further developments, details regarding specific automation would be needed. Only the volume required to place larger components, such as motors and generators, were provided. For such a robot many sensors and actuators would be required, and also many different types of cameras and navigation systems. The most important parts will be the control and communication unit.

Additional areas to be covered

- Material selection
- Topology
- Transport to the Moon (first setting up to starting operation)
- Manufacturing
- Maintenance aspects
- Tribology
- Fail safe properties
- Interface with conveyor unit
- Navigation and obstacle detection
- Interaction with other robots
- Research for a promising landing an excavation area

11 Conclusion

The moon landing in 1969 was the starting signal for the space age, and after a few quieter years, space exploration is experiencing an upswing again. Reasons for this are, on the one hand, private space companies establishing a new market in that area, and on the other hand, the progressive explorations on Mars, which are becoming more and more in the focus of attention. Nearby this “red planet”, there is another important celestial body, the Moon. The Moon is rated with high potential for being a connection in missions from Earth to Mars, and space exploration in general. One of the crucial indents is the production of oxygen from the lunar surface material, regolith. This oxygen is intended to be used for fuel fabrication and/or for allowing life on lunar bases. Fuel is specifically important because rockets can be designed with a lower starting weight from Earth, as refuelling on Moon would be possible.

Review of the lunar environment

The lunar environment has some peculiarities: The gravity is only a sixth compared to Earth, and there is a thinner atmosphere with 14-times lower gas concentration. Another important parameter is the high-temperature fluctuations depending on the daytime, with a range of -258°C at the poles to $+127^{\circ}\text{C}$ at the equator.

Regolith, the material of interest in this thesis, covers the Moons surface with a layer thickness of 4 to 15 m and was formed by meteorite impacts. This regolith consists of many different materials which are bound as oxides. The average grain size is between

60 and 80 μm at the surface, and it shows a sharp grain shape. Further characteristics are cohesion aspects, and also adhesion of lunar dust to various surfaces due to electrostatic charging.

Oxygen production with ISRU

The mentioned oxygen production should be implemented with in-situ resource utilization (ISRU). This means the use of lunar material (specifically regolith) to produce materials that would otherwise have to be transported to the Moon, which in this case mainly concerns oxygen. The ISRU chain contains excavation, conveying, beneficiation, and processing as the major steps. These four steps, as well as their interfaces, have to work in order to allow ISRU. Especially concerning the stages of beneficiation and processing, various methods for extracting oxygen from regolith are research items in several referenced projects. But on excavation, as the initial stage for ISRU, developments are still required – and that is where this thesis is focused.

Various principles for excavation

For the excavation of regolith various types of machines are generally feasible, and several different operating principles would be possible, like using bucket wheels, bucket drums, pneumatic excavation, etc. In addition to the sharp and wear-increasing particles, gravity is one of the biggest problems. Therefore, scraping the material is more preferred than digging. After a comparison of the different functional principles with their pros and cons, an auspicious concept was chosen.

The basic principle of a bucket chain excavator

The idea was to use a horizontal bucket ladder with excavation capabilities, also referring to a bucket chain excavator. Therefore, the bucket chain is connected horizontally to two robots with a bridge system. Besides the relatively large area to be excavated,



this systems also allows levelling the surface for various lunar bases or launch stations for rockets.

The basic concept consists of a structure with three beams: the main one as an excavation beam, which is hinged on each side to two additional beams. With these two outer beams, it is possible to adjust the main beam and thus the excavation depth; and furthermore also the angle of the main beam to adjust to uneven terrain conditions.

Enhanced discharge mechanism

An important part of this excavation process is the discharge of the bulk material. Instead of typical gravitational or centrifugal discharge, as used on bucket ladders on Earth, this system uses a notching mechanism for its bucket. For this application, a fourth vertical beam is included in the structure at the discharge section. While the rotatably mounted bucket is moved along this beam, a locking mechanism gets unlocked, and the bucket swings out (even accelerated with the help of a pre-tensioned spring). At the maximum swing position, there is a punch block. After hitting this block, an impact ensures further discharging of the excavated material, thus decreasing the discharge time. Furthermore, the bucket is locked after this punch so that it does not swing back.

Design-accompanying simulation

For the finding of a suitable bucket design, five basic approaches were designed and compared in a DEM simulation. The simulation covers the excavation process (for surface and subsurface regolith) and the discharge process. After a comparison of reaction forces and the amount of scooped material, a promising solution is used as the basis for further design. The discharge simulation is furthermore used for the determination of the pivot point of the bucket to swing out as intended. The used springs to decrease the discharge time, adding initial speed to the buckets, are also included in this simulation.



Mechanical design

For a better illustration of the concept, a 3D model is created, whereby the model is focused on the excavator as the main mechanical setup. For the model as shown, one out of various feasible solutions is considered and respectively realised as a visualising 3D model. Especially the relevant components for the excavation process are shown in more detail, such as the bucket mechanisms. The two robots, required to move the excavator, as well as other additional components, are in their principles also embedded.

Overview of the excavator

This designed concept is developed to fulfil the requirements of the maximum dimensions, to make it transportable in a spaceship, and it is designed to excavate about $0.4 \text{ dm}^3/\text{s}$; meaning the gathering of enough material to launch three rockets every two lunar days.

Outlook

The result of this thesis shows a promising mechanical concept for lunar excavation, thus as equipment for the initial step for successful ISRU. To get this basic principal concept to further development stages, a large number of further steps are still necessary to reach an overall functional system. These steps include a high number of different – and also interdisciplinary – fields of technology, like materials science, tribology, logistics, energy management, automation, etc. Furthermore, solutions for dust protection, as well as decreasing dust generation in general, are necessary. Other important aspects are self-maintenance and fail-safe properties.

As the basis for these further steps required, this design concept proposed represents a promising concept for lunar excavation from its mechanical side. With several system-specific side-advantages, such as levelling possibilities for the surface, relatively low



dust generation, relatively high volume flow, and offroad capabilities, this concept, or at least subsystems, may be impulses for future developments in this area.

Certain features, such as the notching mechanism, could also be useful for certain applications on Earth. A possible use would be its application with sticky materials or those with a high risk of clogging. Because of the impulse when hitting the punch block, those types of bulk materials would be discharged more effectively. Conclusively, with this concept, a step was taken towards excavation on the Moon, initialising ISRU for oxygen production, and further contribute to space exploration in general perspective – and besides this space-related aspect, also contribute technology concepts for special applications on Earth.

List of Figures

2.1	The Moon surface with mares and highlands [65]	5
2.2	Moon mares [65]	6
2.3	The Apennines on the Moon [65]	6
2.4	Crater landscape [65]	7
2.5	Oriente Basin [58]	8
2.6	Distribution of water ice at the northern and southern polar regions [35]	9
2.7	Temperature profile at the Moon's surface [58]	11
2.8	Lunar agglutinate [58]	13
3.1	ISRU process chain [32]	18
3.2	Moonraker robot [39]	20
3.3	Backhoe as an excavator system [32]	20
3.4	Graphic of pneumatic conveyor [40]	21
3.5	Future design of a pneumatic conveyor [58]	21
3.6	Diagram of a free fall type separator [52]	23
3.7	Diagrammatic representation of an IRMS [52]	23
3.8	Different types of reduction reactors [57]	25
3.9	Sketch of the carbothermal reduction of lunar regolith [5]	26
4.1	Spirit and Opportunity [49]	29
4.2	Structure of Spirit and Opportunity [44]	30
4.3	Curiosity [46]	31



4.4	Curiosity's turret [46]	32
4.5	Structure of Curiosity's turret [45]	32
4.6	Perseverance [42]	33
4.7	Perseverance and its cameras [42]	33
4.8	Ingenuity [42]	34
4.9	NASA Rassor [48]	35
5.1	Vulcan Centaur [66]	37
5.2	European Large Logistics Lander [18]	38
5.3	NASA Lunar Lander [34]	39
5.4	Peregrine [3]	40
5.5	Starship: crew configuration and uncrewed configuration [62]	41
5.6	Starship payload volume [62]	42
5.7	Blue Moon [8]	42
8.1	Functional principles [32]	51
8.2	Backhoe loader [9]	52
8.3	Scraper [53]	54
8.4	Bucket-wheel excavator for coal mining [55]	55
8.5	Lunar excavator by the Colorado School of Mines [15]	56
8.6	Bucket-wheel excavator with a bucket wheel in the middle [32]	56
8.7	Bucket drum concept [50]	57
8.8	Bucket drum DEM simulation [50]	57
8.9	Shaftless screw conveyor [11]	58
8.10	Concept bilateral screw conveyor	59
8.11	Sweeper concept for dismantling regolith	60
8.12	Types of pneumatic systems [21]	61
8.13	Bucket elevator [20]	63
8.14	Bucket chain excavator [54]	64
8.15	Vertical bucket ladder [21]	66

8.16	Methods of discharging a bucket [21]	67
8.17	Forces of a bucket ladder at the discharge [21]	68
8.18	Different principles of bucket attachment [28]	70
8.19	Concept bucket ladder with boom	71
8.20	Excavation area boom concept	71
8.21	Concept bucket ladder with bridge [26]	72
8.22	Variation of the middle segment	73
8.23	Excavation areas bridge [26]	73
9.1	Density calibration: cylinder filling	76
9.2	Density calibration: full cylinder	76
9.3	DEM Calibration Tool	77
9.4	Angle of repose for the subsurface Regolith	78
9.5	Sublayer	80
9.6	Field setup for surface Regolith	80
9.7	Shovel shapes	80
9.8	Bucket plunging Form A	81
9.9	Bucket turning out Form A	81
9.10	Force progression - Surface - All values	82
9.11	Force progression - Subsurface - All values	82
9.12	Force progression - Surface - Smoothed curve	82
9.13	Force progression - Subsurface - Smoothed curve	83
9.14	Force progression - Surface - Detail bucket plunging	84
9.15	Force progression - Subsurface - Detail bucket plunging	84
9.16	Force progression - Surface - Detail bucket turning out	84
9.17	Force progression - Subsurface - Detail bucket turning out	84
9.18	Number of scooped particles - Surface	85
9.19	Number of scooped particles - Subsurface	85
9.20	Chosen bucket design	86
9.21	Function of the notching mechanism [26]	87



9.22	Pivot-Point: x-axis positions	88
9.23	Pivot-Point: y-axis positions	89
9.24	Possible pivot-point	90
9.25	Bucket spin out	90
9.26	Bucket before hitting the block	90
9.27	Bucket after hitting the block	90
10.1	Design explanation	92
10.2	Carrier clamping station	93
10.3	Main beam	93
10.4	Connector	93
10.5	Discharge carrier	93
10.6	Basic structure	94
10.7	Bearing combination	95
10.8	Clamping station	96
10.9	Two shafts connected via shaft coupling	97
10.10	Second deflection of the drive shaft	97
10.11	Robot at clamping station	98
10.12	Revolute joint for offroad driving	98
10.13	Robot at ejector station	99
10.14	Ball joint against unevenness	100
10.15	Chute	100
10.16	Chute in the assembly	100
10.17	Overview of the bucket mechanism	102
10.18	Bucket at swing-out end position	102
10.19	Positions of the activation rollers	103
10.20	Steel cable attachment	103
10.21	Bearing of the bucket	104
10.22	Cover of the bearing	104
10.23	Locked hooks	104



10.24	Unlocked hooks	104
10.25	Adjusting roller	105
10.26	Punching block before locking	105
10.27	Locked punching block	105
10.28	Unlock rollers tensioning station	106
10.29	Bucket reset	107
10.30	Resetting rollers	107
10.31	Final bucket design	107
10.32	Bucket unlocking timeline	108
10.33	Bucket resetting timeline	108
10.34	Lower end position - maximum excavation depth	109
10.35	Upper end position	109
10.36	Lower end position - isometric view	110
10.37	Upper end position - isometric view	111
10.38	Excavation System from the top	112
10.39	Excavation System from clamping station side	112
10.40	Lunar excavation in operation [23]	113
10.41	Lunar excavation concept on the Moon (Background: [1])	114

List of Tables

2.1	Overview of properties Moon and Earth [58]	4
2.2	Gas composition of the lunar atmosphere [24]	10
2.3	Major and trace elements of regolith [58]	13
2.4	Cohesion and internal friction angle of regolith [24, 36]	14
2.5	Particle size distribution in lunar soil [12]	15
4.1	Facts about the missions Spirit and Opportunity [49]	29
4.2	The Curiosity mission [46, 45]	31
6.1	Design materials for lunar applications [67]	46
8.1	Mass flow & depth of different functional concepts [32]	65
9.1	Density calibration: results	77
9.2	Internal friction calibration: results	78
9.3	Used DEM parameters	79

Bibliography

- [1] grahmbo7 (Username). *Moon surface texture*. blenderartists.org, April 2019. URL: <https://blenderartists.org/t/moon-surface-texture/1154765> (cit. on p. 114).
- [2] Ahmad Anwar et al. "Vacuum Effect on Spacecraft Structure Materials." In: *International Conference on Aerospace Sciences and Aviation Technology 16.AEROSPACE SCIENCES (2015)*, pp. 1–10. DOI: 10.21608/asat.2015.22908 (cit. on p. 45).
- [3] Astrobotic Technology. *Peregrine Lunar Lander Payload User's Guide*. Ed. by Astrobotic Technology. URL: <https://www.astrobotic.com/payload-user-guide> (cit. on pp. 39, 40).
- [4] Viorel Badescu. *Moon [recurso electrónico]: Prospective Energy and Material Resources*. Alemania: Springer Healthcare Ltd, 2012. ISBN: 9783642279690. DOI: 10.1007/978-3-642-27969-0. URL: <http://site.ebrary.com/lib/alltitles/docDetail.action?docID=10545842> (cit. on pp. 4, 12, 19, 20, 24–27).
- [5] R. Balasubramaniam et al. "Carbothermal Processing of Lunar Regolith Using Methane." In: *AIP Conference Proceedings*. AIP, 10–14 February 2008, pp. 157–161. DOI: 10.1063/1.2844962 (cit. on p. 26).
- [6] BECKER 3D. *ThreeParticle/CAE*. URL: <https://www.becker3d.com/> (cit. on p. 76).
- [7] Berner Michael. *Vorlesungsskriptum Gewinnungsmaschinen -280.026: Obertage*. WS20/21 (cit. on p. 55).



- [8] Blue Origin. *Blue Moon*. Ed. by Blue Origin. URL: <https://www.blueorigin.com/blue-moon/> (cit. on pp. 42, 43).
- [9] Marshall Brain and Tom Harris. *Backhoe Loaders / Backhoe Tractors | Cat | Caterpillar*. 4.11.2020. URL: https://www.cat.com/en_US/products/new/equipment/backhoe-loaders.html (cit. on p. 52).
- [10] C. I. Calle. "The electrostatic environments of Mars and the Moon." In: *Journal of Physics: Conference Series* 301 (2011), p. 012006. DOI: 10.1088/1742-6596/301/1/012006 (cit. on p. 45).
- [11] Christian Cavallo. "All About Screw Conveyors - Types, Design, and Uses." In: *Thomas* (). URL: <https://www.thomasnet.com/articles/materials-handling/all-about-screw-conveyors/> (cit. on p. 58).
- [12] J. E. Colwell et al. "Lunar surface: Dust dynamics and regolith mechanics." In: *Reviews of Geophysics* 45.2 (2007). ISSN: 8755-1209. DOI: 10.1029/2005RG000184 (cit. on pp. 12, 15, 16).
- [13] Heather Couper et al. *The planets: The definitive visual guide to our Solar System*. First American edition. London: Dorling Kindersley, 2014. ISBN: 9781409353058 (cit. on p. 4).
- [14] Dallas Bienhoff. *The Future of Commercial Space Transportation*. Ed. by The Space Review. URL: <https://thespacereview.com/article/3776/1> (cit. on p. 36).
- [15] Bruce Damer, Dave Rasmussen, and Peter Newman. "Design Simulation in Support of NASA's Robotic and Human Lunar Exploration Program." In: *Space 2006*. [Reston, Va.]: [American Institute of Aeronautics and Astronautics], 2006. ISBN: 978-1-62410-049-9. DOI: 10.2514/6.2006-7397 (cit. on p. 56).
- [16] Dassault Systèmes SolidWorks Corporation. *SolidWorks*. URL: <https://www.solidworks.com/de> (cit. on p. 92).

- [17] European Cooperation for Space Standardization. *Space product assurance: Kinetic outgassing of materials for space*. Ed. by ESA Requirements and Standards Division. Netherlands, 2011. URL: <https://ecss.nl/hbstms/ecss-q-tm-70-52a-kinetic-outgassing-of-materials-for-space/> (cit. on p. 45).
- [18] European Space Agency. *European Large Logistics Lander*. URL: http://www.esa.int/Science_Exploration/Human_and_Robotic_Exploration/Exploration/European_Large_Logistics_Lander (cit. on pp. 37, 38).
- [19] Leo Ferguson. "What Our Future Will Look Like on Mars - Predict - Medium." In: *Predict* (7.11.2020). URL: <https://medium.com/predict/what-our-future-will-look-like-on-mars-30984b08632c> (cit. on p. 1).
- [20] Ilchmann Fördertechnik GmbH. *Becherwerke Hersteller, Fotogalerie*. 5.11.2020. URL: <https://www.ilchmann.biz/de/produkte/becherwerke/fotogalerie.html> (cit. on p. 63).
- [21] Rudolf Griemert and Peter Römisch. *Fördertechnik: Auswahl und Berechnung von Elementen und Baugruppen*. 12., überarb. u. erw. Auflage 2018. Wiesbaden: Springer Fachmedien Wiesbaden, 2018. ISBN: 9783658214142. DOI: 10.1007/978-3-658-21414-2 (cit. on pp. 61, 62, 66–70).
- [22] Hanneke Weitering. *Blue Moon: Here's How Blue Origin's New Lunar Lander Works*. Ed. by Space.com. 10.05.2019. URL: <https://www.space.com/blue-origin-blue-moon-lander-explained.html> (cit. on p. 43).
- [23] Philipp Hartlieb et al. *Excavation & Conveying for Lunar Materials*. 2021. DOI: 10.5281/ZENODO.4707306 (cit. on pp. x, 113).
- [24] Grant H. Heiken, ed. *Lunar sourcebook: A user's guide to the moon*. Cambridge: Univ. Press, 1991. ISBN: 0521334446 (cit. on pp. 6, 8, 10, 11, 14, 15).
- [25] Helmut Hasler. "Development of a Tool to Assist the Calibration Process of Bulk Density in DEM Simulation." Bachelor Thesis. Montanuniversität Leoben, 2020/21. URL: <https://dem.hasler.co.at/> (cit. on p. 76).

- [26] Dominik Höber, Andreas Taschner, and Eric Fimbinger. "Excavation and Conveying Technologies for Space Applications." In: *BHM Berg- und Hüttenmännische Monatshefte* 166.2 (2021), pp. 95–103. ISSN: 0005-8912. DOI: 10.1007/s00501-020-01073-z (cit. on pp. ix, 50, 72, 73, 87).
- [27] "How Caterpillar Backhoe Loaders Work." In: *HowStuffWorks* (5.03.2001). URL: <https://science.howstuffworks.com/transport/engines-equipment/backhoe-loader1.htm> (cit. on p. 52).
- [28] pewag International AG. *Becherwerke - Fördertechnik*. 15.11.2020. URL: <https://www.pewag.at/shop/conveyortechnik/becherwerke-4.html> (cit. on p. 70).
- [29] Alexander M. Jablonski and Kelly A. Ogden. "Technical Requirements for Lunar Structures." In: *Journal of Aerospace Engineering* 21.2 (2008), pp. 72–90. ISSN: 0893-1321. DOI: 10.1061/(ASCE)0893-1321(2008)21:2(72) (cit. on pp. 44, 45).
- [30] Telana L. Jackson, William M. Farrell, and Michael I. Zimmerman. "Rover wheel charging on the lunar surface." In: *Advances in Space Research* 55.6 (2015), pp. 1710–1720. ISSN: 0273-1177. DOI: 10.1016/j.asr.2014.12.027. URL: <http://www.sciencedirect.com/science/article/pii/S0273117714008035> (cit. on p. 45).
- [31] Zilong Jiao et al. "Outgassing Environment of Spacecraft: An Overview." In: *IOP Conference Series: Materials Science and Engineering* 611 (2019), p. 012071. DOI: 10.1088/1757-899X/611/1/012071 (cit. on p. 45).
- [32] G. H. Just et al. "Parametric review of existing regolith excavation techniques for lunar In Situ Resource Utilisation (ISRU) and recommendations for future excavation experiments." In: *Planetary and Space Science* 180 (2020), p. 104746. ISSN: 00320633. DOI: 10.1016/j.pss.2019.104746 (cit. on pp. 18–20, 51, 56, 65).
- [33] K. Hadler, D. J. P. Martin, J. Carpenter, and J. J. Cilliers, ed. *A UNIVERSAL FLOWSHEET AND TERMINOLOGY FOR IN SITU RESOURCE UTILIZATION (ISRU)*. 2019 (cit. on p. 18).



- [34] L.D. Kennedy. *NASA Lunar Lander Reference Design*. Ed. by National Aeronautics and Space Administration. Marshall Space Flight Center and Huntsville, Alabama 35812. URL: <https://ntrs.nasa.gov/citations/20190033128> (cit. on pp. 38, 39).
- [35] Shuai Li et al. "Direct evidence of surface exposed water ice in the lunar polar regions." In: *Proceedings of the National Academy of Sciences of the United States of America* 115.36 (2018), pp. 8907–8912. DOI: 10.1073/pnas.1802345115 (cit. on p. 9).
- [36] Tianxi LIU et al. "Simulation and Analysis of the Lunar Regolith Sampling Process Based on the Discrete Element Method." In: *TRANSACTIONS OF THE JAPAN SOCIETY FOR AERONAUTICAL AND SPACE SCIENCES* 57.6 (2014), pp. 309–316. ISSN: 0549-3811. DOI: 10.2322/tjsass.57.309 (cit. on p. 14).
- [37] *Mars 2020 Perseverance Landing Press Kit | Introduction*. 7.03.2021. URL: https://www.jpl.nasa.gov/news/press_kits/mars_2020/landing/ (cit. on pp. 32, 33).
- [38] Mike Brown. *SPACEX STARSHIP: STUNNING IMAGE SHOWS HOW IT MAY DEPLOY 240 STARLINK CRAFT*. Ed. by Bustle Digital Group. NYC 315 Park Avenue South 12th Floor NY 10010, 17.6.2020. URL: <https://www.inverse.com/innovation/spacex-starship-stunning-image-shows-how-it-may-deploy-240-starlink-craft> (cit. on p. 41).
- [39] "Moonraker robots dig for victory in lunar challenge." In: *New Scientist* 204.2731 (2009), p. 21. ISSN: 02624079. DOI: 10.1016/S0262-4079(09)62803-7 (cit. on p. 20).
- [40] Robert P. Mueller, III Ivan I. Townsend, and James G. Mantovani. "Pneumatic Regolith Transfer Systems for In Situ Resource Utilization." In: *Earth & Space 2010*. Ed. by Gangbing Song and Ramesh B. Malla. Reston, VA: American Society of Civil Engineers, 2010, pp. 1353–1363. ISBN: 9780784410967. DOI: 10.1061/41096(366)122 (cit. on p. 21).
- [41] Robert P. Mueller et al. "Regolith Advanced Surface Systems Operations Robot (RASSOR)." In: *IEEE Aerospace Conference, 2013*. Piscataway, NJ: IEEE, 3/2/2013 -



- 3/9/2013, pp. 1–12. ISBN: 978-1-4673-1813-6. DOI: 10.1109/AERO.2013.6497341 (cit. on pp. 34, 35, 56).
- [42] NASA. *Mars 2020 Perseverance Launch Press Kit*. 6/2020. URL: https://www.jpl.nasa.gov/news/press_kits/mars_2020/launch/ (cit. on pp. 32–34).
- [43] NASA. *Mars Exploration Rover Landings Press Kit*. 1/2004. URL: https://mars.nasa.gov/internal_resources/826/ (cit. on p. 30).
- [44] NASA. *Mars Exploration Rover Launches Press Kit*. 6/2003. URL: https://mars.nasa.gov/internal_resources/827/ (cit. on pp. 29, 30).
- [45] NASA. *Mars Science Laboratory Landing Press Kit*. 7/2012. URL: https://www.jpl.nasa.gov/news/press_kits/MSLLanding.pdf (cit. on pp. 30–32).
- [46] NASA. *Mars Science Laboratory: Curiosity Rover*. 1/2013. URL: <https://mars.nasa.gov/files/resources/MSLLithoSet2013.pdf> (cit. on pp. 30–32).
- [47] NASA. *Opportunity's Mission Is Complete*. 2/2019. URL: <https://mars.nasa.gov/mer/mission/rover-status/#recent> (cit. on pp. 28, 29).
- [48] NASA. *Regolith Advanced Surface Systems Operations Robot (RASSOR) Excavator*. 2/2013. URL: <https://technology.nasa.gov/patent/KSC-TOPS-7> (cit. on pp. 34, 35, 56).
- [49] NASA. *The Mars Exploration Rovers: Spirit and Opportunity*. 12/2013. URL: https://mars.nasa.gov/system/downloadable_items/44694_MER10-YearAnniversaryLithograph.pdf (cit. on pp. 28, 29).
- [50] NASA *Bucket Drum Double-Helix* | 3D CAD Model Library | GrabCAD. 4.11.2020. URL: <https://grabcad.com/library/nasa-bucket-drum-double-helix-1> (cit. on pp. ix, 57).
- [51] Prenner Michael. *Vorlesungsskriptum Stetige Fördersysteme 280.002*. Montanuniversität Leoben, WS2019 (cit. on pp. 53, 69, 70).



- [52] J. N. Rasera et al. "The beneficiation of lunar regolith for space resource utilisation: A review." In: *Planetary and Space Science* 186 (2020), p. 104879. ISSN: 00320633. DOI: 10.1016/j.pss.2020.104879. URL: <http://www.sciencedirect.com/science/article/pii/S0032063319301266> (cit. on pp. 22–24).
- [53] RHO. "Katalog Kratzerförderketten deutsch.indd." In: (). URL: https://www.pfeifer.info/out/assets/PFEIFER-ISOFER_KRATZERFOERDERKETTEN_PPDE.PDF (cit. on p. 54).
- [54] Tenova S.p.A. *Bucket-Chain Excavators - TENOVA*. 5.11.2020. URL: <https://www.tenova.com/product/bucket-chain-excavators/> (cit. on p. 64).
- [55] Tenova S.p.A. *Bucket-Wheel Excavators - TENOVA*. 4.11.2020. URL: <https://www.tenova.com/product/bucket-wheel-excavators/> (cit. on p. 55).
- [56] Kurt Sacksteder and Gerald Sanders. "In-Situ Resource Utilization for Lunar and Mars Exploration." In: *Aerospace Sciences Meetings*. [Place of publication not identified]: [publisher not identified], 2007. ISBN: 978-1-62410-012-3. DOI: 10.2514/6.2007-345 (cit. on pp. 17, 48).
- [57] G. B. Sanders and W. E. Larson. "Progress Made in Lunar In Situ Resource Utilization under NASA's Exploration Technology and Development Program." In: *Earth and Space 2012*. Ed. by Kris Zacny, Ramesh B. Malla, and Wieslaw K. Binienda. Reston, VA: American Society of Civil Engineers, 2012, pp. 457–478. ISBN: 9780784412190. DOI: 10.1061/9780784412190.050 (cit. on pp. 25, 48).
- [58] David G. Schrunk. *The moon: Resources, future development, and settlement*. 2. ed. Springer-Praxis books in space exploration. Berlin: Springer, 2008. ISBN: 9780387360553 (cit. on pp. 3, 4, 8–14, 16, 17, 19, 21, 50).
- [59] Siceloff S. *Engineers Building Hard-working Mining Robot*. Ed. by Kennedy Space Center. 1/2013. URL: <https://www.nasa.gov/topics/technology/features/RASSOR.html> (cit. on pp. 34, 35, 56).

- [60] Hermann Sicius. *Erdalkalimetalle: Elemente der zweiten Hauptgruppe: Eine Reise durch das Periodensystem*. 1. Aufl. 2016. essentials. Wiesbaden: Springer Fachmedien Wiesbaden, 2016. ISBN: 9783658118778. DOI: 10.1007/978-3-658-11878-5. URL: <http://gbv.eblib.com/patron/FullRecord.aspx?p=4178835> (cit. on p. 46).
- [61] *Soviet Missions to the Moon*. 3.03.2021. URL: <https://nssdc.gsfc.nasa.gov/planetary/lunar/lunarussr.html> (cit. on p. 3).
- [62] Space Exploartion Technologies Corp. *Starship Users Guide*. Ed. by Space Exploartion Technologies Corp. URL: https://www.spacex.com/media/starship_users_guide_v1.pdf (cit. on pp. 41, 42).
- [63] The MathWorks, Inc. *MATLAB 2017b*. URL: <https://de.mathworks.com/products/matlab.html> (cit. on p. 81).
- [64] Wolfgang Torge. *Geodäsie*. 2., vollständig überarbeitete und erw. Aufl. De Gruyter Lehrbuch. Berlin and New York: De Gruyter, 2003. ISBN: 3110198177 (cit. on p. 9).
- [65] Erich Übelacker and Frank Kliemt. *Der Mond*. [Nachdr.] Vol. 21. Tessloff Wissen. Nürnberg: Tessloff, 2010. ISBN: 9783788602611 (cit. on pp. 5–7).
- [66] United Launch Alliance. *Vulcan Centaur* (cit. on p. 37).
- [67] Wolfgang Weissbach, Michael Dahms, and Christoph Jaroschek. *Werkstoffe und ihre Anwendungen: Metalle, Kunststoffe und mehr*. 20., überarbeitete Auflage. Springer-Link Bücher. s.l.: Springer Vieweg, 2018. ISBN: 9783658198916. DOI: 10.1007/978-3-658-19892-3 (cit. on pp. 45, 46).
- [68] Don E. Wilhelms, with sections by McCauley, John F., and Newell J. Trask. *The geologic history of the Moon*. 1987. DOI: 10.3133/pp1348 (cit. on pp. 6, 7).
- [69] Elmar Witten, ed. *Handbuch Faserverbundkunststoffe: Grundlagen, Verarbeitung, Anwendungen*. 4th ed. Wiesbaden: Springer Fachmedien Wiesbaden, 2013. ISBN: 9783658027544. URL: <http://lib.myilibrary.com/detail.asp?id=601673> (cit. on p. 46).